LILIANA LUZ

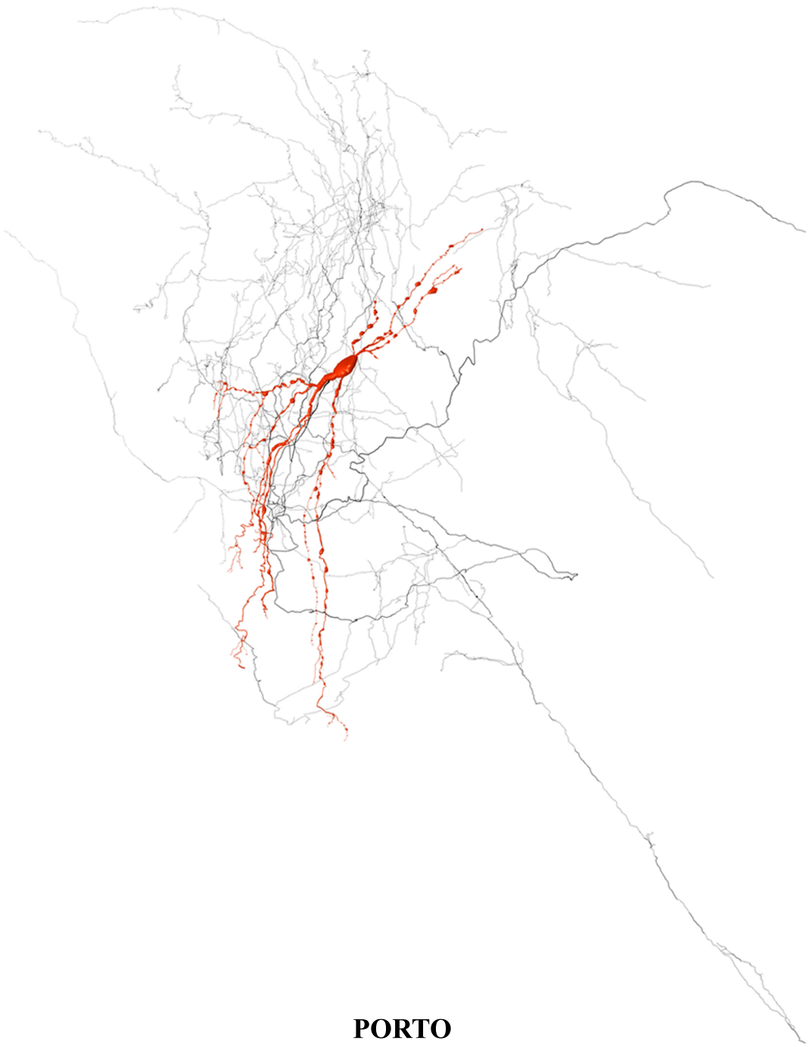
U.PORTO
FMUP FACULDADE DE MEDICINA
UNIVERSIDADE DO PORTO

NOCICEPTIVE PROCESSING ON PROJECTION AND NON-PROJECTION LAMINA I NEURONS

PORTO 2011

LILIANA ALEXANDRA LARACHO DA SILVA LUZ

NOCICEPTIVE PROCESSING ON PROJECTION AND NON-PROJECTION LAMINA I NEURONS



PORTO
2011

LILIANA ALEXANDRA LARACHO DA SILVA LUZ

NOCICEPTIVE PROCESSING ON PROJECTION AND NON-PROJECTION LAMINA I NEURONS

Dissertação de candidatura ao grau de Doutor em Neurociências apresentada à Faculdade de Medicina da Universidade do Porto

PORTO

2011

Artigo 48º, § 3º

“ A Faculdade não responde pelas doutrinas expendidas na dissertação”

(Regulamento da Faculdade de Medicina do Porto, Decreto-Lei nº 19337 de 29 de Janeiro de 1931)

Esta investigação foi realizada no Instituto de Biologia Molecular e Celular. A candidata realizou o trabalho experimental com o apoio de uma bolsa de Doutoramento (SFRH/BD/36401/2007) atribuída pela Fundação para a Ciência e a Tecnologia (FCT).

Orientador: Professor Doutor Boris V. Safronov
Co-orientador: Professora Doutora Deolinda Maria Valente Alves de Lima Teixeira
Co-orientador: Doutor Peter Szucs

CORPO CATEDRÁTICO DA FACULDADE DE MEDICINA DO PORTO

Professores Efectivos

Doutor Alberto Manuel Barros da Silva
Doutor Altamiro Manuel Rodrigues Costa Pereira
Doutor Álvaro Jerónimo Leal Machado de Aguiar
Doutor António Carlos Freitas Ribeiro Saraiva
Doutor Daniel Filipe de Lima Moura
Doutora Deolinda Maria Valente Alves Lima Teixeira
Doutor Francisco Fernandes Rocha Gonçalves
Doutora Isabel Maria Amorim Pereira Ramos
Doutor João Francisco Montenegro A. Lima Bernardes
Doutor Jorge Manuel Mergulhão Castro Tavares
Doutor José Agostinho Marques Lopes
Doutor José Carlos da Cunha Areias
Doutor José Eduardo Torres Eckenroth Guimarães
Doutor José Henrique Dias Pinto Barros
Doutor José Manuel Lopes Teixeira Amarante
Doutor José Manuel Pereira Dias de Castro Lopes
Doutor Manuel Alberto Coimbra Sobrinho Simões
Doutor Manuel António Caldeira Pais Clemente
Doutor Manuel Jesus Falcão Pestana Vasconcelos
Doutora Maria Amélia Duarte Ferreira
Doutora Maria Dulce Cordeiro Madeira
Doutora Maria de Fátima Machado Henriques Carneiro
Doutora Maria Leonor Martins Soares David
Doutor Patrício Manuel Vieira Araújo Soares Silva
Doutor Rui Manuel Almeida Mota Cardoso
Doutor Rui Manuel Lopes Nunes

Professores Jubilados ou Aposentados

Doutor Abel José Sampaio da Costa Tavares
Doutor Abel Vitorino Trigo Cabral
Doutor Alexandre Alberto Guerra Sousa Pinto
Doutor Amândio Gomes Sampaio Tavares
Doutor António Augusto Lopes Vaz
Doutor António Carvalho Almeida Coimbra
Doutor António Fernandes da Fonseca
Doutor António Fernandes Oliveira Barbosa Ribeiro Braga
Doutor António Germano Pina Silva Leal
Doutor António José Pacheco Palha
Doutor António Luís Tomé da Rocha Ribeiro
Doutor António Manuel Sampaio de Araújo Teixeira
Doutor Belmiro dos Santos Patrício
Doutor Cândido Alves Hipólito Reis
Doutor Carlos Rodrigues Magalhães Ramalhão
Doutor Cassiano Pena de Abreu e Lima
Doutor Daniel Santos Pinto Serrão
Doutor Eduardo Jorge Cunha Rodrigues Pereira
Doutor Fernando de Carvalho Cerqueira Magro Ferreira
Doutor Fernando Tavarela Veloso
Doutor Francisco de Sousa Lé
Doutor Henrique José Ferreira Gonçalves Lecour de Menezes
Doutor Joaquim Germano Pinto Machado Correia da Silva
Doutor José Augusto Fleming Torrinha
Doutor José de Carvalho Oliveira
Doutor José Fernandes Barros Castro Correia
Doutor José Luís Medina Vieira
Doutor José Manuel Costa Mesquita Guimarães
Doutor Levi Eugénio Ribeiro Guerra
Doutor Luís Alberto Martins Gomes de Almeida
Doutor Manuel Augusto Cardoso de Oliveira
Doutor Manuel Machado Rodrigues Gomes

Doutor Manuel Maria Paula Barbosa

Doutor Manuel Teixeira Amarante Júnior

Doutora Maria da Conceição Fernandes Marques Magalhães

Doutora Maria Isabel Amorim de Azevedo

Doutor Mário José Cerqueira Gomes Braga

Doutor Serafim Correia Pinto Guimarães

Doutor Valdemar Miguel Botelho dos Santos Cardoso

Doutor Walter Friedrich Alfred Osswald

JÚRI DE PROVAS DE DOUTORAMENTO EM NEUROCIÊNCIAS

Presidente

Director da Faculdade de Medicina (por delegação reitoral)

Vogais

Doutora Ana Maria Ferreira de Sousa Sebastião, Professora Associada da Faculdade de Medicina da Universidade de Lisboa;

Doutor Andrew J. Todd, Professor of Neuroscience, Institute of Neuroscience and Psychology, University of Glasgow;

Doutora Isaura Ferreira Tavares, Professora Associada da Faculdade de Medicina da Universidade do Porto;

Doutor Nokolai Lukoyanov, Professor Associado da Faculdade de Medicina da Universidade do Porto;

Doutor Rui Manuel Cardoso Vaz, Professor Associado da Faculdade de Medicina da Universidade do Porto;

Doutor Boris Safronov, Professor Auxiliar Convidado da Faculdade de Medicina da Universidade do Porto.

Ao Professor Doutor Boris V. Safronov

Ao Doutor Peter Szucs

À Professora Doutora Deolinda Maria Valente Alves de Lima Teixeira

Aos meus pais e à minha irmã

Ao meu avô Licínio

Ao Nuno

AGRADECIMENTOS

Uma dissertação, apesar de ser processo solitário a que qualquer investigador está destinado, reúne contributos de várias pessoas. Desde o início do doutoramento, contei com a confiança e o apoio de inúmeras pessoas sem os quais, esta investigação não teria sido possível.

Em primeiro lugar quero agradecer à pessoa responsável pelos meus primeiros passos na área das neurociências e orientador desta dissertação, o Doutor Boris Safronov. As notas dominantes da sua orientação foram contribuições essenciais para este trabalho. Acima de tudo, obrigada por me continuar a acompanhar nesta jornada e por estimular o meu interesse pelo conhecimento e pela investigação científica.

I thank my co-supervisor Doctor Peter Szucs for his guidance throughout my studies. His availability for helping with my project, constructive criticism, numerous advices, encouragement, enthusiasm and patience made my stay in the lab a great experience. Köszönöm, hogy követendő példát mutattál és hogy jó barátomnak tudhatlak!

Agradeço também à minha co-orientadora Professora Doutora Deolinda Lima que sempre me inspirou através das suas palavras e paixão pela investigação científica.

Gostaria também de agraciar algumas pessoas com quem contactei durante estes anos em que estive no Instituto de Biologia Molecular e Celular. Agradeço à Sónia Santos e Mafalda Sousa pelo apoio, companheirismo e partilha do aparelho de *patch-clamp* e ainda ao Doutor Paulo Aguiar pela atenção, apoio e disponibilidade constante. Um obrigado muito especial à Raquel Pinho por toda a sua amizade, boa disposição, paciência e apoio constante durante todo o trabalho.

À Fundação para a Ciência e a Tecnologia declaro o meu reconhecimento pela Bolsa de Doutoramento concedida.

Um especial agradecimento a todos meus amigos que me apoiaram nas horas difíceis.

E por fim mas não os menos importantes, agradeço aos meus pais, irmã e avós pelo apoio que sempre me deram. Um agradecimento especial aos meus pais pelo constante encorajamento a fim de prosseguir a elaboração deste trabalho. Sei que é a vós que devo o facto de ser aquilo que sou hoje.

Dedico esta dissertação a duas pessoas que de modo particular são muito importantes na minha vida. Ao meu avô Licínio, onde quer que esteja, espero que tenha orgulho do meu percurso... Ao Nuno, companheiro e amigo, que me apoiou nos bons e maus momentos. Por todo o amor e carinho, toda a confiança em mim depositada, pela ajuda e motivação, pela companhia...

Em obediência ao disposto no Decreto-Lei nº388/70, artigo 8º, parágrafo 2, declaro que efectuei o planeamento e execução das experiências, observações do material e análise dos resultados discutidos durante esta dissertação. Declaro ainda que participei activamente na redacção de todas as publicações que fazem parte integrante desta dissertação:

I Szucs P*, **Luz LL***, Lima D & Safronov BV. (2010). Local axon collaterals of lamina I projection neurons in the spinal cord of young rats. *J Comp Neurol* 518, 2645-2665 (* the first two authors contributed equally to this work.).

II **Luz LL***, Szucs P*, Pinho R & Safronov BV. (2010). Monosynaptic excitatory inputs to spinal lamina I anterolateral-tract-projecting neurons from neighbouring lamina I neurons. *J Physiol* 588, 4489-4505 (* the first two authors contributed equally to this work.).

III Szucs P, **Luz LL**, Pinho R, Aguiar P, Antal Zs, Tiong SY, Todd A, Safronov BV. (2011). Morphological analysis of lamina I local-circuit neurons of the lumbar spinal dorsal horn of rats (In preparation).

Com excepção do resumo, a restante parte desta dissertação será escrita em inglês.

ABBREVIATIONS

ALT	Anterolateral tract
AMPA	α-amino-3-hydroxy-5-methyl-4-isoxazolepropionate
AMPAR	AMPA receptor
CI-AMPAR	Calcium-impermeable-AMPAR
COLD	Thermoreceptive (neuron)
CP-AMPAR	Calcium-permeable-AMPAR
CV	Conduction velocity
CVLM	Caudal ventrolateral medulla
DRt	Dorsal reticular nucleus
EPSC	Excitatory postsynaptic current
GABA	Gamma-amino butyric acid
HPC	Polimodal nociceptive (neuron)
iGluR	Ionotropic glutamate receptor
IR-LED	Infrared light-emitting diode
LCN	Local-circuit neuron
LPB	Lateral parabrachial nucleus
LSN	Lateral spinal nucleus
MCT	Mixed-collateral type
mGluR	Metabotropic glutamate receptor
NK1r	Neurokinin-1 receptor
NMDA	N-methyl-D-aspartate
NMDAR	NMDA receptor
NRM	Nucleus raphe magnus
NS	Nociceptive-specific (neuron)
PAG	Periaqueductal grey matter
RVM	Rostral ventromedial medulla
SDH	Superficial dorsal horn
SHT	Spinohypothalamic tract
SMT	Spinomesencephalic tract
SRT	Spinoreticular tract
STT	Spinothalamic tract
VCT	Ventral-collateral type

CONTENTS

INTRODUCTION ---------- - 1 -

1. Pain and nociceptive processing ---------- - 2 -

1.1 Transmission of nociceptive signals to the spinal cord ---------- - 2 -

1.2 Spinal ascending pathways ---------- - 3 -

1.3 Descending spinal modulation ---------- - 5 -

2. Spinal lamina I ---------- - 7 -

2.1 Afferent input to lamina I ---------- - 7 -

2.2 Lamina I neurons ---------- - 7 -

2.3 Morphology of lamina I neurons ---------- - 8 -

2.4 Neurochemistry of lamina I neurons ---------- - 9 -

2.5 Functional aspects of lamina I ---------- - 12 -

3. Organization of neuronal network in lamina I remains unknown ------ - 14 -

4. Work objectives ---------- - 16 -

PUBLICATIONS ---------- - 18 -

Publication I ---------- - 20 -

Publication II ---------- - 44 -

Publication III ---------- - 64 -

FINAL REMARKS ---------- - 70 -

1. Local axon collaterals of lamina I projection neurons ---------- - 72 -

2. Organization of synaptic connections in lamina I ---------- - 74 -

3. Morphological description of LCNs ---------- - 76 -

4. Remaining questions and future directions ---------- - 78 -

REFERENCES ---------- - 80 -

ABSTRACT ---------- - 98 -

RESUMO ---------- - 102 -

INTRODUCTION

1. Pain and nociceptive processing

The ability to detect noxious stimuli is essential to an organism's survival and wellbeing (Basbaum *et al.*, 2009). Pain allows the body to recognize factors threatening its integrity and respond with behaviour that will remove the organism from the source of potential injury. According to the International Association for the Study of Pain (IASP), pain is defined as an unpleasant sensory and emotional experience associated with actual or potential tissue damage, or described in terms of such damage. Pain is also considered as a complex phenomenon which has an individual connotation and can be substantially influenced by previous experiences (reviewed by Almeida *et al.*, 2004).

A peripheral nociceptive stimulus triggers a cascade of physiological events that are progressively transmitted to, and processed in, higher nervous centres leading to integration of the information encoding the various facets of pain (reviewed by Millan, 1999; Calvino & Grilo, 2006). An important role in nociception is attributed to the spinal dorsal horn, where internal processing of peripheral input is also subjected to the supraspinal control.

In this introduction, I shall first review the basic steps of pain processing including the activation of nociceptive afferents, signal integration at the spinal and supraspinal levels, and the role of descending modulation. The second part will be focused on the spinal dorsal horn neurons of the most superficial layer (lamina I) describing anatomical and physiological properties of projection neurons which are the major spinal nociceptive output elements.

1.1 Transmission of nociceptive signals to the spinal cord

Nociception begins in the periphery, where stimuli are translated into nerve signals by nociceptors, which are free nerve endings of primary afferents disseminated throughout the skin, muscles, joints and viscera. The peripheral nociceptors can be activated by mechanical, chemical or thermal stimulation as well as by release of inflammatory mediators like bradykinin, prostaglandins, histamine or serotonin (reviewed by Gardner *et al.*, 2000; Calvino & Grilo, 2006).

From peripheral receptors, the information is transmitted to the spinal cord via primary afferents, which are divided, on the basis of their conduction velocity (CV), in three principal groups: Aβ-, Aδ- and C-type afferents. Large-diameter myelinated Aβ-fibres conduct action potentials at highest CV (36-72 m/s). Small-diameter thinly-myelinated Aδ-fibres conduct at lower CV of 4-36 m/s. Thin and unmyelinated C-fibres are conducting at lowest CV (0.4-2.0 m/s). Aβ-fibres innervate peripheral mechanoreceptors and are thought to be involved mainly in proprioception, whereas both Aδ- and C-fibres were found to function as nociceptors or thermoreceptors (LaMotte, 1977; reviewed by Gardner *et al.*, 2000; Todd & Koerber, 2006). Primary afferent neurons are pseudounipolar, with the cell bodies located in the dorsal root ganglia. Aδ- and C-afferents have medium and small-sized somata, respectively. Small neurons can express peptides, for example, substance P (Snider & McMahon, 1998; reviewed by Willis & Coggeshall, 2004).

Sensory fibres enter the spinal cord via the dorsal roots and terminate with a fibre-specific pattern. The unmyelinated C-fibres first enter Lissauer's tract as well as the dorsal columns and the dorsolateral fasciculus and then terminate in the grey matter within one or two segments (LaMotte, 1977; Light & Perl, 1979; Cruz *et al.*, 1987; Todd & Koerber, 2006; Pinto *et al.*, 2010). Aδ- and C-type primary afferents target mostly the superficial dorsal horn (SDH), laminae I-II, but they also send collaterals to deep laminae (V-VII and X) (reviewed by Willis & Coggeshall, 1991; Calvino & Grilo, 2006; D'Mello & Dickenson, 2008). Central terminals of peptidergic C-fibre afferents terminate mainly in lamina I and outer lamina II (Averill *et al.*, 1995; reviewed by Willis & Coggeshall, 2004), while nonpeptidergic C-fibres project deeper to the inner lamina II (reviewed by Willis & Coggeshall, 2004; Basbaum *et al.*, 2009).

Such functional organization indicates that superficial laminae of the dorsal horn are involved in processing of diverse modalities of nociceptive input.

1.2 Spinal ascending pathways

Within the spinal cord, nociceptive signals are processed by complex neuronal networks that involve neurons of the superficial layers. This information is then projected through diverse ascending pathways directly to the brainstem and thalamus, and indirectly, to the cerebral cortex, where the complex pattern of pain

perception is formed. Since organization of ascending pathways varies between mammals, I will focus on major pathways involving lamina I neurons described for our experimental model (rat): the spinothalamic tract (STT), the spinoreticular tract (SRT), the spinomesencephalic tract (SMT) and the spinohypothalamic tract (SHT).

The STT is the most prominent ascending nociceptive pathway in the spinal cord of most mammals and is also referred to as the anterolateral system, although several other pathways (e.g. the SMT and SRT) accompany the STT in the ventrolateral quadrant of the white matter. The STT terminates in three main areas of the lateral thalamus; the ventral posterior lateral nucleus, the intralaminar nuclei and the posterior complex (Willis *et al.*, 1979; reviewed by Willis & Westlund, 1997; Tracey, 2004). Most of the cells project to the contralateral thalamus, although a small fraction projects ipsilaterally (reviewed by Willis & Westlund, 1997). Interestingly, in rats the direct projections to the thalamus are outnumbered by those to other supraspinal sites, like the lateral parabrachial nucleus (LPB) of the brainstem. The STT is formed by axons of nociceptive-specific and wide-dynamic-range neurons in lamina I, laminae V-VII and also lamina X (Kevetter & Willis, 1982, 1983; Harmann *et al.*, 1988; Lima & Coimbra, 1988; Burstein *et al.*, 1990; reviewed by Willis & Coggeshall, 1991; Willis & Westlund, 1997; Basbaum & Jessel, 2000).

Although the majority of axons forming the SRT originate from neurons in laminae V, VII, VIII and X (reviewed by Basbaum & Jessel, 2000; Almeida *et al.*, 2004), there is a separate projection from lamina I and X to the dorsal reticular nucleus (DRt) of the medulla (Bing *et al.*, 1990; Lima, 1990; Lima & Coimbra, 1990; reviewed by Willis *et al.*, 2004). There are three targets of this tract in the brainstem: the precerebellar nucleus in the lateral reticular formation, the medial pontobulbar reticular formation and the DRt (Lima & Coimbra, 1990; reviewed by Tracey, 2004). In contrast to the STT, many of the axons of the SRT do not cross the midline (reviewed by Basbaum & Jessel, 2000).

The SMT seems more suited to contribute to the motivational-affective aspects of pain (Bernard & Besson, 1990; reviewed by Basbaum & Jessel, 2000; Willis *et al.*, 2004), as well as to trigger activity in descending control systems (Willis & Coggeshall, 2004). The location of the neurons that give origin to this tract is overlapping with that of the neurons of the STT: laminae I, II, IV-VII and X (Menetrey *et al.*, 1982; Hylden *et al.*, 1986a; Cliffer *et al.*, 1991; reviewed by Willis & Westlund, 1997; Millan, 1999). In rats, the axons of this pathway originating from

neurons in lamina I and the lateral spinal nucleus (LSN) ascend in the dorsal part of the lateral funiculus rather than in the anterolateral quadrant (McMahon & Wall, 1983, 1985; Swett *et al.*, 1985; reviewed by Basbaum & Jessel, 2000). Supraspinal targets of this tract include the mesencephalic reticular formation, the periaqueductal grey matter (PAG) and the LPB (reviewed by Basbaum & Jessel, 2000).

Neurons giving rise to the SHT are located bilaterally, mostly in the deeper laminae of the dorsal horn, but also in lamina I and the LSN (Burstein *et al.*, 1990; reviewed by Basbaum & Jessel, 2000; Almeida *et al.*, 2004). The SHT ascend directly to the lateral, posterior, and dorsal hypothalamic areas (Cliffer *et al.*, 1991; reviewed by Basbaum & Jessel, 2000; Tracey, 2004), where they synapse with neurons that give rise to the hypothalamospinal tract. This pathway is accompanied by axons that project directly from the spinal cord to several regions of the telencephalon, including the amygdala, septal nuclei, nucleus accumbens, and other limbic system structures (Burstein *et al.*, 1987; Cliffer *et al.*, 1991).

1.3 Descending spinal modulation

Nociceptive processing in the spinal dorsal horn is modulated by a complex neuronal network of several brain areas collectively known as the supraspinal endogenous pain control systems (Melzack & Wall, 1965; reviewed by Tavares & Lima, 2007). According to the type of transmitter released the three major descending modulation systems are classified as noradrenergic, serotonergic and opioidergic. The descending axons terminate diffusely throughout the dorsal horn, and although some form synapses, the majority of their action is mediated through volume transmission (Zoli *et al.*, 1999; reviewed by Todd, 2010). The pain control systems interact with each other and, beside the well-known anti-nociceptive effects, can also trigger the pain facilitation, pronociception (Jones, 1991; reviewed by Tavares & Lima, 2007).

One of the major systems includes PAG and the rostral ventromedial medulla (RVM), PAG-RVM system. Although, some neurons in the PAG project directly to the spinal cord, most of the connections between PAG and the spinal cord are indirect, through the RVM nuclei like the nucleus raphe magnus (NRM) and the nuclei of reticular formation (reviewed by Willis & Westlund, 1997; Gebhart, 2004; Fields *et al.*, 2006). Descending modulation from the PAG-RVM system is mainly

serotonergic (Bowker *et al.*, 1981) with some contribution of GABAergic and/or glycinergic pathways (Antal *et al.*, 1996; reviewed by Millan, 2002).

The PAG also projects to parabrachial areas, including the locus coeruleus and the A5 and A7 groups (Jones, 1991; reviewed by Millan, 2002; Fields *et al.*, 2006). The spinal projections from these parabrachial areas are noradrenergic. The activation of these pathways leads to a release of norepinephrine and inhibition of primary afferent terminals via alpha-2A-adrenoceptors (reviewed by Pertovaara, 2006).

In addition, two areas of the caudal medulla, the DRt and caudal ventrolateral medulla (CVLM) also participate in descending modulation (reviewed by Tavares & Lima, 2002). The DRt is reciprocally connected with the dorsal horn and its stimulation results in pain facilitation (reviewed by Lima & Almeida, 2002).

It is important to note that modulation of nociception occurs at several targets including the primary afferent terminals, projection neurons, excitatory and inhibitory interneurons, and terminals of other descending pathways (reviewed by Willis & Coggeshall, 1991; Millan, 1999, 2002; Fields *et al.*, 2006).

2. Spinal lamina I

Lamina I is the key output layer of the SDH containing several types of projection neurons. They receive nociceptive primary afferent input, integrate it and transmit to higher brain centres. The integration process also includes inputs from the local neuronal networks, propriospinal neurons and descending systems. Despite its obvious importance, the complex neuronal and synaptic organization in lamina I is still poorly understood (reviewed by Willis & Coggeshall, 2004; Todd, 2010).

2.1 Afferent input to lamina I

Lamina I, also known as the marginal zone, is the most superficial dorsal horn layer, located just below the dorsal columns and Lissauer`s tract (Rexed, 1952; reviewed by Todd & Koerber, 2006). Ventrally, it is delimited by the translucent layer of lamina II or substantia gelatinosa. The dark appearance of lamina I is due to the higher percentage of termination of weakly-myelinated Aδ-fibres in comparison with lamina II, where most unmyelinated C-fibres terminate. Individual lamina I neurons can receive monosynaptic inputs from both Aδ- and C-type afferents (Grudt & Perl, 2002; Ikeda *et al.*, 2003; Pinto *et al.*, 2010). Thin afferents entering the spinal cord terminate not only in the segment of root entrance but also one to two segments above and below (Szentagothai, 1964; Cruz *et al.*, 1987). In agreement with this, it has recently been shown that individual lamina I neurons receive and integrate broad intersegmental monosynaptic inputs from Aδ- and C-fibres (Pinto *et al.*, 2010).

2.2 Lamina I neurons

Results from anatomical studies with Golgi technique or intercellular injection methods have shown that most of the neurons in lamina I give rise to axons that arborize in the same segment and generally close to the cell body. These neurons contribute either to local spinal and propriospinal circuits (Bennett *et al.*, 1981; Bice & Beal, 1997b). According to Bice & Beal (1997b), as few as 11% of lamina I cells are true local-circuit neurons, with no axon extending further than one segment away. Over half of lamina I cells are short propriospinal neurons extending

their axons for 2-7 segments. The remaining population included both long propriospinal neurons and projection neurons.

Although lamina I contains the highest density of supraspinally projecting neurons, these make up only 5-10 % of its population (Bice & Beal, 1997b, a; Spike *et al.*, 2003). Axons of lamina I projection neurons typically cross the midline and ascend in the contralateral white matter through the anterolateral tract (ALT) (Ramon y Cajal, 1909; Kuru, 1949; Willis & Coggeshall, 1991). In the rat, many of their supraspinal targets also receive ipsilateral projections from lamina I neurons (Spike *et al.*, 2003). It was also shown that many lamina I neurons can project to more than one brain region (Hylden *et al.*, 1989; Spike *et al.*, 2003; Al-Khater & Todd, 2009; Polgar *et al.*, 2010b).

Early studies in the rat suggested a lack of correlation between cell morphology and functional properties of lamina I cells (Light *et al.*, 1979; Woolf & Fitzgerald, 1983; Steedman *et al.*, 1985; Hylden *et al.*, 1986b; Rethelyi *et al.*, 1989). More recently, however, it has been suggested that the different somatodendritic morphologies of lamina I neurons represent particular patterns of supraspinal connectivity (Lima, 1998) and form distinct functional classes (Han *et al.*, 1998). Several attempts have also been made to correlate basic physiological properties with somatodendritic morphology and/or supraspinal targets (Prescott & De Koninck, 2002; Ruscheweyh *et al.*, 2004).

2.3 Morphology of lamina I neurons

Lamina I neurons vary widely in size and shape. The characteristic feature of this region is the presence of large medio-laterally oriented neurons, known as giant marginal cells of Waldeyer, that contrast with the surrounding tightly-packed smaller neurons (reviewed by Willis & Coggeshall, 2004). With an exception of size, these giant neurons fit into the same morphological categories as other lamina I cells (Molony *et al.*, 1981; Lima & Coimbra, 1983).

The somatodendritic structures of lamina I neurons have been extensively studied (Ramon y Cajal, 1909; Gobel, 1978; Light *et al.*, 1979; Lima & Coimbra, 1986). Their first comprehensive classification was done in the cat spinal trigeminal nucleus by Gobel (1978), who identified pyramidal and multipolar neurons. Later studies done in the rat described four major types of lamina I neurons: fusiform,

multipolar, flattened and pyramidal (Lima & Coimbra, 1983, 1986). Fusiform cells have longitudinal spindle-shaped perikarya with bipolar (less frequently unipolar) dendritic trees rich in pedicled spines. Such neurons were mainly found in the lateral part of lamina I. Multipolar cells have a dense dendritic arbour originating from numerous primary trunks and they predominate in the medial part of lamina I. Flattened aspiny neurons, with a polygonal body flattened in the horizontal plane and a horizontal dendritic arbour, were confined to lamina I predominating in its middle part. Pyramidal neurons have longitudinally elongated perikarya that bulge into the white matter. The arbour has a large longitudinal and mediolateral spread and includes branches which ramify in the white matter (Lima & Coimbra, 1983, 1986). Flattened and pyramidal lamina I neurons, which show the classical mediolateral orientation of the marginal cells described in the older literature, have been suggested to make up the bulk of the projection neurons of lamina I in the rat (Lima & Coimbra, 1986). These two cell types, along with the multipolar (type IIB) neurons, possess the largest cell bodies among the lamina I neuronal population (Lima & Coimbra, 1986).

However, much less is known about the axon trajectories and axon collaterals of projection neurons. Axon collaterals of some lamina I projection neurons have been shown at the supraspinal level (Liu, 1986; Harmann *et al.*, 1988; Hylden *et al.*, 1989; Spike *et al.*, 2003; Al-Khater & Todd, 2009). In addition, local (spinal) axon collaterals were described in some reports; lamina I neurons were shown to issue collaterals in laminae I–IV of the spinal cord in monkey (Beal *et al.*, 1981), cat (Light *et al.*, 1979; Bennett *et al.*, 1981; Hylden *et al.*, 1986b) and rat (Cheunsuang & Morris, 2000; Grudt & Perl, 2002) as well as in the medullary dorsal horn of rats (Li *et al.*, 2000).

2.4 Neurochemistry of lamina I neurons

The neurochemical characteristics of different lamina I neurons and the relationships between morphological classification and transmitter/receptor phenotype have been studied by several groups. In the following part, I will discuss the most relevant transmitters and neuromodulators: glutamate, gamma-amino butyric acid (GABA), glycine and substance P.

- **Glutamate**

Glutamate is the main excitatory neurotransmitter in the spinal cord and is released by primary afferents, excitatory interneurons and some descending axons (Broman, 1994; Todd *et al.*, 2003). It is likely that most dorsal horn neurons that do not use GABA or glycine as their transmitter are glutamatergic (Todd & Spike, 1993; Todd *et al.*, 2003; Todd & Ribeiro-da-Silva, 2005). Glutamate acts on ionotropic glutamate receptors (iGluRs) and metabotropic glutamate receptors (mGluRs), which are widely expressed by spinal neurons (Coggeshall & Carlton, 1997).

The iGluRs can be divided into three classes on the basis of their preference for agonists *N*-methyl-D-aspartate (NMDA), kainic acid or α-amino-3-hydroxy-5-methyl-4-isoxazolepropionate (AMPA). NMDA receptors (NMDARs) comprise a hetero- or homomeric assembly of receptor subunits, NR 1-3. NMDARs are ligand- and voltage- gated, show high permeability to Ca^{2+} and are considered to play an essential role in activity-dependent synaptic plasticity (Katano *et al.*, 2008). In contrast, the AMPA receptors (AMPARs) mediate fast excitatory postsynaptic potentials in spinal neurons (Yoshimura & Jessell, 1990; Yoshimura & Nishi, 1992). AMPARs have a tetrameric structure and are made up from four subunits (GluR1-4, also known as GluR-A-D). AMPARs that lack the GluR2 subunit show significant Ca^{2+}-permeability, while those that possess subunits with long C-terminal tails (GluR1 and GluR4) have been shown to undergo activity-dependent insertion, leading to long-term potentiation (Spike *et al.*, 1998; Polgar *et al.*, 2008). Polgar *et al.* (2008) showed that synapses in laminae I (and also lamina II) contain GluR2 together with GluR1 and/or GluR3, while the long form of GluR4 is restricted to specific neuronal populations, which may include some lamina I projection cells. In spinothalamic neurons, there was also detected the presence of GluR1 and GluR2/3 receptors (Zou *et al.*, 2000). Large lamina I projection cells (that also express the neurokinin-1 receptor; see later) had clusters of synaptic AMPARs that contained the GluR4 subunit, whereas small cells possessed GluR1-containing AMPARs (Polgar *et al.*, 2010a).

The mGluRs couple via G-proteins to the intracellular second messenger cascades (Pin & Duvoisin, 1995). Based on sequence homology, transduction mechanisms, and pharmacological characteristics, the eight mGluR subtypes cloned so far, have been subdivided into three families (Pin & Bockaert, 1995). From these subtypes

high levels of staining for mGlu1, mGlu5 and mGlu7 receptors are found in laminae I and II in rats (Shigemoto *et al.*, 1992; Vidnyanszky *et al.*, 1994; Berthele *et al.*, 1999; Alvarez *et al.*, 2000), with the mGlu5 receptor being predominantly located on the soma and dendrites of dorsal horn neurons (Vidnyanszky *et al.*, 1994; Jia *et al.*, 1999).

- **GABA and glycine**

GABA and glycine are the principal inhibitory neurotransmitters in superficial spinal dorsal horn and they act on $GABA_A$/$GABA_B$/$GABA_C$ and glycine receptors, respectively (Todd & Spike, 1993; Todd *et al.*, 1995; Todd *et al.*, 1996).

Dorsal horn GABAergic neurons are concentrated in the superficial laminae (I-III). Todd & Sullivan (1990) reported that nearly all glycine-immunoreactive cells in lamina I also contain GABA, and although co-localized, they can still mediate distinct synaptic events in the SDH (Todd *et al.*, 1996; Chery & De Koninck, 1999). Polgar *et al.* (2003) also estimated that in lamina I, the proportion of neurons with GABA-immunoreactivity was 23-29 % (present in both cell bodies and axon terminals) and with glycine-immunoreactivy was 9-12 %. GABAergic terminals within lamina I appear to originate mainly from local neurons or other spinal neurons (from deeper layers or other segments) (Todd & Spike, 1993). GABAergic dorsal horn neurons can also express parvalbumin (Antal et al., 1991), met-enkephalin (Todd *et al.*, 1992), and nitric oxide synthase (Valtschanoff *et al.*, 1992).

In lamina I, glycine receptors are located synaptically but $GABA_A$ receptors are located extrasynaptically, suggesting distinct functional properties of inhibition mediated by these two transmitters. As a consequence, the majority of miniature inhibitory postsynaptic currents are glycinergic, and GABAergic component is only seen in large evoked inhibitory postsynaptic currents (Chery & De Koninck, 1999; Keller *et al.*, 2001).

- **Substance P**

Substance P is the most abundant tachykinin peptide present in the mammalian spinal cord. It is released from small diameter primary afferents after noxious stimulation (Littlewood *et al.*, 1995; Lawson *et al.*, 1997; Todd *et al.*, 2000) implying

a significant role of substance P in pain mechanism (Mantyh *et al.*, 1997; reviewed by Hunt & Mantyh, 2001).

Substance P acts mainly on the G-protein-coupled neurokinin-1 receptor (NK1r), which is expressed in the dorsal horn with the highest density in lamina I (Nakaya *et al.*, 1994; Littlewood *et al.*, 1995; Mantyh *et al.*, 1995; Marshall *et al.*, 1996). Activation of NK1r leads to a sustained depolarization of the neuron that is often enough to trigger action potential discharge (King *et al.*, 1997).

There is a considerable heterogeneity in the expression pattern of the NK1r. In the rat, around 45 % of lamina I neurons are NK1r-immunoreactive (Todd *et al.*, 1998). Since only 5–10 % of neurons in lamina I are projecting (Bice & Beal, 1997b, a; Spike *et al.*, 2003), essential part of this immunoreactivity can be attributed to the population of interneurons (Littlewood *et al.*, 1995). It should be noted, however, that the expression level of NK1r, as well as a percentage of immunoreactive cells, is much higher for projection neurons than for interneurons (Todd *et al.*, 2002; Al Ghamdi *et al.*, 2009). NK1r is presented in 80 % of the projection neurons retrogradely labelled from thalamus, PAG, CVLM or LPB (Marshall *et al.*, 1996; Todd *et al.*, 2000; Al-Khater *et al.*, 2008). Besides, the NK1r expressing lamina I neurons project to the brainstem area RVM involved in the descending modulation of spinal cord activity (Khasabov *et al.*, 2002; Suzuki *et al.*, 2002).

2.5 Functional aspects of lamina I

- Intrinsic properties of lamina I neurons

Electrophysiological studies done both *in vivo* and *in vitro* preparations identified types of neurons according to their action potential discharge patterns observed during the depolarizing current injection. The major classes include tonic firing neurons, delayed firing neurons, initial bursting neurons and single spiking neurons (Thomson *et al.*, 1989; Lopez-Garcia & King, 1994; Grudt & Perl, 2002; Prescott & De Koninck, 2002; Ruscheweyh & Sandkuhler, 2002; Graham *et al.*, 2004).

Tonic-firing neurons discharged action potentials during the whole current pulse. Delayed-firing neurons showed a delayed onset of firing in response to current

injections that was due to activation of a transient voltage-dependent K^+ A-type current. Another group of neurons fired a short initial burst of action potentials. Single-spiking neurons discharged only one action potential at the onset of a depolarising pulse. These firing properties are not unique to lamina I as they have been observed in other dorsal horn regions (Hochman *et al.*, 1997; Santos *et al.*, 2007). Two additional firing patterns, the gap and bursting firing pattern, were described in some projection neurons (Ruscheweyh *et al.*, 2004). The majority of spino-parabrachial neurons showed the gap firing patter while the spino–periaqueductal neurons presented the burst firing pattern. This observation implies that that firing properties of lamina I neurons may correlate with their projection target (Ruscheweyh *et al.*, 2004).

- **Lamina I neuron modalities**

Electrophysiological studies in the cat and primate identified three functional classes of lamina I neurons according to their responsiveness to different modalities of peripheral stimulation. Nociceptive-specific (NS) neurons responded only to pinch and/or noxious heat. Innocuous thermoreceptive (COLD) neurons responded only to innocuous cooling and were inhibited by warming, while polimodal nociceptive (HPC) neurons responded to heat and/or pinch and also to cold (Christensen & Perl, 1970; Woolf & Fitzgerald, 1983; Dostrovsky & Craig, 1996). Another study (Han *et al.*, 1998) tried to reveal a certain correlation between the cell morphology and its physiological response. The NS cells were identified as fusiform, COLD cells were morphologically identified as pyramidal and HPC cells had a multipolar shape. However, this correlation has not been confirmed in rodents (Todd *et al.*, 2002; Todd *et al.*, 2005).

- **Synaptic connections of lamina I neurons**

Lamina I neurons form a complex network with other laminae in the dorsal horn, in particular with lamina II. Lamina I neurons were shown to receive local monosynaptic inputs from both excitatory and inhibitory lamina II neurons (Lu & Perl, 2005; Graham *et al.*, 2007; Santos *et al.*, 2007; Kato *et al.*, 2009; Santos *et al.*, 2009). Two types of connections were repeatedly observed and proposed as defining a “circuit” (Lu & Perl, 2005). In lamina II, central neurons excited vertical neurons, and they in turn excited neurons in lamina I, some of which were identified as

putative projection neurons. These two connections (central to vertical and vertical to projection) potentially form a circuit capable of processing mixed primary afferent inputs and subsequently relaying signals out of the SDH through lamina I projection neurons. In addition, lamina I neurons can receive direct monosynaptic mixed input from Aδ- and C-fibres (Pinto *et al.*, 2010). Inputs from both lamina II excitatory interneurons and primary afferents can be sufficiently strong to excite postsynaptic neurons (Santos *et al.*, 2009; Pinto *et al.*, 2010).

Lamina I neurons also have axon collaterals extending to deeper laminae (Lima & Coimbra, 1986), suggesting that they may directly interact with deeper dorsal horn neurons. Indeed, paired extracellular recordings from rat deep dorsal horn cells following the stimulation of neurons in the superficial layers suggested that lamina I neurons had a modulatory effect there (Biella *et al.*, 1997).

3. Organization of neuronal network in lamina I remains unknown

In spite of the substantial progress achieved during the last decades, we still know very little about the detailed organization of the lamina I neuronal network. Experimental techniques used so far did not allow deep insights into the structural and functional organization of neuronal circuits.

The anatomical structure of lamina I neurons was mostly investigated using the Golgi method and the retrograde labelling technique. They allowed to describe the somatodendritic organization of the neurons and to determine the major supraspinal projection areas. However, the techniques available so far could not be used for a systematic labelling of the entire extension of the fine axonal branches of projection and local-circuit neurons. For this reason, the structural organization of local branches of lamina I neurons and their functional intraspinal projections remain a mystery.

The synaptic connectivity in the spinal neuronal circuits is usually studied by simultaneous recording from pairs of monosynaptically connected neurons in the spinal cord slice. However, this technique is hardly applicable to lamina I neurons, most of which have large somata and do not survive the slicing procedure. Moreover, according to the lamina I orientation the most connections between the neurons are expected in sections parallel to the dorsal surface of the spinal cord.

However, such slices cannot be done for the most superficial 20-µm-thick cell layer forming lamina I. Therefore, functional connection between lamina I neurons have not been studied.

During the last years, our laboratory developed several unique methods that enable us to overcome technical obstacles and to study unknown principles of organization of lamina I neuron circuits:

i) We have found that by using an infrared light-emitting-diode (IR-LED) as a source of oblique illumination, it is possible to visualize through the white matter living unstained lamina I neurons in the entire (non-sliced) spinal cord. Experimentation with the entire spinal cord preparation allowed to record from lamina I neurons which preserved all their synaptic contacts (Safronov *et al.*, 2007; Szucs *et al.*, 2009). Moreover, during the patch-clamp recordings, the visually-identified lamina I neurons could be filled with biocytin to achieve a detailed labelling of all axonal branches and dendrites.

ii) We have also established an alternative method of effective and rapid filling of the neurons with biocytin through the cell-attached pipette (Szucs *et al.*, 2009).

iii) We have developed the technique of the fast identification of monosynaptically connected neuron pairs in a tissue with a low percentage of connected neurons (Santos *et al.*, 2007), giving a great advantage for studies in lamina I.

4. Work objectives

The major goal of the experimental work was to study unknown basic principles of the organization of neuronal circuits in spinal lamina I. We focused on the axonal morphology of lamina I neurons and their synaptic interactions. The experiments were performed in the rat, an animal extensively used in electrophysiological studies.

The present dissertation includes three publications arranged chronologically.

Local axon collaterals of lamina I projection neurons in the spinal cord of young rats.

We were interested in studying axonal morphology and branching of lamina I projection neurons. Neurons were visualized in the spinal cord through the intact dorsal white matter by using the oblique IR-LED illumination technique (Szucs *et al.*, 2009). Individual visually identified lamina I neurons were filled in whole-cell mode or cell-attached mode (a modified version of the technique introduced by Pinault, 1996). After the recording session the tissue was fixed and biocytin was revealed by the avidin/peroxidase method. Finally, we performed complete reconstructions of projecting lamina I neurons from serial sections using a Neurolucida system.

Monosynaptic excitatory inputs to spinal lamina I anterolateral-tract-projecting neurons from neighbouring lamina I neurons.

In this second publication we studied the local inputs to projection neurons from other lamina I neurons. We combined single-cell imaging in the isolated spinal cord, paired recordings, 3-D reconstructions of biocytin-labelled neurons and computer simulations to study the monosynaptic input to large ALT-projecting neurons from neighbouring (somata separated by less than 80 µm) large lamina I neurons.

Morphological analysis of lamina I local-circuit neurons of the lumbar spinal dorsal horn of rats (in preparation).

In this last task we characterized non-projecting neurons of lamina I. The electrophysiological and morphological methods used in this study were identical to those utilized in the previous two.

With this set of experiments we intended to provide new important insights into the functional and structural organization of neuronal circuits in the principal spinal nociceptive projecting area (lamina I). This knowledge is currently in acute deficit in the field but is absolutely essential for understanding the processing in spinal nociceptive circuitry.

PUBLICATIONS

Publication I

Local axon collaterals of lamina I projection neurons in the spinal cord of young rats.
Szucs P, Luz LL, Lima D & Safronov BV.
J Comp Neurol 518, 2645-2665, 2010.

RESEARCH ARTICLE

Local Axon Collaterals of Lamina I Projection Neurons in the Spinal Cord of Young Rats

Peter Szucs,[1]* Liliana L. Luz,[1,2] Deolinda Lima,[1,2] and Boris V. Safronov[1,2]

[1]Instituto de Biologia Molecular e Celular (IBMC), Universidade do Porto, 4150-180 Porto, Portugal
[2]Laboratório de Biologia Celular e Molecular, Faculdade de Medicina, Universidade do Porto, 4200-319 Porto, Portugal

ABSTRACT

Large, mediolaterally oriented neurons in lamina I of the spinal cord, frequently referred to as *marginal cells of Waldeyer*, are known to project to supraspinal targets via the anterolateral tract (ALT). Although dendritic organization of lamina I neurons has been extensively studied, little is known about their local axonal morphology and branching. With the help of oblique illumination, we visually identified large lamina I neurons in the isolated lumbar enlargement (L1–L6) of the spinal cord of P14–P20 rats. By using intracellular and cell-attached biocytin injections, we achieved extensive axonal and dendritic labeling in 77 lamina I cells, 40 of which were identified as ALT projection neurons. In the majority of the cases (n = 28), the main axon of these projection neurons gave rise to one or more thin collaterals on the ipsilateral side. Based on their trajectory and location, these collaterals could be divided into three major categories: dorsal, lateral, and ventral. Lamina I projection neurons had dorsal (n = 5), lateral (n = 8), or ventral (n = 6) collaterals only or a combination of these collateral types (n = 9). Our results suggest that lamina I ALT projection neurons can additionally function as local-circuit and propriospinal neurons participating in intra- and intersegmental spinal cord processing. J. Comp. Neurol. 518:2645–2665, 2010.

© 2010 Wiley-Liss, Inc.

INDEXING TERMS: cells of Waldeyer; anterolateral tract; biocytin labeling; oblique illumination; infrared light-emitting diode (IR-LED)

The marginal zone of the dorsal horn, defined by Rexed (1952) as lamina I, is an important relay station in the somatosensory ascending pathway for nociceptive information transmitted via small-diameter unmyelinated and myelinated primary afferent fibers (Bester et al., 2000; Christensen and Perl, 1970; Craig et al., 2001; Light and Perl, 1979; Sugiura et al., 1986; Willis and Coggeshall, 1991). Apart from excitatory and inhibitory intrinsic neurons (Cervero et al., 1979; Dickenson et al., 1997; Hunt et al., 1981), lamina I also contains projection neurons. Some of them project supraspinally through the anterolateral tract (ALT), with axons crossing the midline and ascending in the contralateral white matter (Kuru, 1949; Ramon y Cajal, 1909; Willis and Coggeshall, 1991). In the rat, lamina I projection neurons target the caudal ventrolateral medullary reticular formation (Lima et al., 1991), the nucleus tractus solitarius (Esteves et al., 1993), and the parabrachial nuclei and periaqueductal gray (Lima and Coimbra, 1989), but only a small percentage project to the thalamus (Al-Khater et al., 2008). Many of these supraspinal targets also receive ipsilateral projections from lamina I neurons (Lima, 1998).

Based on their somatodendritic organization, lamina I neurons in the rat have been classified as fusiform (IA and IB), multipolar (IIA and IIB), flattened (III), and pyramidal (IV; Lima and Coimbra, 1986). Because of the difficulty of detecting ventrally oriented dendrites of multipolar neurons in horizontal sections that are commonly used in morphological studies (Spike et al., 2003), flattened cells are not always distinguished from multipolar cells (Zhang et al., 1996). It has been suggested that the different somatodendritic morphologies of lamina I neurons present particular patterns of supraspinal

© 2010 Wiley-Liss, Inc.

The first two authors contributed equally to this work.

Grant sponsor: Portuguese Foundation for Science and Technology, funded by POCTI2010 and FEDER (to B.V.S.).

*CORRESPONDENCE TO: Peter Szucs, Instituto de Biologia Molecular e Celular (IBMC), Universidade do Porto, Rua do Campo Alegre 823, 4150-180 Porto, Portugal. E-mail: szucs@ibmc.up.pt

Received November 5, 2009; Revised March 18, 2010; Accepted March 31, 2010
DOI 10.1002/cne.22391
Published online April 14, 2010 in Wiley InterScience (www.interscience.wiley.com)

connectivity (Lima, 1998) and form distinct functional classes (Han et al., 1998). Several attempts have also been made to correlate basic physiological properties with somatodendritic morphology and/or supraspinal targets (Prescott and De Koninck, 2002; Ruscheweyh et al., 2004). Flattened and pyramidal lamina I neurons, which show the classical mediolateral orientation of the marginal cells described in the older literature, have been suggested to make up the bulk of the projection neurons of lamina I in rat (Lima and Coimbra, 1986). These two cell types, along with the multipolar IIB neurons, possess the largest cell bodies among the lamina I neuronal population.

The role of a neuron in a network is determined by two key factors, input and output, which, from an anatomical point of view, depend on the organization of its dendritic and axonal trees, respectively. The dendritic structure of lamina I neurons has been extensively studied (Light et al., 1979; Lima and Coimbra, 1986; Ramon y Cajal, 1909). However, much less is known about the organization of the axons of local-circuit lamina I neurons and the axon collaterals of projection neurons. Axon collaterals of some lamina I projection neurons have been shown at the supraspinal level (Al-Khater and Todd, 2009) by employing retrograde tracers from more than one supraspinal areas (Harmann et al., 1988; Hylden et al., 1989; Liu, 1986; Spike et al., 2003). In addition, local (spinal) axon collaterals were described in some reports; lamina I neurons were shown to issue collaterals in laminae I–IV of the spinal cord in monkey (Beal et al., 1981), cat (Bennett et al., 1981; Hylden et al., 1986; Light et al., 1979) and rat (Cheunsuang and Morris, 2000; Grudt and Perl, 2002) as well as in the medullary dorsal horn of rats (Li et al., 2000). However, either these neurons were filled in slice preparations, in which neither the collateral nor the main axon could be followed to confirm the trajectories, or the branching patterns of the collaterals were not analyzed. Although authors generally agree that local axon collaterals may have a significant contribution to intraspinal connections, collaterals of lamina I projection neurons have not been described systematically.

This lack of knowledge is due, at least in part, to the technical difficulty associated with blind filling of neurons within the thin superficial layer of the spinal cord or the unavoidable truncation of cell processes in slices. To overcome these obstacles, we used a new imaging technique (Safronov et al., 2007; Szucs et al., 2009) that allowed us to perform visually controlled labeling of selected lamina I neurons in the isolated lumbar enlargement (L1–L6) of rats. We succeeded in performing intracellular and cell-attached labeling, along with complete anatomical reconstruction of the local axonal arbors of lamina I projection neurons. We demonstrate that projection neurons in the lateral aspect of lamina I give rise to various types of ipsilateral local axon collaterals, which may establish diverse intra- and intersegmental connections.

MATERIALS AND METHODS

Preparation

Laboratory Wistar rats (P14–P20) were killed in accordance with the national guidelines (Direcção Geral de Veterinária, Ministério da Agricultura) after anesthesia by intraperitoneal injection of Na^{+}-pentobarbital (30 mg/kg) and subsequent check for lack of pedal withdrawal reflexes. The procedure was approved by the Ethics Committee of the Instituto de Biologia Molecular e Celular (Porto, Portugal). The vertebral column was quickly cut out and immersed in oxygenated artificial cerebrospinal fluid (ACSF) at room temperature. The lumbar enlargement (L1–L6) of the spinal cord was dissected; dorsal roots were cut; and, on one side, the pia mater was locally removed along the lateral part of the dorsal surface to provide access for the pipettes. The ventrolateral surface opposite the cleaned part was glued with cyanoacrylate adhesive to a 0.7-mm-thick golden plate and transferred to the recording chamber (Fig. 1A,B). The metal plate provided mechanical stability for the preparation throughout the recording and/or labeling procedure.

Visualization and identification of lamina I neurons in the intact spinal cord

Neurons were visualized through the intact dorsal white matter by using the oblique infrared light-emitting diode (IR-LED) illumination technique (Szucs et al., 2009). The IR-LED (L850F-02U; Marubeni Japan) was positioned outside the solution meniscus (Fig. 1A). The LED had its emission peak at 850 nm, a narrow beam of $\pm 5^{\circ}$ and maximum radiant intensity of 270 mW/sr. The images were obtained with a digital CCD camera (C4742-95; Hamamatsu Japan).

Neurons were visualized in the most superficial layer of the dorsal gray matter lateral to the dorsal root entry point. The white matter in this region is thin in young animals (Fig. 1B) and has virtually no ascending/descending primary afferent fibers (Pinto et al., 2008; Szucs et al., 2009). The rostrocaudally orientated myelinated fibers in the dorsolateral white matter served as indicators of the lateral edge of the dorsal gray matter (Fig. 1B). The large size and mediolateral orientation of the somatodendritic domain are generally considered as characteristic features of lamina I projection neurons (Kandel et al., 2000). Therefore, to increase the probability of recording from projection neurons, in accordance with the classical (Ramon y Cajal, 1909) and more recent (Lima and

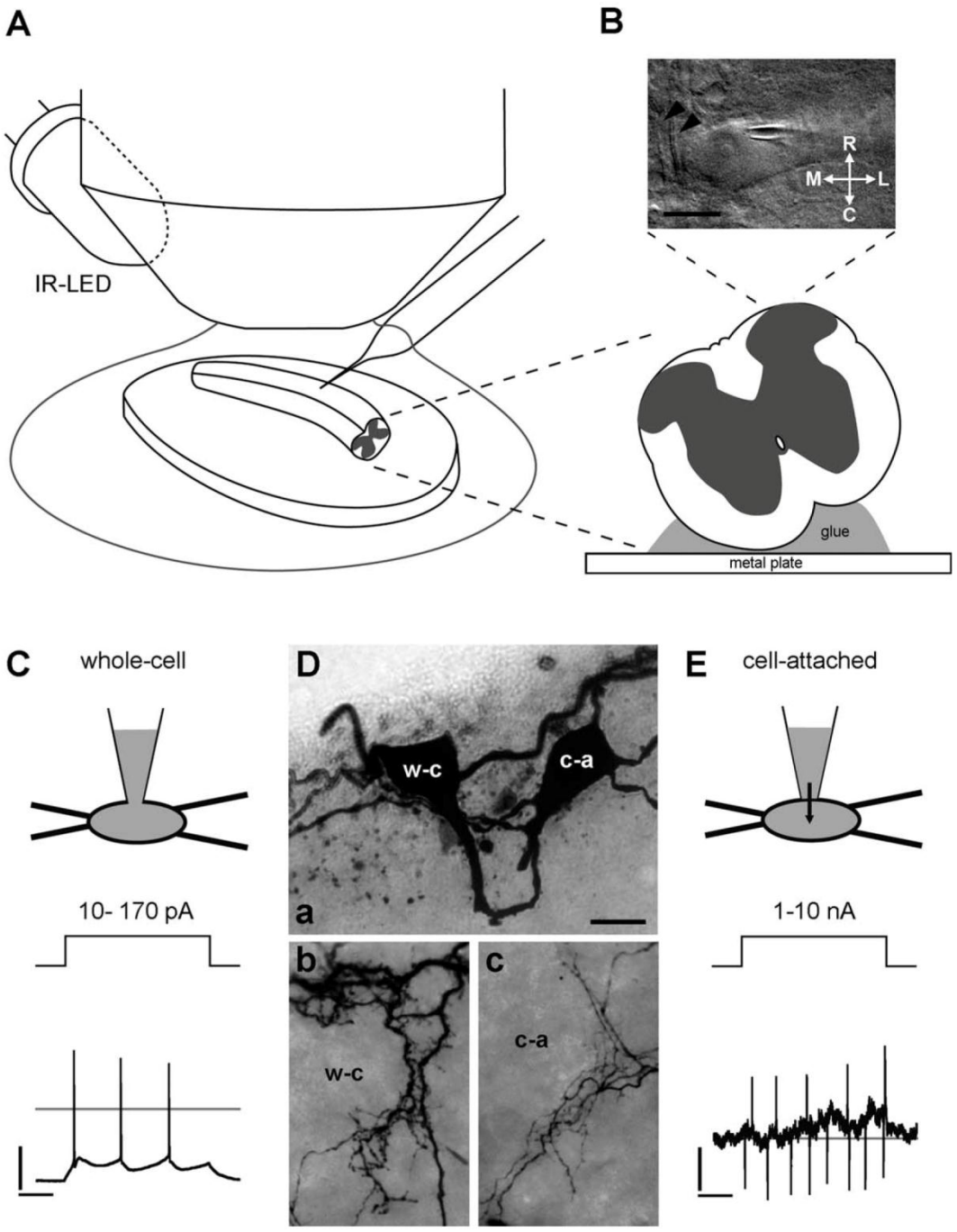


Figure 1. Visualization and labeling of lamina I neurons in the isolated lumbar enlargement. **A:** Outline of the experimental setup. The spinal cord was glued to a metal plate (enlarged drawing at right) to provide mechanical stability throughout the recording/labeling session. The spinal cord preparation was placed under the objective lens (×40) and illuminated with an IR-LED. **B:** Infrared image of a mediolaterally oriented cell body with the tip of the labeling pipette. Arrowheads point to the rostrocaudally oriented fibers in the dorsal funiculus, marking the medial border of the accessible part of the dorsal gray matter. Compass indicates the main directions: R, rostral; C, caudal; M, medial; L, lateral. **C:** Schematic illustration of the whole-cell labeling configuration (top). Middle trace shows the square current pulse with the range of currents applied through the labeling electrode. Bottom trace shows an example of the voltage response recorded in the cell during the labeling procedure. Gray horizontal line indicates 0 mV. **Da:** Photomicrographs of two lamina I projection neurons labeled with whole-cell intracellular (w-c) and cell-attached transmembrane (c-a) methods. **Db,Dc:** Terminal dendritic branches from the corresponding cell shown in Da. **E:** Schematic illustration of the cell-attached filling configuration (top). Middle trace shows the square current pulse applied through the electrode. Bottom trace depicts the voltage readout from the pipette with small extracellular spikes. Gray horizontal line, 0 mV. Scale bars = 20 μm in B,D; 100 msec horizontally in C,E; 40 mV vertically in C; 5 mV vertically in E.

Coimbra, 1986) descriptions, we searched for mediolaterally oriented, large cell bodies with the largest diameter greater than 25 μm (Fig. 1B). The neurons in the dorsal gray matter medial to the dorsal root entry point were not accessible for tight-seal recordings because of the thick dorsal white matter formed by ascending and descending afferent fibers.

Solutions

The ACSF had a composition (in mM): NaCl 115, KCl 3, $CaCl_2$ 2, $MgCl_2$ 1, NaH_2PO_4 1, $NaHCO_3$ 25, and glucose 11 (pH 7.4 when bubbled with 95–5% mixture of O_2–CO_2). The pipette solution for recording and filling neurons in the whole-cell mode contained (in mM): KCl 3, K-gluconate 150, $MgCl_2$ 1, BAPTA 1, HEPES 10 (pH 7.3 adjusted with KOH, final $[K^+]$ was 160 mM) and biocytin (1%). The pipettes used for the cell-attached transmembrane filling contained a solution of 500 mM NaCl and 1.5% biocytin.

Recording and biocytin filling

Recordings were made with an EPC-10 amplifier (Heka, Lambrecht, Germany). The patch pipettes were pulled (MF-830; Narishige) from thick-walled borosilicate glass tubes with 1.5 mm outer diameter and 0.86 mm inner diameter (Biomedical Instruments) and had after fire-polishing a resistance of 3–5 MΩ. Offset potentials were compensated directly before the seal formation. Liquid junction potentials were calculated and corrected for in all experiments.

In whole-cell mode, neurons were filled by passive diffusion of biocytin from the pipette. A current protocol consisting of depolarizing current pulses (500 msec) of increasing amplitude (10–170 pA, 10 pA increment) was repeatedly applied for 10 minutes to facilitate diffusion of biocytin from the recording pipette (Fig. 1C,Da,Db).

As an alternative, a modified version of the technique introduced by Pinault (1996) was applied to label individual visually identified lamina I neurons (Szucs et al., 2009). Fire-polished and filled pipettes had a resistance of ~10 MΩ. After the cell had been touched, a slight suction was applied to the pipette to form a loose seal. Transmembrane entry of biocytin into the cell was facilitated by a stimulation protocol repeatedly applied for 10 minutes. It consisted of depolarizing current pulses (500 msec) of increasing amplitude (1–10 nA, 1 nA increment) applied at 1 Hz. Some neurons started to discharge spikes at a certain level of depolarization that could be judged from the appearance of 1–5-mV extracellular action potentials (Fig. 1Da,Dc,E). In these cases, the amplitude of the current pulse was kept at that level during the whole stimulation period.

The maximum number of neurons filled in the same spinal cord was five. In cases of multiple staining, special care was taken to ensure that neighboring cells had sufficient distance between them, allowing enough separation of their processes to be identified and reconstructed.

Histological processing

Horizontal sections of the spinal cord are commonly used for morphological studies of dendrites of lamina I neurons, because, in the medial aspect of the dorsal horn, these are mainly in the horizontal plane (Spike et al., 2003). However, for three major reasons, we chose to use parasagittal sections. First, the lateral part of lamina I follows the curvature of the dorsal horn surface, and lamina I projection neurons, especially their main axons, have larger projection in the sagittal plane (Fig. 2A). Second, the use of sagittal sections also allows for differentiation between flattened and multipolar cell types based on the presence or absence of ventrally oriented dendrites (Lima and Coimbra, 1986). Third, the precise reconstruction of the main axon descending ventrally is easier in sagittal sections.

After fixation (4% paraformaledhyde; 4°C for at least 12 hours), the spinal cord was embedded in agar with the recorded side facing upward, and serial sagittal 100-μm-thick sections (Fig. 2B) were prepared with a vibrating microtome (Leica VT 1000S). Individual sections were collected serially into phosphate-buffered saline (0.1 M, pH 7.0–7.2) in the wells of a 24-multiwell flat-bottomed plate. To reveal the biocytin, the free-floating sections were permeabilized with 50% ethanol, treated according to the avidin-biotinylated horseradish peroxidase method (ExtrAvidin-peroxidase, diluted 1:1,000), and the histochemical reaction was completed with a diaminobenzidine chromogen reaction. Sections were serially mounted on gelatin-coated glass slides and left to dry for at least 4 hours. After rehydration, sections were counterstained with 1% toluidine blue to help in determining borders of the gray matter and laminae during reconstruction. Finally, sections were dehydrated, cleared, and coverslipped with DPX. All chemicals were purchased from Sigma (St. Louis, MO), with the exception of DPX (Fluka, Buchs, Switzerland).

Measurements and cell reconstruction

Photomicrographs were taken with a Primo Star (Zeiss) microscope equipped with a Guppy (Allied Vision Technologies) digital camera. Contrast and brightness of the images used for the figures were adjusted in Adobe Image Ready software. Perimeter and area of filled neuronal somata were measured using the ImageTool software (University of Texas Health Science Center at San Antonio) by tracing the outline of the cell body with a mouse

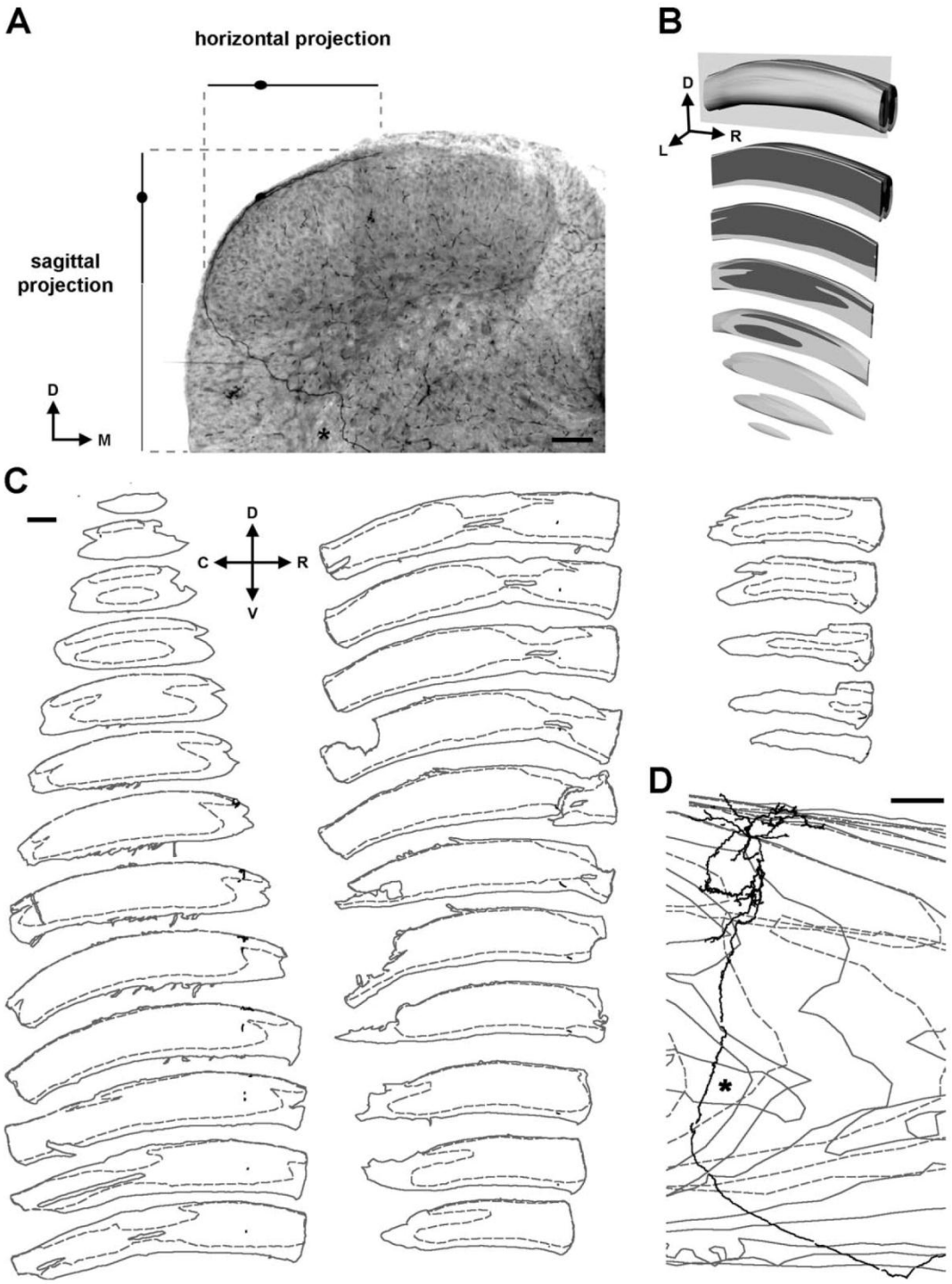


Figure 2. Two-dimensional reconstruction of the labeled neurons. **A:** Horizontal and sagittal projections of a superficial lamina I neuron following the curvature of the gray matter in a photomicrograph of a transverse spinal cord section. A mediolaterally oriented neuron in the lateral part of lamina I appears as vertical in the sagittal plane. The projecting axon is indicated by asterisk. **B:** Characteristic appearance of the spinal gray matter in the sagittal sections. Serial transverse sections from A were used to build a three-dimensional computer model. **C:** Two-dimensional reconstructions of all the serial sections from a lumbar enlargement. First section at top left is from that side of the spinal cord where the labeled neuron was located. Solid gray lines indicate the bottom contour of the section and the central canal; dashed gray lines show the border of the gray matter; solid black lines depict the labeled cell processes. **D:** Image of the reconstructed neuron (cell ID: L130-E1) with a long projection axon (asterisk) from the overlaid and aligned serial sections. R, rostral; C, caudal; D, dorsal; V, ventral; L, lateral; M, medial (throughout the figures). Scale bars = 100 μm in A; 1,000 μm in C; 200 μm in D.

on digital images taken with ×10 objective lens. The angle between the longest diameter of the cell body and the rostrocaudal axis of the spinal cord was also determined on these images. Digital images for the measurements of axonal diameters were taken with a ×100 oil immersion objective lens.

We performed complete reconstructions of 16 ALT-projecting lamina I neurons (in 10 spinal cords) from serial sections as follows: a window of the Neurolucida (MBF Bioscience, workstation version) software was dimmed and superimposed on the live digital image of the section (×40 objective lens) by means of the freeware Transparent Windows 2.2 application. All dendrites, somata, main axons, and axon collaterals as well as contours of the gray and white matter were completely traced into a two-dimensional serial section data file (Fig. 2C). Alignment of the microscope stage during the reconstruction was performed manually. The location of the parts of the axon collaterals and the main axon was determined on reconstructions of individual sections in which borders of the gray and white matter could be well identified (Fig. 2C). Corresponding ends of neuronal processes in the consecutive reconstructed sections have not been connected with Neurolucida, so the neurons did not form a continuous tree. The two-dimensional serial sections were overlaid, aligned with Neuroexplorer (MBF Bioscience) software (Fig. 2D), and exported as bitmap images.

It should be noted that, because of the sagittal plane of the sections, the overlaid two-dimensional image of lateral neurons appear vertical (Fig. 2A,D). Because dendritic arbors of lamina I neurons are mostly parallel with the dorsal horn surface (except for fusiform IB and multipolar IIB neurons; Lima and Coimbra, 1986), mediolaterally spreading dendrites projected in the sagittal plane will show a dorsoventral orientation (Fig. 2A,D). For this reason, mediolateral and dorsoventral spread of the dendritic and axonal arbors cannot be measured reliably on these collapsed two-dimensional reconstructions. Therefore, measurements are given only for the rostrocaudal extent of the cells. Shrinkage during histological preparation was not taken into account.

When neurons were not reconstructed, the course and distribution of axon collaterals was evaluated by checking all serial sections with ×40 (dry) and ×100 (oil immersion) objectives. Values are given as mean ± SEM unless otherwise mentioned.

RESULTS

In total, 77 neurons were recorded and/or filled in the lateral half of lamina I in the isolated lumbar enlargement (L1–L6 segments) of the spinal cord. Most lamina I neurons (n = 67) were filled in the whole-cell mode, whereas the remaining (n = 10) were filled by means of the cell-attached transmembrane labeling technique (Szucs et al., 2009). There was no apparent difference in the extent and quality of the labeling between the two methods (Fig. 1Da, Db vs. Dc). Cells labeled through the cell-attached pipette occasionally had a thin hollow around the cell body. This however, did not effect the identification of the main axon and collaterals.

Among these 77 labeled lamina I neurons, 40 had a prominent main axon going ventrally and medially toward the central canal, crossing the midline in the anterior commissure and entering the anterolateral white matter. These neurons (n = 40) projecting through the ALT (Fig. 3A) form the basis of the present study. The remaining cells were not included for any of the following reasons: main axon ascending in regions other than the ALT, lack of a projection axon (local-circuit neurons, see Fig. 3B), or insufficiently filled or truncated axon.

The mean input resistance and membrane time constant of the ALT projection neurons was 0.6 ± 0.1 GΩ and 89.9 ± 5.7 msec (n = 39), respectively. Analysis of physiological parameters of the neurons was beyond the scope of this study.

Basic morphological parameters regarding segmental location, somata and somatodendritic architecture of the ALT projection neurons are listed in Table 1. Somata of the neurons labeled were distributed along the whole extent of the lumbar enlargement (L1–L6). Mean cross-sectional perimeter and area of the filled somata were 100.4 ± 3.2 μm (range 70–152 μm) and 558.4 ± 27.9 μm^2 (range 284–962 μm^2), respectively. The mean angle between the rostrocaudal axis and that of the longest diameter of the somata (when their cross-sections were not circular) was 66.5° ± 4.5°.

Based on their somatodendritic morphology, labeled neurons were divided into four major types using the criteria introduced by Lima and Coimbra (1986). All 40 ALT projection neurons belonged to three types, flattened (n = 27), pyramidal (n = 6), and fusiform (n = 7). The mean rostrocaudal dendritic spread measured for the reconstructed ALT projection neurons was 505.5 ± 44.9 μm (n = 16, range 134–883 μm). Interestingly, all multipolar (type IIA and IIB) neurons labeled in our study (n = 25) either were local-circuit neurons or projected through pathways other then the ALT. Detailed description of the multipolar neurons will be the subject of another study.

Morphology of the main axon of ALT projection neurons

In the majority of cases (n = 30), the axon was traced continuously from the labeled cell body into the ventral part of the lateral funiculus on the contralateral side

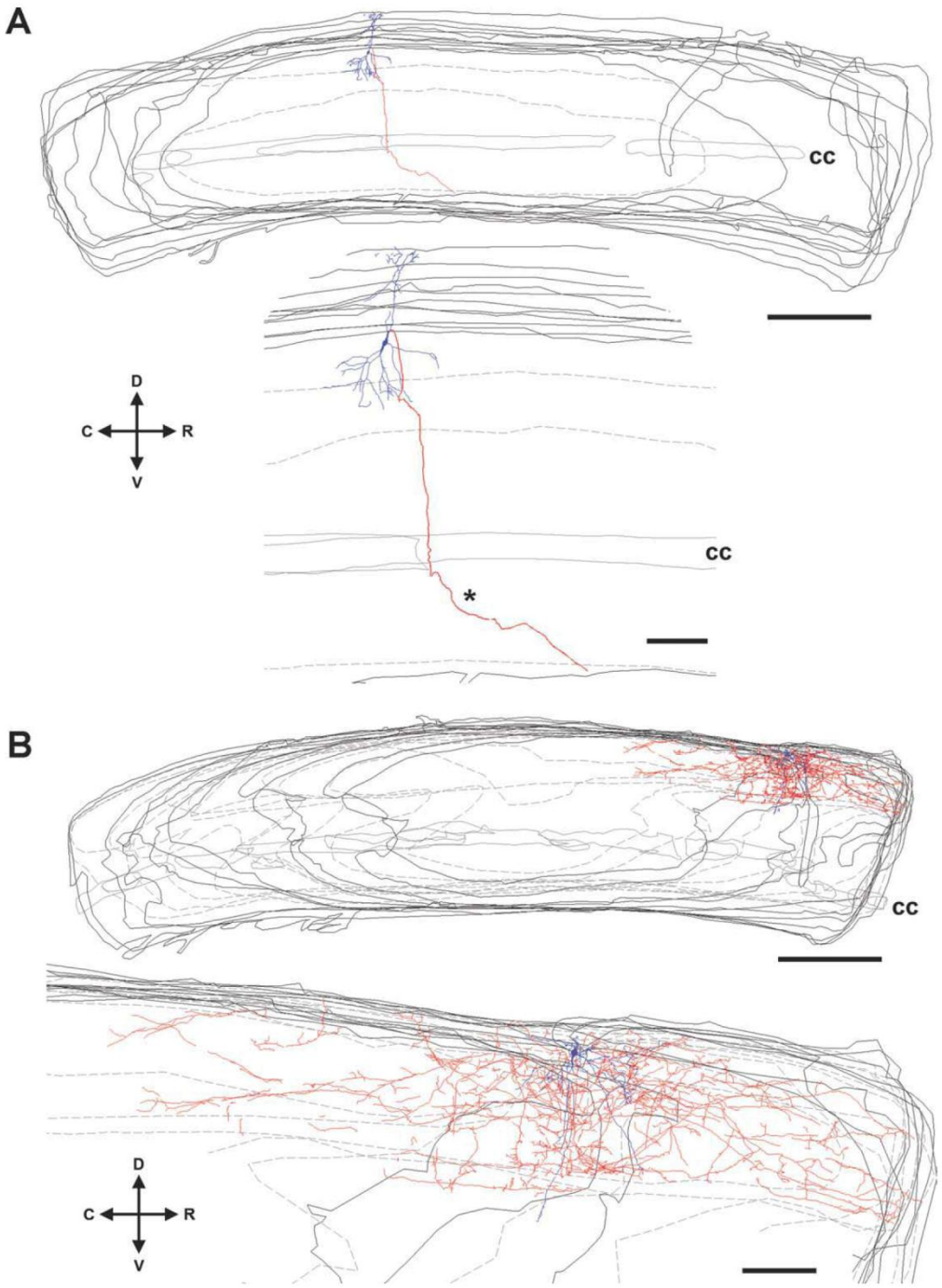


Figure 3. Different appearance of ALT projection neurons and local-circuit neurons. **A:** Mediolaterally oriented lamina I neuron (cell ID: L102-E2) with a single projection axon traversing the spinal cord below the central canal and turning rostrally (top). Bottom: Higher magnification image of the same projection neuron. **B:** Local-circuit neuron in the rostral half of the lumbar enlargement (top) and its higher magnification image (bottom) showing the densely branching axon covering the lateral part of the dorsal horn. Throughout the figures, solid dark gray lines indicate borders of the section; solid light gray lines show the central canal; dashed light gray lines depict the border of the gray matter; neuronal soma and dendrites are blue; axons are red; main (projection) axon is indicated by asterisk; cc, central canal. For clarity reasons, only contours of sections containing the soma and dendrites are superimposed. Scale bars = 1,000 μm in A,B (top); 250 μm in A,B (bottom).

TABLE 1.
Basic Morphological Parameters of ALT Projection Neurons[1]

ID	Lumbar segment	Soma area (μm^2)	Soma angle (degrees)	Type (somatodendritic)
L051-E1	L1	313.86	25	Flattened
L088-E5	L5	409.91	79	Flattened
L102-E2[2]	L4	444.64	75	Flattened
L108-E2[2]	L1	414.25	60	Flattened
L110-E2	L3	815.08	90	Fusiform
L110-E3	L5	680.46	90	Pyramidal
L113-E4	L5	410.4	80	Flattened
L137-E1[2]	L1	519.87	90	Flattened
L140-E3	L5	711.8	90	Fusiform
L142-E1	L1	420.52	n.a.	Flattened
L146-E1	L3	309.13	n.a.	Flattened
L309-E1	L1	538.19	85	Flattened
L039-E1[2]	L2	462.16	90	Flattened
L252-E2	L2	579.67	12	Flattened
L256-E4[2]	L3	863.23	85	Flattened
L259-E4	L4	898.92	90	Flattened
L290-E1	L2	464.89	10	Flattened
L091-E1[2]	L1	503.85	85	Pyramidal
L091-E1pre[2]	L1	585.21	22	Pyramidal
L126-E1	L2	395.5	75	Flattened
L137-E2[2]	L2	557.97	55	Flattened
L137-E3[2]	L2	350	50	Fusiform
L153-E3	L3	749.42	60	Flattened
L274-E1	L1	457.18	90	Fusiform
L280-E1	L2	660.69	60	Pyramidal
L083-E1[2]	L4	283.56	75	Fusiform
L083-E2[2]	L4	419.56	80	Flattened
L117-E2[2]	L5	706.02	55	Flattened
L130-E1[2]	L2	449.46	70	Pyramidal
L144-E4	L5	592.69	80	Pyramidal
L153-E1	L4	491.42	5	Fusiform
L134-E4-3	L4	508.78	88	Flattened
L256-E3[2]	L2	819.35	90	Flattened
L309-E3	L1	962.09	80	Flattened
L060-E5	L5	621.42	n.a.	Flattened
L256-E2[2]	L2	313.95	n.a.	Flattened
L263-E3	L4	677.56	n.a.	Flattened
L273-E3[2]	L6	645.74	80	Flattened
L292-E4	L3	786.55	60	Flattened
L309-E2	L1	541.57	15	Fusiform

[1]Segmental location, cross-sectional soma area, soma angle and somatodendritic type of 40 labeled neurons. Soma angle refers to the angle between the axis of the longest soma diameter and the rostrocaudal axis. Somatodendritic type was determined using the criteria of Lima and Coimbra (1986). ID, cell identification code; n.a., not applicable, in the case of a neuron with a round soma.
[2]Neuron reconstructed.

(Table 2, WM). These axons all crossed the midline in the anterior commissure. In the remaining neurons (n = 10), the axon could be traced until the central canal, where it gradually became fainter (Table 2, CC). These neurons were also considered as ALT projecting, because the initial course and appearance (constant diameter with occasional elongated bead-like structures) of their main axon were identical to those of the other 30 neurons.

The main axon originated directly from the cell body only in 11 cases (Fig. 4A). In 29 neurons, however, the projecting axon branched from a stem dendrite (Fig. 4B). This branching point was frequently located after one or two dendritic branches (Fig. 4C). In cases of dendritic origin, the mean distance from the soma to the beginning of the axon was 26.9 ± 2.8 μm (n = 29).

The course of the main axon was directly ventromedial in 30 cases. However, in 10 neurons, the axon first formed a dorsomedial loop of variable length (Fig. 4D,E), with the dorsal turning point occasionally giving rise to axon collaterals (see Fig. 5A). After the turning point, the axon descended laterally, followed the surface of the dorsal gray matter until its edge and then took a ventromedial course toward the central canal (Fig. 4G) and contralateral white matter.

The main axon of all labeled neurons presented elongated enlargements resembling nodes of Ranvier (Morgan, 2001; Fig. 4E,F). The undulating appearance of the axons (and dendrites) most likely is due to shrinkage that occurred during the histological processing. This technical artifact, however, could not account for sharp turns of the axons observed in our sections (Fig. 4F).

Ipsilateral spinal axon collaterals of ALT projection neurons

The main axon of 28 ALT projection neurons gave rise to one or more thin axon collaterals on the ipsilateral side. The total number of ipsilateral collaterals observed in these 28 neurons was 54. The collaterals of each ALT projection neuron are described in Table 2. The mean diameter of the collaterals (measured within the first 50 μm from the branching point) was 0.21 ± 0.02 μm (n = 10), being approximately one-fourth the mean diameter of the main axon (0.79 ± 0.03 μm; n = 10). Collaterals had numerous en passant varicosities and terminal boutons typical for unmyelinated axons (see Fig. 6A, inset 2). Some varicosities appeared as slight thickenings of the axon, whereas others had diameters of 0.8–1.0 μm. Varicosities were frequently found accumulated along a short piece of the axon.

Based on their trajectory and location, collaterals could be divided into three major categories: dorsal, lateral, and ventral. The lateral type had two subtypes, lateral-rostral and lateral-caudal. From this point onward, ALT projection neurons issuing only one type of collateral are termed as dorsal, lateral, or ventral-collateral type (DCT, LCT, and VCT), respectively. Neurons giving rise to more than one type of collateral are referred to as mixed-collateral type (MCT) ALT projection neurons.

TABLE 2.

Morphological Description of the Main Axon and Ispilateral Collaterals of ALT Projection Neurons[1]

	Main axon					Collaterals				
	Extent/course			Origin						
ID	WM	CC	Loop	Soma	Dendrite	LR	LC	V	D	Type (axon collateral)
L051-E1		+		+						NC
L088-E5	+				+					NC
L102-E2[2]	+				+					NC
L108-E2[2]		+			+					NC
L110-E2	+				+					NC
L110-E3	+		+	+						NC
L113-E4		+	+		+					NC
L137-E1[2]	+				+					NC
L140-E3	+				+					NC
L142-E1	+				+					NC
L146-E1		+	+	+						NC
L309-E1	+				+					NC
L039-E1[2]	+		+		+				1	DCT-I
L252-E2		+	+		+				1	DCT-I
L256-E4[2]		+			+				1	DCT-II
L259-E4		+			+				1	DCT-II
L290-E1	+				+				1	DCT-II
L091-E1[2]	+				+	1				LCT
L091-E1pre[2]	+				+	1				LCT
L126-E1	+				+	1				LCT
L137-E2[2]	+				+	1				LCT
L137-E3[2]	+			+		2				LCT
L153-E3	+		+	+		1				LCT
L274-E1	+				+	1				LCT
L280-E1	+		+	+		1				LCT
L083-E1[2]		+			+			1		VCT
L083-E2[2]	+			+				1		VCT
L117-E2[2]		+			+			4		VCT
L130-E1[2]	+				+			1		VCT
L144-E4	+			+				1		VCT
L153-E1	+			+				2		VCT
L134-E4-3		+			+	1	1			MCT
L256-E3[2]	+				+	1			1	MCT
L309-E3	+		+		+			1	1	MCT
L060-E5	+		+		+		2	1	1	MCT
L256-E2[2]	+				+	2		2	1	MCT
L263-E3	+			+		1		1	1	MCT
L273-E3[2]	+			+		1	1		1	MCT
L292-E4	+				+	1	1	1	1	MCT
L309-E2	+		+		+	1	1	1	2	MCT

[1]Parameters of the main axon and collaterals of lamina I projection neurons. Collaterals, the number of collaterals of each type originating from the main axon. ID, cell identification code; WM, main axon in contralateral white matter; CC, main axon traced until central canal; LR, lateral-rostral; LC, lateral-caudal; V, ventral; D, dorsal; NC, no collateral; DCT, dorsal collateral type; LCT, lateral collateral type; VCT, ventral collateral type; MCT, mixed collateral type.
[2]Neuron reconstructed.

Dorsal collaterals and DCT projection neurons

Dorsal collaterals were branching within the dorsal gray matter (laminae I–IV), occasionally entering the Lissauer tract in the overlying white matter. The collaterals had numerous varicosities. Five ALT projection neurons had only this type of collateral. The origination point of the collaterals varied along the main axon. Two typical cases (DCT-I subtype, n = 2; and DCT-II subtype, n = 3) are shown in Figure 5.

The dorsal collateral of the DCT-I cell originated at the turning point of the dorsomedial loop of the main axon (Fig. 5A). This collateral divided further, and branches were distributed in the most superficial layers of the dorsal gray matter. The collateral became faint and could not be followed beyond the segment where the neuron was located (rostrocaudal extent of the collateral 333 μm). The main axon of this cell could be followed in the contralateral white matter into the next rostral segment. This DCT-I cell in the spinal segment L2 was a flattened

neuron with a mediolaterally oriented soma and extensive dendritic tree (rostrocaudal span 883 μm) presenting long spines (Fig. 5A, inset 2).

In DCT-II neurons (Fig. 5B), the dorsal collateral emerged from the main axon in a recurrent manner at the level of the notch between the dorsal and ventral horns. The collateral ascended dorsally, where it gave numerous side branches. The branches presented a large number of varicosities, presumably forming synaptic contacts with the neurons in the region. The rostrocaudal spread of the collateral was 395 μm. The main axon followed a contorted course and had numerous elongated swellings. Both the soma and the dendritic tree of this neuron had clear mediolateral orientation. The dendritic spread along the rostrocaudal axis was small, 417 μm. According to their somatodendritic architecture, all five DCT ALT projection cells were flattened neurons.

Lateral collaterals and LCT projection neurons

Lateral collaterals originated at the lateral edge of the dorsal horn, from the part of the main axon that traversed through the lateral white matter. These long thin collaterals (single in Fig. 6A or multiple in Fig. 6B) ran parallel with the lateral edge of the dorsal gray matter rostrally, or caudally (not shown in Fig. 6), with no or only a few (one or two) visible branches along their course. The main part of the collateral mostly avoided the gray matter, staying inside the part of the dorsolateral funiculus (DLF) that is considered to be part of the Lissauer tract (Grudt and Perl, 2002). Occasionally, perpendicular side branches with either terminal boutons or high number of varicosities could be observed (see Fig. 8). These varicosities in some cases formed close appositions with counterstained somata of lateral spinal nucleus (LSN) cells and with dorsal horn neurons upon entering the dorsal gray matter (not shown). The longest reconstructed lateral-rostral collateral was greater than 3,000 μm and extended as far as two segments from the location of the cell body.

Eight ALT projection neurons fell into the LCT category. It is important to note that all LCT projection neurons gave rise to lateral-rostral collaterals only. In some cases, lateral collaterals divided into parallel branches and ran together along the same path (not shown). The mean

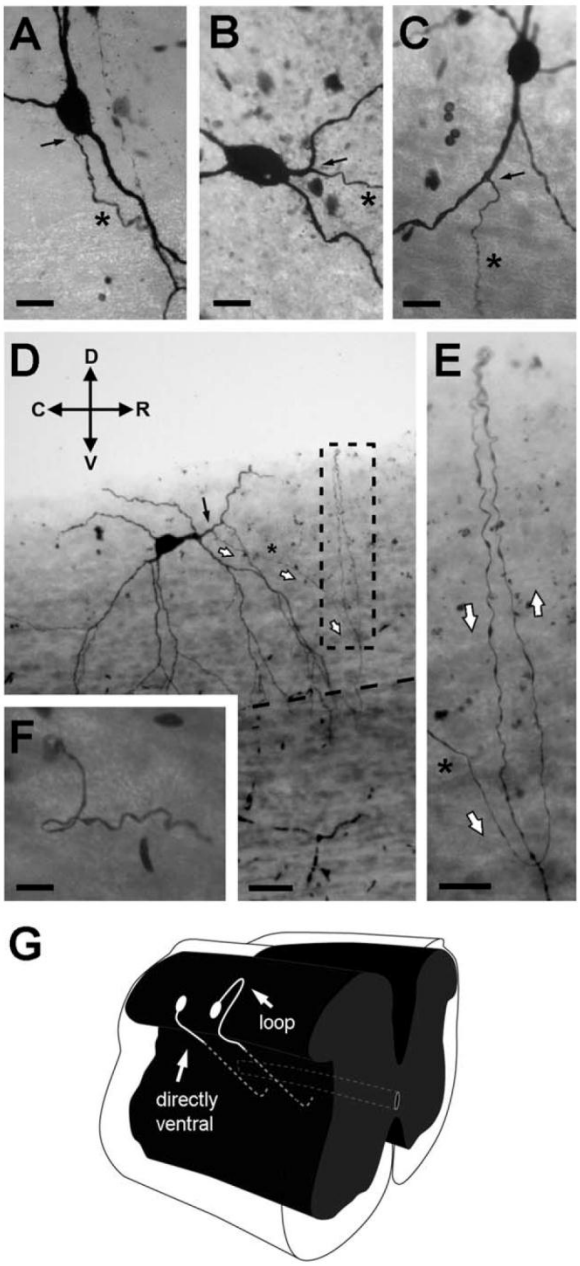


Figure 4. Morphological features of the main axons of ALT projection neurons. **A:** Projection axon originating from the soma of a flattened ALT projection neuron. **B,C:** Projection neurons with axons originating from primary dendrites. Arrows point on the axon origin. **D:** Low-magnification image of a cell (cell ID: L252-E2) with its main axon forming a long dorsomedial loop. The axon originates from a primary dendrite (black arrow), and, after a short lateral course along the surface, it turns in the dorsomedial direction traveling for approximately 80 μm, where it takes a sharp U-turn to run laterally again before starting its ventral descent. Dashed line indicates the edge of the section at its top surface. **E:** Higher magnification image of the dorsomedial axon loop shown in the dashed box in D. Note the undulated appearance of the axon and the numerous elongated swellings. White arrows indicate the direction of the axon. **F:** A short loop formed by a projection axon close to the central canal (another neuron). **G:** Schematic drawing representing the two principal courses of projection axons. Scale bars = 20 μm in A–C; 50 μm in D; 20 μm in E; 10 μm in F.

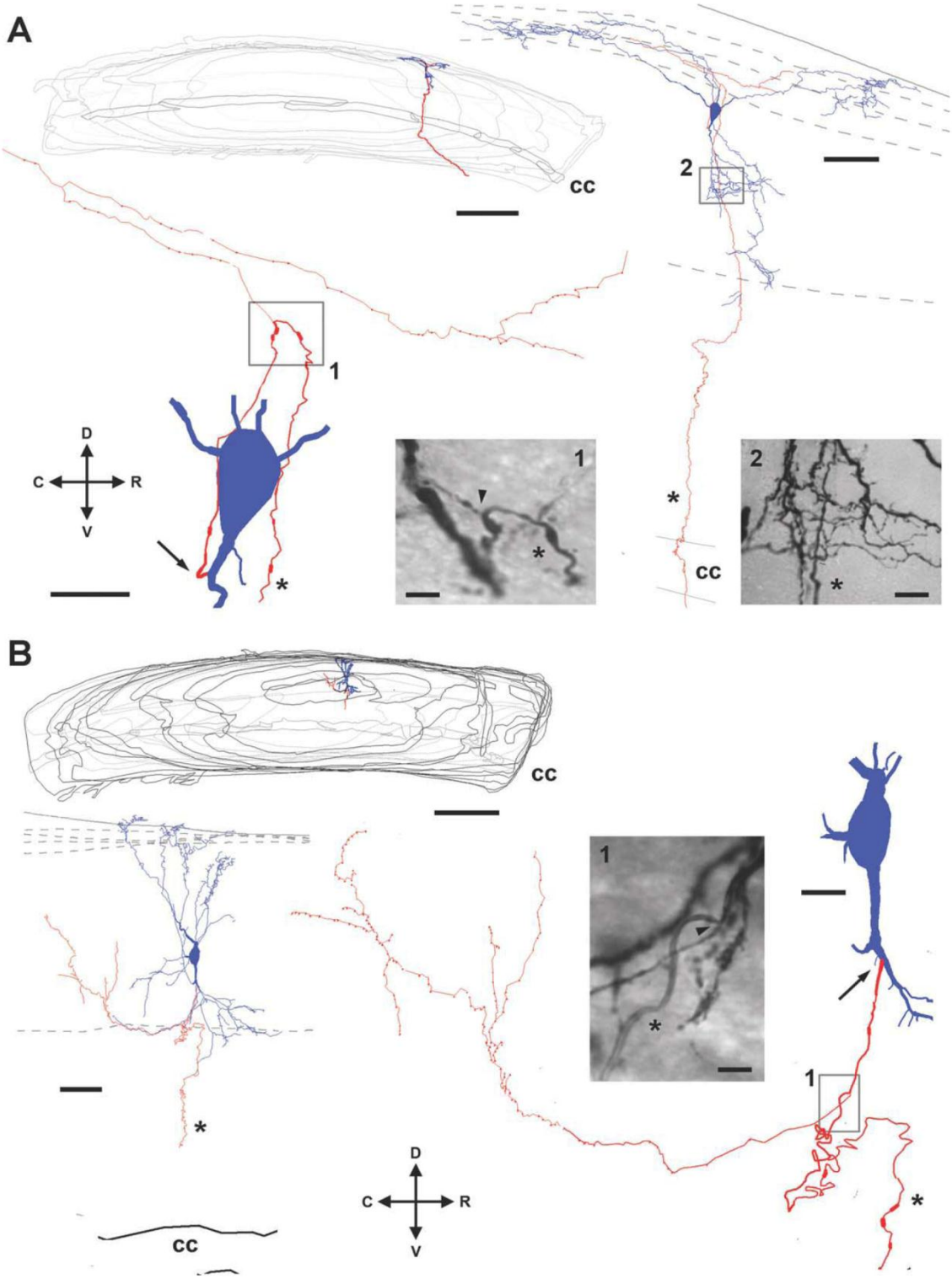


Figure 5. Dorsal collaterals and DCT projection neurons. **A:** Mediolaterally oriented DCT-I neuron (cell ID: L039-E1) with a collateral originating from the top of the dorsomedial loop (inset 1, arrowhead) formed by the main axon originating from a dendrite (arrow). Note the numerous elongated spines on the dendrites surrounding the descending main axon (inset 2). **B:** Example of a DCT-II neuron (cell ID: L256-E4). The collateral, with branches in the dorsal horn, originates in a recurrent manner from the main axon (inset 1, arrowhead) close to its origin from a primary dendrite (arrow). The main axon could not be traced in the contralateral side in this case. Scale bars (left to right) = 25 μm, 1,000 μm, 100 μm in A; 100 μm, 1,000 μm, 25 μm in B; 5 μm in photomicrographs.

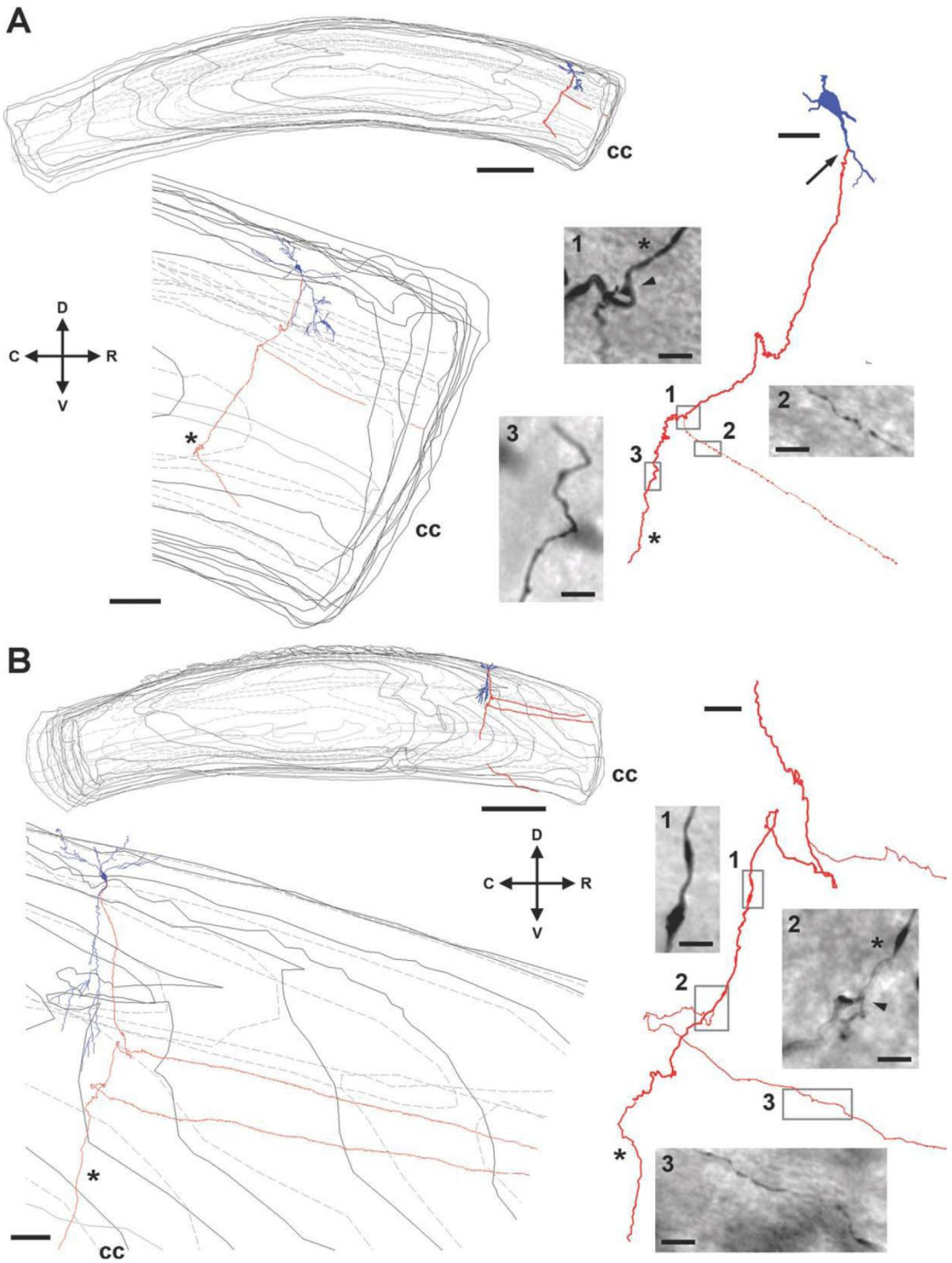


Figure 6. Lateral collaterals and LCT projection neurons. Projection neurons with single (A; cell ID: L091-E1) and multiple (B; cell ID: L137-E3) collaterals. Both neurons are located in the rostral end of the lumbar enlargement. Collaterals follow the edge of the dorsal gray matter, indicated by the dashed gray lines. Insets show high-magnification images of the corresponding areas on the reconstructions. Note the caliber difference between the main axon and the collaterals (presenting frequent varicosities). Arrow in A, origin of the main axon on the dendrite; asterisk, main axon; arrowhead, beginning of the collateral. Scale bars (left to right) = 250 μm, 1,000 μm, 50 μm in A; 100 μm, 1,000 μm, 20 μm in B; 5 μm in photomicrographs.

rostrocaudal spread of axon collaterals for LCT projection neurons was 972.7 ± 238.3 μm (n = 4; reconstructed neurons). It has to be noted, however, that all eight LCT projection neurons were located in the rostral half of the lumbar enlargement (L1–L3), and their rostrally proceeding axon collaterals reached the cut end of the preparation. For this reason, the reported length of the lateral-rostral collaterals should be considered as an underestimate. Based on the somatodendritic classification, LCT projection cells were flattened (n = 3), pyramidal (n = 3), and fusiform (n = 2) neurons.

Ventral collaterals and VCT projection neurons

Ventral collaterals branched from the main axon, mostly below the point of its reentry into the gray matter after the short traversing path in the DLF (Fig. 7). These collaterals usually had few (up to five) visible branches, which often followed the course of the main axon, while staying in its vicinity, and frequently reached laminae V–VII. All ventral collaterals stayed in the ipsilateral ventral horn and presented numerous en passant varicosities along their course inside the ventral gray (Fig. 7, inset 2).

Six ALT projection neurons were of the VCT category. The mean rostrocaudal spread of their collaterals was 190 ± 95.6 μm (n = 4; reconstructed neurons). The most ventral collaterals seen in a VCT ALT projection neuron was four. None of the main axons of the VCT projection neurons (n = 6) had a dorsomedial loop. According to their somatodendritic architecture, the VCT projection neurons were classified as flattened (n = 2), pyramidal (n = 2), and fusiform (n = 2).

MCT projection neurons

Nine lamina I ALT projection neurons had more than one type of ipsilateral axon collaterals. The most collaterals originating from the same main axon was five. Lateral-caudal collaterals were present only in this group. The main axon of MCT cells frequently took sharp turns (Fig. 8) along its path toward the contralateral white matter. The collaterals branched off from various parts of the contorted axon (Fig. 8, insets 2–4) and usually covered a substantial part of the gray matter surrounding the MCT projection neuron. A typical MCT neuron occupying the caudal half of the lumbar enlargement is shown in Figure 8. This neuron had extensive dorsal collaterals and lateral collaterals branching further and running in parallel. Branches of the lateral collateral had shorter and longer side branches. One of these side branches was a terminal branch, with frequent en passant varicosities and terminal boutons, forming close appositions with a group of cell bodies, most likely in the LSN (Fig. 8, inset 1). The overall rostrocaudal extent of the axon collaterals of this MCT projection neuron (3,875 μm) was the largest among the reconstructed cells. The mean rostrocaudal spread of the axon collaterals of MCT neurons was 2,624.7 ± 788.9 μm (n = 3; reconstructed neurons). With the exception of one fusiform neuron, all the MCT cells were of the flattened type.

Laminar location of the major collateral types in the transverse plane

To confirm the trajectory and laminar location of the major collateral types (dorsal, lateral, and ventral), we additionally labeled two ALT projection neurons and reconstructed them from serial transverse sections (Fig. 9). As expected, dorsal collaterals of an MCT projection neuron occupied mostly dorsal laminae I–IV (Fig. 9A), whereas lateral collaterals of the same neuron targeted the dorsal part of the lateral funiculus (Fig. 9B). The single ventral collateral of a VCT projection neuron stayed below the lower border of lamina IV (Fig. 9C). These neurons were excluded from the analysis presented above because of the different sectioning plane.

DISCUSSION

The oblique IR-LED illumination technique allowed us to perform intracellular and cell-attached transmembrane labeling of lamina I projection neurons. The isolated, but otherwise intact, lumbar enlargement allowed complete anatomical reconstruction of labeled cell processes. We have shown that the majority of lamina I ALT projection neurons in the lateral aspect of the dorsal horn give rise to distinct types of ipsilateral axon collaterals, which can serve as basis for cell classification. Certain cells possess single or multiple collaterals of one type, but others have a mixture of collateral types. We have also shown that the main axon of ALT projection neurons in the lateral half of lamina I frequently originates from primary dendrites.

Technical considerations

Our sample consists of neurons from young animals (P14–P20) in which visually controlled recording combined with extensive labeling of surface cells in the entire lumbar enlargement has a high success rate (Szucs et al., 2009). Therefore, one cannot exclude that the described collaterals may change or disappear at later stages of postnatal development. This, however, seems unlikely, in that the presence of axon collaterals of lamina I projection neurons was also reported in adult animals (Hylden et al., 1986). The sample is also biased because medium-sized neurons were not studied, and neurons in the medial part of lamina I close to the dorsal root entry zone were not accessible. Thus, we cannot exclude that

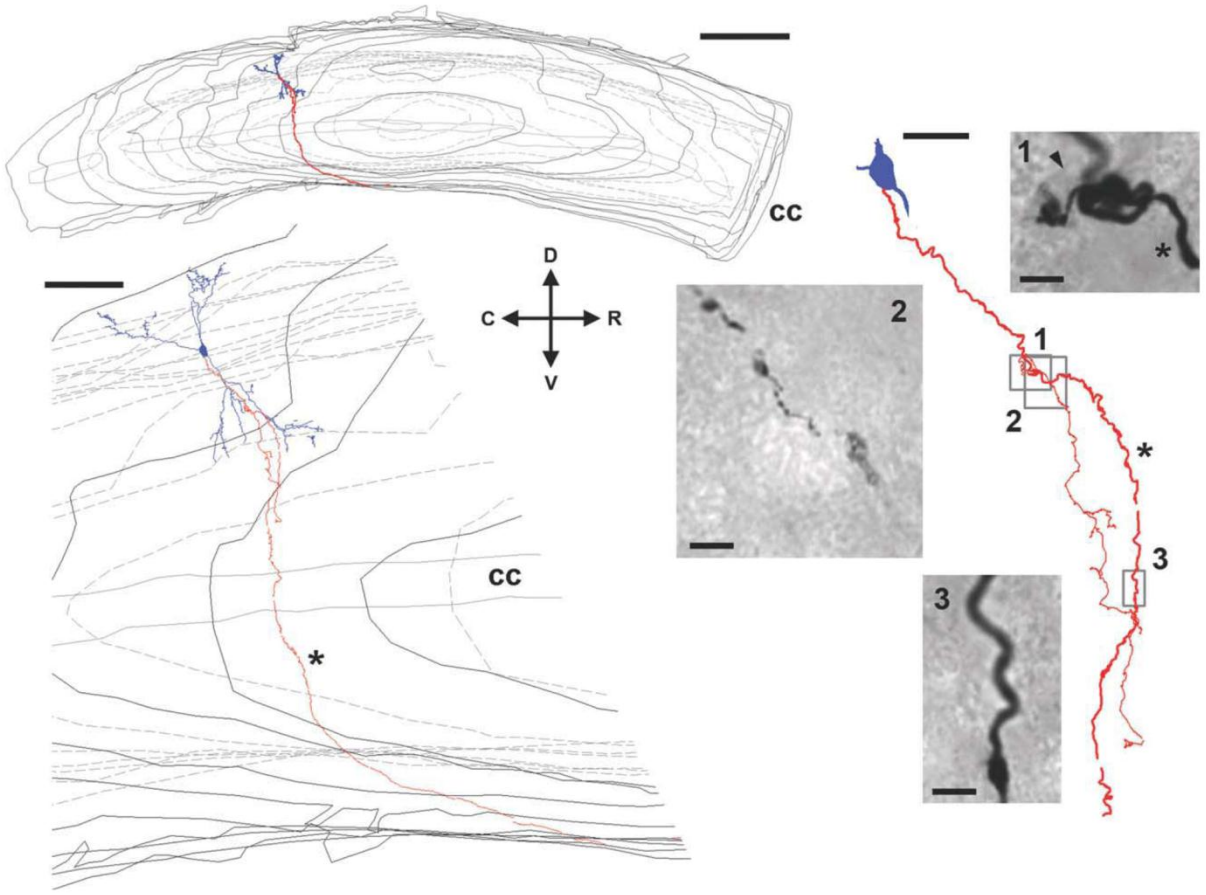


Figure 7. Example of the ventral collateral of a VCT projection neuron. A neuron (cell ID: L083-E2) with a single ventral collateral descending into lamina VII, reaching almost the level of the central canal. Insets show high-magnification images of the corresponding areas on the reconstruction. Scale bars (left to right) = 200 μm, 1,000 μm, 50 μm; 5 μm in photomicrographs.

medium-sized or medially located projection neurons may have different types of collaterals. It should be also noted that our two-dimensional reconstruction approach introduced some distortions and, therefore, did not allow precise measurements of distances along certain axes. These drawbacks, however, did not affect the detection of the collaterals or the classification of the neurons based on the collateral types.

Identity of the neurons: marginal cells of Waldeyer

Although most lamina I neurons are rostrocaudally oriented and medium-sized (compared with small lamina II neurons), several studies have reported the presence of larger neurons with dendrites elongated along the mediolateral axis (Han et al., 1998; Lima and Coimbra, 1983, 1986; Ramon y Cajal, 1909). These cells are generally referred to as *marginal cells of Waldeyer* (Willis and Coggeshall, 1991). Lima and Coimbra (1986) reported that pyramidal and flattened type lamina I neurons show the classical mediolateral orientation of the marginal cells described in the older literature and, probably, make up the bulk of the lamina I projection neurons in rat. These two types, along with the multipolar IIB neurons, also possess the largest cell bodies among the lamina I neuronal population. Indeed, by targeting lamina I neurons with the longest cell body diameter above 25 μm, the majority of our ALT projection neurons proved to be flattened and pyramidal cells. Thus, soma size and the typical orientation of the somatodendritic domain suggest that the majority of our ALT projection neurons were marginal cells of Waldeyer.

It has to be noted that the use of our selection criteria also resulted in filling multipolar neurons (n = 25, mostly type IIB). However, none of these neurons had a projection axon in the contralateral white matter. They either were local-circuit neurons or projected through pathways other then the ALT. This is in line with earlier observations that multipolar neurons make up the bulk of lamina I cells

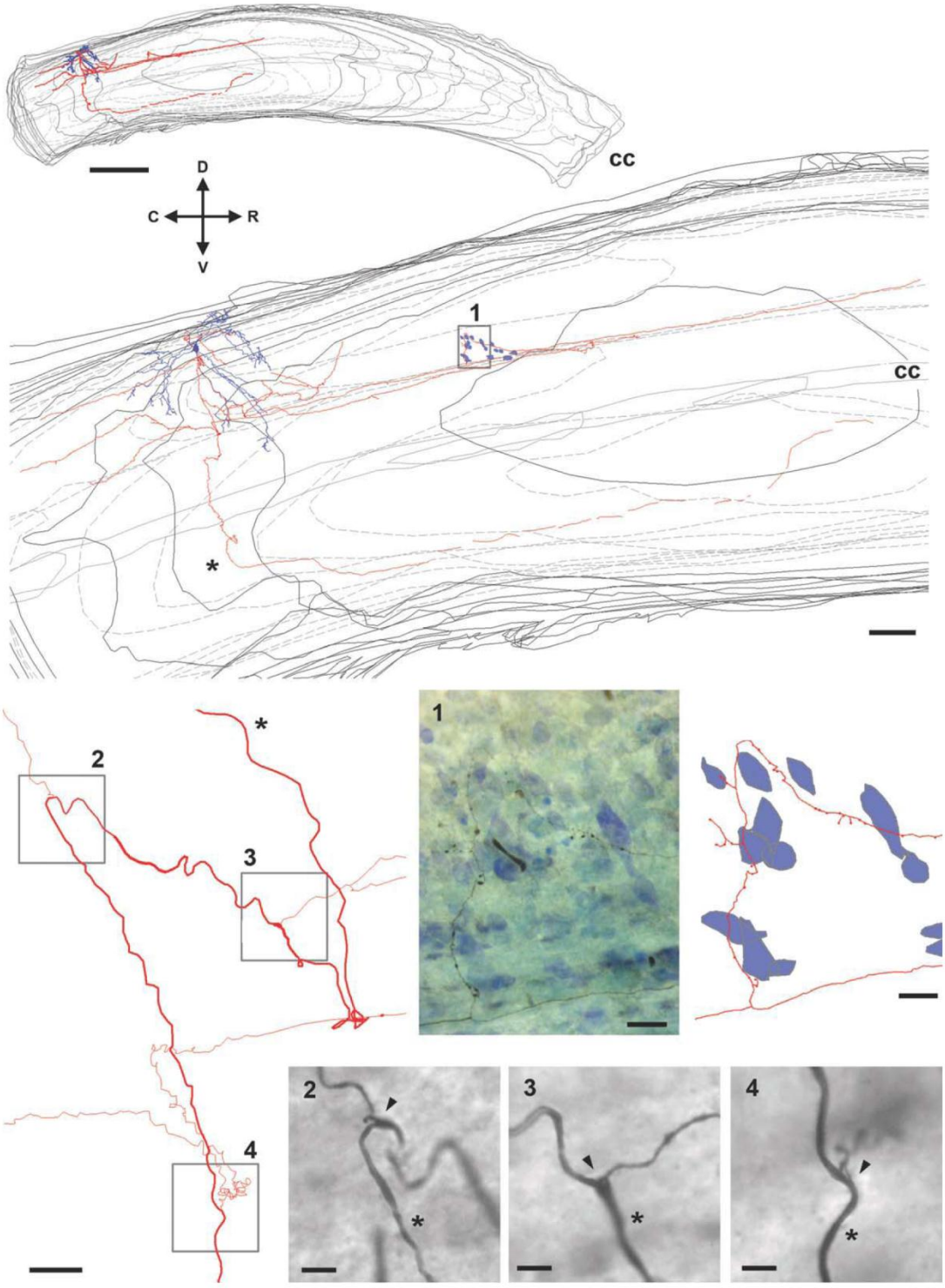


Figure 8. Example of an MCT projection neuron. Lamina I neuron (cell ID: L273-E3), located in the caudal part of the lumbar enlargement, with three (two lateral and one dorsal) collaterals. The collaterals branch further, and the resulting axons cover a substantial part of the dorsal gray matter in the segment where the neuron is located. Two axon branches shoot out and extend rostrally for several segments, where they could not be followed further. Inset 1 and its reconstruction (at right) show close appositions between varicosities of a terminal side branch and a group of larger cell bodies most likely located in the lateral spinal nucleus (LSN). Insets 2–4 show high-magnification images of the corresponding areas on the reconstruction of the axon. Scale bars (top to bottom) = 1,000 μm, 200 μm, 20 μm, 20 μm; 20 μm in photomicrograph 1; 5 μm in photomicrographs 2–4.

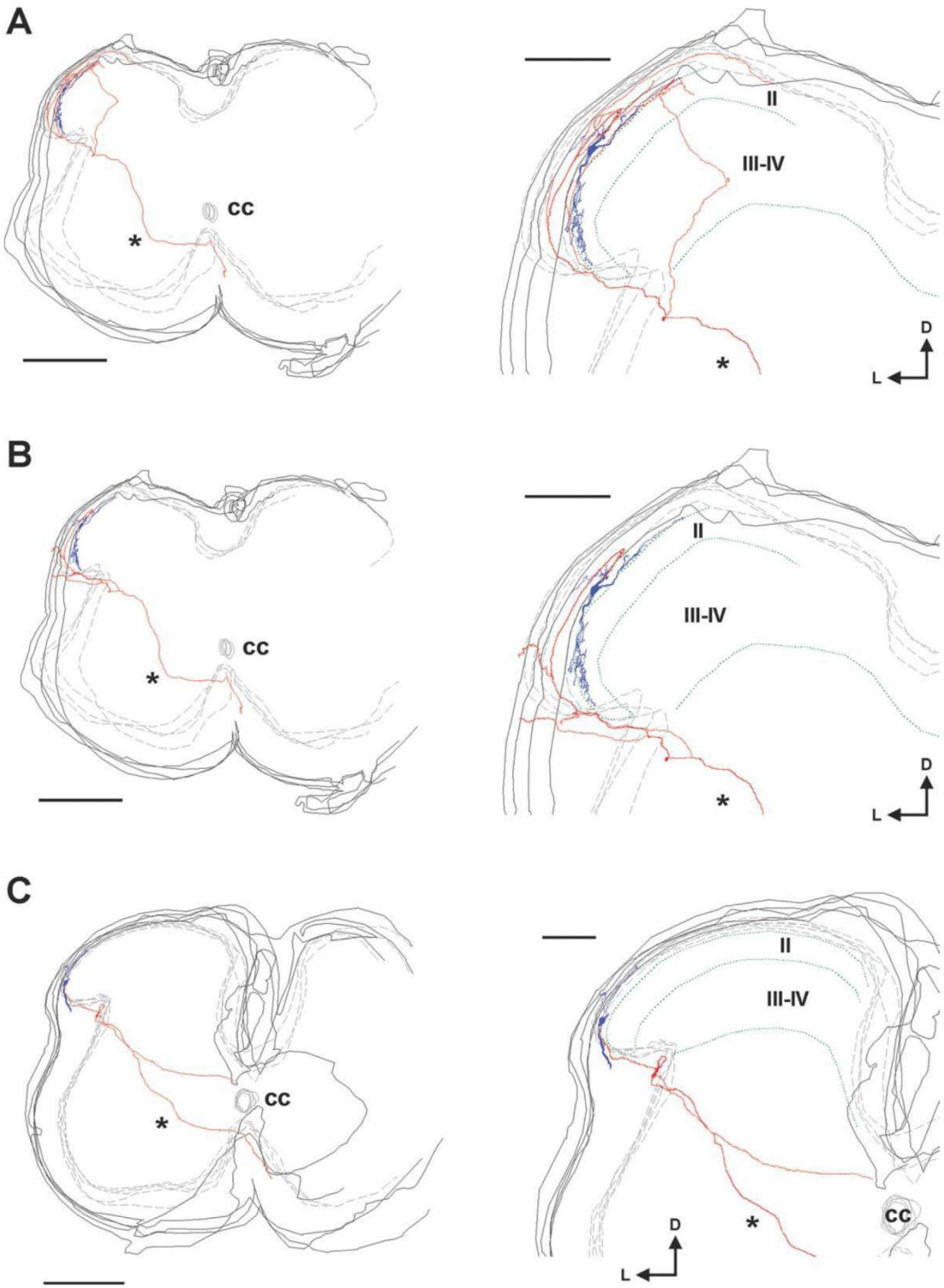


Figure 9. Laminar location of the major collateral types in the transverse plane. **A:** Dorsal collaterals of an MCT lamina I projection neuron at the L6 level of the spinal cord (age P18) at low (left) and high (right) magnification. The collaterals mostly occupy the dorsal laminae I–IV. **B:** Lateral collaterals of the same MCT projection neuron. Collaterals target the dorsal part of the lateral funiculus. **C:** Ventral collateral of a VCT projection neuron located at the L3 level (age P14). The collateral stays below the lower border of lamina IV, initially runs together with the main axon, and then aims toward the dorsal commissure. Reconstructions were made from six to eight transverse serial sections (thickness 100 μm). Dotted green lines indicate the borders of spinal laminae (II, III–IV). Some contour lines were omitted for clarity. Scale bars (left to right) = 500 μm, 200 μm.

projecting ipsilaterally to the dorsal reticular nucleus (Lima, 1998).

Dendritic origin of the projection axons

Dendritic origin of the axon has been previously reported for lamina I neurons (Cheunsuang and Morris, 2000; Hylden et al., 1986). Similar observations were also made in cat preganglionic sympathetic neurons (Morgan, 2001), in rat substantia nigra neurons (Hausser et al., 1995), and in hippocampal interneurons of the rat (Martina et al., 2000). In this report, we show that this anatomical variation is frequent in lamina I ALT projection neurons.

The functional significance of a dendritic origin of the main axon could be a matter of speculation. For example, targeted synaptic input to the intermittent dendritic region between the soma and the axon origin can effectively modulate spike generation. In addition, computer simulation based on anatomical data showed that such synapses could regulate the relative efficacy of other inputs arising from different regions of the dendritic tree (Lee et al., 2005). In an extreme case, strong inhibitory input to the intermittent dendritic region may discouple the axon from the soma electrically. Determining the ultrastructure of the intermittent dendritic region, together with mapping of the expression pattern of transmitter receptors and voltage-gated ion channels, will be necessary to elucidate the physiological role of this anatomical variation in lamina I neurons.

Ipsilateral axon collaterals of lamina I projection neurons

Ipsilateral axon collaterals of lamina I neurons have been previously reported by a number of groups. In an intracellular labeling study in the cat spinal cord, Bennett et al. (1981) found two lamina I neurons that issued local (laminae I–IV) axon branches that were rich in varicosities. These two neurons, however, were not confirmed to be projection cells. Other sharp-electrode studies in vivo (Beal et al., 1981; Hylden et al., 1986; Light et al., 1979) and in spinal cord slices (Cheunsuang and Morris, 2000) have reported unmyelinated collaterals of lamina I neurons branching in the superficial laminae. Although not reconstructed in detail, they resembled our dorsal collaterals. Among these studies, however, only that of Hylden et al. (1986) confirmed the projection nature of their cells. Short pieces of thin axon collaterals from the main axon of two putative lamina I projection neurons were reported in the DLF (Grudt and Perl, 2002). Although collaterals and main axon of these neurons were filled in spinal cord slices and, therefore, could only be partially followed, their description fits that of our LCT neurons.

For the medullary dorsal horn of rats, Li et al. (2000) described large local axonal arbors in the vicinity of the somata of putative projection neurons. The overall appearance of some of those cells (see Figs. 2–4 from Li et al., 2000) was very similar to that of our local circuit interneurons described in Figure 3B.

Dorsal collaterals: contribution to local circuits

The distribution of dorsal collaterals suggests that the postsynaptic target areas of the DCT-I neurons include neighboring lamina I, whereas those of the DCT-II neurons include laminae II–IV. The rostrocaudal extent of the collaterals implies that their postsynaptic targets are located within the same segment (Fig. 10A).

Previous observations of propriospinal lamina I axons in the ipsilateral Lissauer tract (Craig, 1991) and lamina I neurons with collaterals in the dorsal horn (Beal et al., 1981; Bennett et al., 1981; Light et al., 1979) led to the suggestion that some lamina I neurons may have both segmental and supraspinal connections (Hylden et al., 1986). Our results strongly support this idea and indicate two possible functions of dorsal collaterals. First, lamina I ALT projection neurons could recruit neighboring lamina I neurons, some of which may also be projection neurons targeting the same (or other) supraspinal areas. In this case, activity of a DCT projection neuron would amplify (or extend) the supraspinally directed signal. Second, the collaterals may excite inhibitory interneurons in the superficial laminae. In this way they either inhibit their own activity (negative feedback) or provide collateral inhibition of neighboring dorsal horn regions.

Lateral collaterals: intersegmental connections/propriospinal projections

Lateral collaterals occupied the dorsal part of the lateral funiculus (LF) targeting rostral segments (Figs. 9B, 10B) and, occasionally, extending caudally. Several previous studies have reported ipsilateral axons originating from lamina I in various parts of the LF. Lamina I axon longitudinal connections have been demonstrated by Szentagothai (1964). An anterograde labeling study in cat (Craig, 1991) revealed propriospinal lamina I axons ascending for several segments, predominantly ipsilaterally, also in the white matter adjacent to the superficial dorsal horn. These fibers were suggested to be unmyelinated and to terminate in lamina I. Ipsilateral axons in the LF of segments as rostral as Th13 have also been reported in rat after the injection of anterograde tracers into the lateral half of the dorsal horn of L2–L4 segments (Petko and Antal, 2000). Retrograde labeling results

obtained with various methods indicated that ipsilateral propriospinal cells projecting more than two segments rostrally are also located in lamina I in cat (Molenaar and Kuypers, 1978; Verburgh et al., 1989; Yezierski et al., 1980) and in rat (Dutton et al., 2006). These results demonstrated that multisegmental integration can occur within lamina I, and most authors attributed this role to specific sets of propriospinal neurons. However, our results imply that some of these propriospinal axons are ipsilateral collaterals of ALT projection neurons located in the lateral half of lamina I.

The small diameter and en passant varicosities of lateral collaterals observed in our study are in good agreement with earlier observations that many propriospinal axons in the DLF are unmyelinated (Chung and Coggeshall, 1988), and the ipsilaterally ascending axons of lamina I cells are slowly conducting (Cervero et al., 1979; Craig and Kniffki, 1985). Our results also support Cervero et al. (1979) in showing that 15% of lamina I cells can be antidromically activated from the ipsilateral Lissauer tract as far as three segments rostrally.

Furthermore, lateral collaterals of ALT projection neurons may provide input for the LSN. Indeed, Olave and Maxwell (2004) demonstrated that axons originating, presumably, from excitatory interneurons are contacting LSN neurons. They also suggested that lamina I projection neurons activate LSN neurons through collaterals. This assumption was based on the observation (Grudt and Perl, 2002) that some lamina I neurons with thick axons that cross the midline possess occasional axon collaterals entering the DLF. The trajectory of the lateral collaterals revealed in our study strongly supports this idea. One of the lateral-rostral collaterals of the MCT projection neuron shown in Figure 8 actually gave a side branch with numerous varicosities forming putative contacts on large

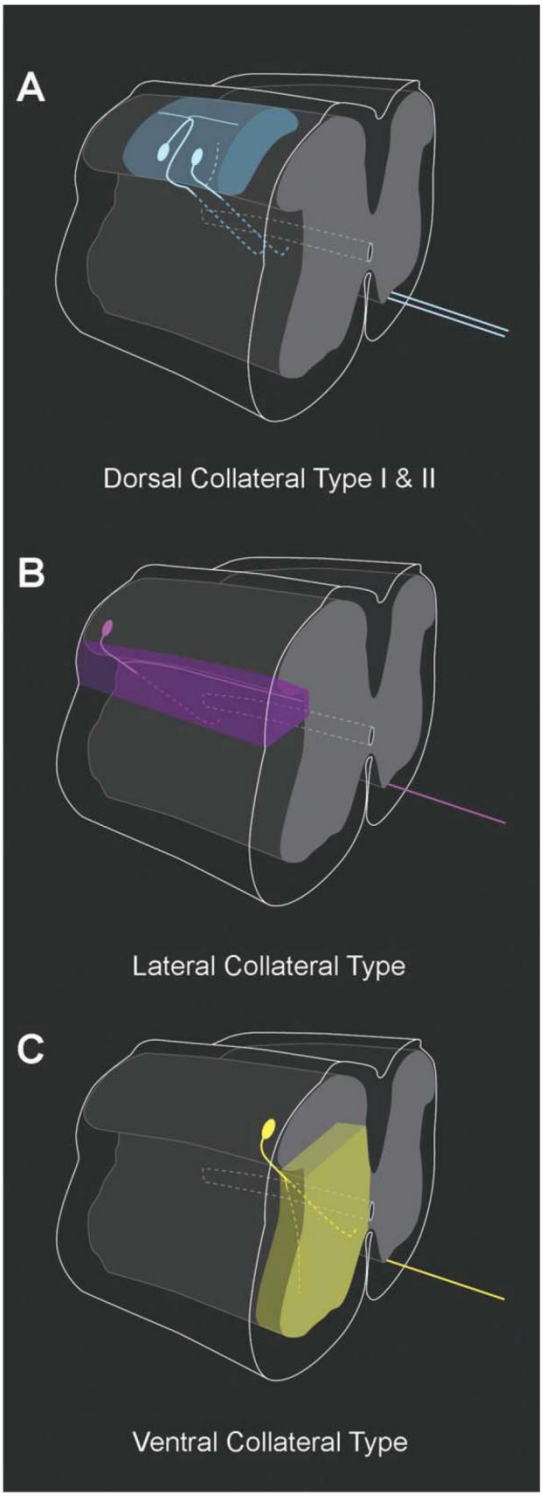


Figure 10. Ipsilateral spinal cord areas occupied by axon collaterals of different types of ALT projection neurons. Colored areas show the approximate 3-D spread of each axon collateral type. These collateral areas were constructed based on the courses of all the collaterals in a given group. **A:** The area (blue) covered by collaterals of DCT-I and DTC-II projection neurons is not extending beyond the segment where the soma is located, but it may extend dorsally into the overlying white matter. **B:** The collateral area (purple) of LCT neurons extends beyond the segment of the neuron; includes LSN, a part of the DLF; and may extend into the neighboring gray matter (lateral part of laminae I–V). **C:** The area covered by VCT neurons (yellow) could best be described as a transverse slice of the gray matter ventral to lamina IV, centered on the rostrocaudal position of the neuron soma. The collateral area of an MCT projection neuron would be a combination of the areas described above. Continuous colored lines indicate axons running in the white matter or close to the gray/white matter border. Dashed colored lines represent axons running inside the gray matter. Continuous white lines around the gray matter indicate the contours of the white matter.

neurons located, presumably, in the LSN. Putative contacts between lateral collaterals and LSN neurons were also observed in transverse sections (two cases, not included in this study). Taken together, our data suggest that, besides their principal function, lamina I projection neurons with lateral collaterals (LCT or MCT) can be involved in inter- and/or multisegmental integration and can provide input for LSN neurons.

Ventral collaterals: intrasegmental connections with deep laminae

Ventral collaterals typically had a limited rostrocaudal spread but also had larger and variable mediolateral and dorsoventral extents. The schematic area occupied by all the ventral collaterals could be best described as a few-hundred-micrometers-thick transverse slice of the gray matter, centered (rostrocaudally) on the position of the neuronal soma (Fig. 10C). This distribution suggests that neurons giving rise to ventral collaterals establish connections with neurons in deeper laminae (V–VII). Therefore, approximately one-third of ALT projection neurons (n = 6, VCT; n = 6, MCT) could project to the ventral horn.

Ventral projections of lamina I neurons can explain the observation that application of substance P in spinal cord slices increases the frequency of spontaneous excitatory postsynaptic potentials in lamina V–VII neurons (Szucs et al., 2004). This increase could be abolished by tetrodotoxin or by an incision below lamina IV, suggesting that neurokinin-1 receptor-positive neurons in the dorsal horn excite lamina V–VII neurons in a spike-dependent manner. Ventral collaterals of the lamina I projection neurons could provide such excitation, and their narrow rostrocaudal spread explains why they remain preserved in transverse slice preparations.

A recent study by Braz and Basbaum (2009) demonstrated that neurons in deep laminae (III–V) receive polysynaptic inputs from unmyelinated primary afferents. The authors presumed that this input is via interneurons of laminae I–II. Apart from some lamina II islet and stalked neurons projecting to deeper laminae (Eckert et al., 2003), the ventral collaterals of VCT and MCT lamina I neurons described here may also establish such connections. In this way the ventral collaterals can link parallel pain pathways originating from lamina I and lamina V (Braz et al., 2005). Thus, our findings further support the hypothesis of sensory information "flow" from superficial to deeper laminae of the dorsal horn (Braz and Basbaum, 2009; Wall, 1960).

Elucidating the role of ipsilateral collaterals

Identifying the postsynaptic targets of ipsilateral collaterals may reveal local network functions of lamina I projection neurons. Collaterals of other principal neurons in the spinal cord are known to contribute to such networks. For example, motoneurons receive feedback inhibition from Renshaw cells excited by local collaterals of motoneuron axons (Renshaw, 1946). Sacral preganglionic neurons issue a large number of intraspinal collaterals covering broad areas of the ventral horn, indicating their widespread integrative functions within the spinal cord (Morgan et al., 1991). To the best of our knowledge, involvement of ALT-projecting lamina I neurons in local spinal processing has not been described so far.

From this point of view, MCT cells with diverse types of collaterals form probably the most intriguing group of lamina I neurons. They seem to play a very complex role involving participation in local circuits, establishing propriospinal connections, and at the same time serving as major supraspinal output elements of the dorsal horn network. MCT neurons with extensive dendritic trees and diverse axon collaterals are capable of interconnecting broad spinal cord regions.

In conclusion, lamina I ALT projection neurons give rise to distinct types of ipsilateral axon collaterals. We propose that these collaterals are important determinants of the complex function of projection neurons and can serve as basis for their classification. Eventually, detailed description of collateral connections of lamina I projection neurons will be crucial for a better understanding of their roles in spinal sensory processing.

ACKNOWLEDGMENTS

The authors thank Zita Puskár for her constructive comments on the manuscript and technical aspects of histological processing and Francis Odeh for language correction.

LITERATURE CITED

Al-Khater KM, Todd AJ. 2009. Collateral projections of neurons in laminae I, III, and IV of rat spinal cord to thalamus, periaqueductal gray matter, and lateral parabrachial area. J Comp Neurol 515:629–646.

Al-Khater KM, Kerr R, Todd AJ. 2008. A quantitative study of spinothalamic neurons in laminae I, III, and IV in lumbar and cervical segments of the rat spinal cord. J Comp Neurol 511:1–18.

Beal JA, Penny JE, Bicknell HR. 1981. Structural diversity of marginal (lamina I) neurons in the adult monkey (*Macaca mulatta*) lumbosacral spinal cord: a golgi study. J Comp Neurol 202:237–254.

Bennett GJ, Abdelmoumene M, Hayashi H, Hoffert MJ, Dubner R. 1981. Spinal cord layer I neurons with axon collaterals that generate local arbors. Brain Res 209:421–426.

Bester H, Chapman V, Besson JM, Bernard JF. 2000. Physiological properties of the lamina I spinoparabrachial neurons in the rat. J Neurophysiol 83:2239–2259.

Braz JM, Basbaum AI. 2009. Triggering genetically-expressed transneuronal tracers by peripheral axotomy reveals convergent and segregated sensory neuron-spinal cord connectivity. Neuroscience 163:1220–1232.

Braz JM, Nassar MA, Wood JN, Basbaum AI. 2005. Parallel "pain" pathways arise from subpopulations of primary afferent nociceptor. Neuron 47:787–793.
Cervero F, Iggo A, Molony V. 1979. Ascending projections of nociceptor-driven lamina I neurones in the cat. Exp Brain Res 35:135–149.
Cheunsuang O, Morris R. 2000. Spinal lamina I neurons that express neurokinin 1 receptors: morphological analysis. Neuroscience 97:335–345.
Christensen BN, Perl ER. 1970. Spinal neurons specifically excited by noxious or thermal stimuli: marginal zone of the dorsal horn. J Neurophysiol 33:293–307.
Chung K, Coggeshall RE. 1988. Propriospinal fibers in the white matter of the cat sacral spinal cord. J Comp Neurol 269:612–617.
Craig AD. 1991. Spinal distribution of ascending lamina I axons anterogradely labeled with *Phaseolus vulgaris* leucoagglutinin (PHA-L) in the cat. J Comp Neurol 313:377–393.
Craig AD, Kniffki KD. 1985. Spinothalamic lumbosacral lamina I cells responsive to skin and muscle stimulation in the cat. J Physiol 365:197–221.
Craig AD, Krout K, Andrew D. 2001. Quantitative response characteristics of thermoreceptive and nociceptive lamina I spinothalamic neurons in the cat. J Neurophysiol 86: 1459–1480.
Dickenson AH, Chapman V, Green GM. 1997. The pharmacology of excitatory and inhibitory amino acid-mediated events in the transmission and modulation of pain in the spinal cord. Gen Pharmacol 28:633–638.
Dutton RC, Carstens MI, Antognini JF, Carstens E. 2006. Long ascending propriospinal projections from lumbosacral to upper cervical spinal cord in the rat. Brain Res 1119:76–85.
Eckert WA 3rd, McNaughton KK, Light AR. 2003. Morphology and axonal arborization of rat spinal inner lamina II neurons hyperpolarized by mu-opioid-selective agonists. J Comp Neurol 458:240–256.
Esteves F, Lima D, Coimbra A. 1993. Structural types of spinal cord marginal (lamina I) neurons projecting to the nucleus of the tractus solitarius in the rat. Somatosens Mot Res 10:203–216.
Grudt TJ, Perl ER. 2002. Correlations between neuronal morphology and electrophysiological features in the rodent superficial dorsal horn. J Physiol 540:189–207.
Han ZS, Zhang ET, Craig AD. 1998. Nociceptive and thermoreceptive lamina I neurons are anatomically distinct. Nat Neurosci 1:218–225.
Harmann PA, Carlton SM, Willis WD. 1988. Collaterals of spinothalamic tract cells to the periaqueductal gray: a fluorescent double-labeling study in the rat. Brain Res 441: 87–97.
Hausser M, Stuart G, Racca C, Sakmann B. 1995. Axonal initiation and active dendritic propagation of action potentials in substantia nigra neurons. Neuron 15:637–647.
Hunt SP, Kelly JS, Emson PC, Kimmel JR, Miller RJ, Wu JY. 1981. An immunohistochemical study of neuronal populations containing neuropeptides or gamma-aminobutyrate within the superficial layers of the rat dorsal horn. Neuroscience 6:1883–1898.
Hylden JL, Hayashi H, Dubner R, Bennett GJ. 1986. Physiology and morphology of the lamina I spinomesencephalic projection. J Comp Neurol 247:505–515.
Hylden JL, Anton F, Nahin RL. 1989. Spinal lamina I projection neurons in the rat: collateral innervation of parabrachial area and thalamus. Neuroscience 28:27–37.
Kandel ER, Shchwartz JH, Jessel TM. 2000. Principles of neural science. New York: McGraw-Hill.
Kuru M. 1949. The sensory paths in the spinal cord and brain stem of man. Tokyo: Sogensya.
Lee DC, Jensen AL, Schiefer MA, Morgan CW, Grill WM. 2005. Structural mechanisms to produce differential dendritic gains. Brain Res 1033:117–127.
Li YQ, Li H, Yang K, Kaneko T, Mizuno N. 2000. Morphologic features and electrical membrane properties of projection neurons in the marginal layer of the medullary dorsal horn of the rat. J Comp Neurol 424:24–36.
Light AR, Perl ER. 1979. Spinal termination of functionally identified primary afferent neurons with slowly conducting myelinated fibers. J Comp Neurol 186:133–150.
Light AR, Trevino DL, Perl ER. 1979. Morphological features of functionally defined neurons in the marginal zone and substantia gelatinosa of the spinal dorsal horn. J Comp Neurol 186:151–171.
Lima D. 1998. Anatomical basis for the dynamic processing of nociceptive input. Eur J Pain 2:195–202.
Lima D, Coimbra A. 1983. The neuronal population of the marginal zone (lamina I) of the rat spinal cord. A study based on reconstructions of serially sectioned cells. Anat Embryol 167:273–288.
Lima D, Coimbra A. 1986. A Golgi study of the neuronal population of the marginal zone (lamina I) of the rat spinal cord. J Comp Neurol 244:53–71.
Lima D, Coimbra A. 1989. Morphological types of spinomesencephalic neurons in the marginal zone (lamina I) of the rat spinal cord, as shown after retrograde labelling with cholera toxin subunit B. J Comp Neurol 279:327–339.
Lima D, Mendes-Ribeiro JA, Coimbra A. 1991. The spino-latero-reticular system of the rat: projections from the superficial dorsal horn and structural characterization of marginal neurons involved. Neuroscience 45:137–152.
Liu RP. 1986. Spinal neuronal collaterals to the intralaminar thalamic nuclei and periaqueductal gray. Brain Res 365: 145–150.
Martina M, Vida I, Jonas P. 2000. Distal initiation and active propagation of action potentials in interneuron dendrites. Science 287:295–300.
Molenaar I, Kuypers HG. 1978. Cells of origin of propriospinal fibers and of fibers ascending to supraspinal levels. A HRP study in cat and rhesus monkey. Brain Res 152:429–450.
Morgan CW. 2001. Axons of sacral preganglionic neurons in the cat: I. Origin, initial segment, and myelination. J Neurocytol 30:523–544.
Morgan CW, de Groat WC, Felkins LA, Zhang SJ. 1991. Axon collaterals indicate broad intraspinal role for sacral preganglionic neurons. Proc Natl Acad Sci U S A 88:6888–6892.
Olave MJ, Maxwell DJ. 2004. Axon terminals possessing alpha2C-adrenergic receptors densely innervate neurons in the rat lateral spinal nucleus which respond to noxious stimulation. Neuroscience 126:391–403.
Petko M, Antal M. 2000. Propriospinal afferent and efferent connections of the lateral and medial areas of the dorsal horn (laminae I–IV) in the rat lumbar spinal cord. J Comp Neurol 422:312–325.
Pinault D. 1996. A novel single-cell staining procedure performed in vivo under electrophysiological control: morphofunctional features of juxtacellularly labeled thalamic cells and other central neurons with biocytin or neurobiotin. J Neurosci Methods 65:113–136.
Pinto V, Szucs P, Derkach VA, Safronov BV. 2008. Monosynaptic convergence of C- and Adelta-afferent fibres from different segmental dorsal roots on to single substantia gelatinosa neurones in the rat spinal cord. J Physiol 586: 4165–4177.
Prescott SA, De Koninck Y. 2002. Four cell types with distinctive membrane properties and morphologies in lamina I of the spinal dorsal horn of the adult rat. J Physiol 539: 817–836.

Ramon y Cajal S. 1909. Histologie du systeme nerveux de l'homme et des vertebres. Paris: A. Maloine.
Renshaw B. 1946. Central effects of centripetal impulses in axons of spinal ventral roots. J Neurophysiol 9:191–204.
Rexed B. 1952. The cytoarchitectonic organization of the spinal cord in the cat. J Comp Neurol 96:415–495.
Ruscheweyh R, Ikeda H, Heinke B, Sandkuhler J. 2004. Distinctive membrane and discharge properties of rat spinal lamina I projection neurones in vitro. J Physiol 555:527–543.
Safronov BV, Pinto V, Derkach VA. 2007. High-resolution single-cell imaging for functional studies in the whole brain and spinal cord and thick tissue blocks using light-emitting diode illumination. J Neurosci Methods 164:292–298.
Spike RC, Puskar Z, Andrew D, Todd AJ. 2003. A quantitative and morphological study of projection neurons in lamina I of the rat lumbar spinal cord. Eur J Neurosci 18: 2433–2448.
Sugiura Y, Lee CL, Perl ER. 1986. Central projections of identified, unmyelinated (C) afferent fibers innervating mammalian skin. Science 234:358–361.
Szentagothai J. 1964. Neuronal and synaptic arrangement in the substantia gelatinosa Rolandi. J Comp Neurol 122: 219–239.
Szucs P, Szokol K, Veress G, Antal M, Poisbeau P. 2004. Modulation of neuronal excitability by substance P in neurons of laminae V–VII of the neonatal spinal cord. FENS Abstr 2:A04611.
Szucs P, Pinto V, Safronov BV. 2009. Advanced technique of infrared LED imaging of unstained cells and intracellular structures in isolated spinal cord, brainstem, ganglia and cerebellum. J Neurosci Methods 177:369–380.
Verburgh CA, Kuypers HG, Voogd J, Stevens HP. 1989. Spinocerebellar neurons and propriospinal neurons in the cervical spinal cord: a fluorescent double-labeling study in the rat and the cat. Exp Brain Res 75:73–82.
Wall PD. 1960. Cord cells responding to touch, damage, and temperature of skin. J Neurophysiol 23:197–210.
Willis WD, Coggeshall RE. 1991. Sensory mechanisms of the spinal cord. New York: John Wiley & Sons.
Yezierski RP, Culberson JL, Brown PB. 1980. Cells of origin of propriospinal connections to cat lumbosacral gray as determined with horseradish peroxidase. Exp Neurol 69: 493–512.
Zhang ET, Han ZS, Craig AD. 1996. Morphological classes of spinothalamic lamina I neurons in the cat. J Comp Neurol 367:537–549.

Publication II

Monosynaptic excitatory inputs to spinal lamina I anterolateral-tract-projecting neurons from neighbouring lamina I neurons.

Luz LL, Szucs P, Pinho R & Safronov BV.

J Physiol 588, 4489-4505, 2010

J Physiol 588.22 (2010) pp 4489–4505

The Journal of Physiology

Monosynaptic excitatory inputs to spinal lamina I anterolateral-tract-projecting neurons from neighbouring lamina I neurons

Liliana L. Luz[1,2], Peter Szucs[1], Raquel Pinho[1] and Boris V. Safronov[1,2]

[1] *Instituto de Biologia Molecular e Celular – IBMC, Universidade do Porto, Rua do Campo Alegre 823, 4150-180 Porto, Portugal*
[2] *Laboratório de Biologia Celular e Molecular, Faculdade de Medicina, Universidade do Porto, Alameda Professor Hernâni Monteiro, 4200-319 Porto, Portugal*

Spinal lamina I receives nociceptive primary afferent input to project through diverse ascending pathways, including the anterolateral tract (ALT). Large projection neurons (PNs) form only a few per cent of the cell population in this layer, and little is known about their local input from other lamina I neurons. We combined single-cell imaging in the isolated spinal cord, paired recordings, 3-D reconstructions of biocytin-labelled neurons and computer simulations to study the monosynaptic input to large ALT-PNs from neighbouring (somata separated by less than 80 μm) large lamina I neurons. All 11 connections identified were excitatory. We have found that an axon of a presynaptic neuron forms multiple synapses on an ALT-PN, and both Ca^{2+}-permeable and Ca^{2+}-impermeable AMPA receptors are involved in transmission. The monosynaptic EPSC latencies (1–12 ms) are determined by both post- and presynaptic factors. The postsynaptic delay, resulting from the electrotonic EPSC propagation in the dendrites of an ALT-PN, could be 4 ms at most. The presynaptic delay, caused by the spike propagation in a narrow highly branched axon of a local-circuit neuron, can be about 10 ms for neighbouring ALT-PNs and longer for more distant neurons. In many cases, the EPSPs evoked by release from a lamina I neuron were sufficient to elicit a spike in an ALT-PN. Our data show that ALT-PNs can receive input from both lamina I local-circuit neurons and other ALT-PNs. We suggest that lamina I is a functionally interconnected layer. The intralaminar network described here can amplify the overall output from the principal spinal nociceptive projection area.

(Received 28 July 2010; accepted after revision 27 September 2010; first published online 27 September 2010)
Corresponding author B. V. Safronov: Instituto de Biologia Molecular e Celular – IBMC, Universidade do Porto, Rua do Campo Alegre 823, 4150-180 Porto, Portugal. Email: safronov@ibmc.up.pt

Abbreviations ALT, anterolateral tract; CI-AMPAR, Ca^{2+}-impermeable AMPA receptor; CP-AMPAR, Ca^{2+}-permeable AMPA receptor; PN, projection neuron; SDH, superficial dorsal horn; SG, substantia gelatinosa (lamina II).

Introduction

Spinal lamina I processes diverse modalities of nociceptive input and projects through ascending tracts to specific areas of the brainstem and thalamus (Willis & Coggeshall, 1991; Todd *et al.* 2000; Lima & Almeida, 2002). Individual lamina I neurons receive and integrate monosynaptic Aδ- and C-fibre afferent inputs (Grudt & Perl, 2002; Ikeda *et al.* 2003) originating from several segmental dorsal roots (Pinto *et al.* 2010). Lamina I neurons were shown to receive local monosynaptic inputs from excitatory and inhibitory lamina II (substantia gelatinosa, SG) neurons (Lu & Perl, 2005; Graham *et al.* 2007; Santos *et al.* 2007; Kato *et al.* 2009; Santos *et al.* 2009). The input from an SG excitatory interneuron can be sufficiently strong to excite a postsynaptic neuron (Santos *et al.* 2009). The functional connectivity between lamina I neurons, to our knowledge, has not been described so far.

Lamina I contains both projection neurons (PNs) and non-projection, or local-circuit, neurons. PNs form only less than 5% of the neuronal population (Spike *et al.* 2003; Todd & Koerber, 2006). The main axon of some PNs crosses the spinal grey matter and ascends in the contralateral anterolateral tract (ALT). It has recently been shown that the main axon of large mediolaterally oriented ALT-PNs from the lateral lamina I gives rise to ipsilateral collaterals which can spread to the dorsal, lateral or ventral

L. L. Luz and P. Szucs contributed equally to this work.

© 2010 The Authors. Journal compilation © 2010 The Physiological Society

DOI: 10.1113/jphysiol.2010.197012

regions of the spinal cord (Szucs *et al.* 2010). According to their size and morphology, these ALT-PNs most likely correspond to Waldeyer cells of the classical literature (Waldeyer, 1889; Cajal, 1909). The majority of lamina I neurons, however, are local-circuit neurons (Bice & Beal, 1997). Some of them can also have large cell bodies and extensive axons forming a dense network interconnecting the dorsal grey matter of several spinal cord segments (Szucs *et al.* 2010), suggesting a possibility of numerous contacts with other lamina I neurons. In spite of this, the functional role of lamina I local-circuit neurons as well as their interaction with the ALT-PNs is poorly understood. One reason for this is that a low percentage (<5%) of PNs, together with a low probability (∼10%) of finding pairs of monosynaptically connected superficial dorsal horn (SDH) neurons in spinal cord slices (Santos *et al.* 2007), makes a systematic study of the ALT-PN connections extremely difficult. Furthermore, large lamina I neurons are most sensitive to damage introduced by a slicing procedure, and therefore, their properties and functional connectivity could hardly be studied using slices.

For these reasons, we used the isolated spinal cord preparation (Szucs *et al.* 2009) preserving large ALT-PNs and local-circuit neurons, along with their connections via long axodendritic pathways (Szucs *et al.* 2010), to study whether (1) an ALT-PN can receive inputs from another lamina I neuron, (2) the synaptic transmission involves Ca^{2+}-permeable AMPA receptors (CP-AMPARs) and Ca^{2+}-impermeable AMPA receptors (CI-AMPARs), (3) release from a lamina I neuron can be sufficient to excite an ALT-PN, and whether (4) spinal lamina I can be considered as an interconnected cell layer.

Methods

Ethical approval

Laboratory Wistar rats (P14–P20) were killed by decapitation in accordance with Portuguese national guidelines (Direcção Geral de Veterinária, Ministério da Agricultura) after anaesthesia with intraperitoneal injection of sodium pentobarbital (30 mg kg^{-1}) and subsequent check for lack of pedal withdrawal reflexes. The experiments were carried out according to the guidelines laid down by the institution's animal welfare committee (Comissão de Ética do Instituto de Biologia Molecular e Celular) and comply with the policies and regulations of *The Journal of Physiology* (Drummond, 2009). The number of animals used in this study was 84.

Preparation of the spinal cord

The vertebral column was quickly cut out and immersed in oxygenated artificial cerebrospinal fluid (ACSF) at room temperature. The lumbar spinal cord was dissected and the pia mater was locally removed in the region of interest with forceps and scissors, to provide access for the recording and stimulating pipettes. The spinal cord was glued with cyanoacrylate adhesive to a golden plate (the dorsolateral spinal cord surface was up) and transferred to the recording chamber (Fig. 1*A*). All measurements were done at 22–24°C.

Visualization of lamina I neurons

Lamina I neurons were visualized (Fig. 1*A*) through the intact dorsolateral white matter in the lumbar spinal cord using the oblique infrared light-emitting-diode (LED) illumination technique (Safronov *et al.* 2007; Szucs *et al.* 2009). Lamina I was identified on the basis of orientation of myelinated fibres in the dorsal white matter (Pinto *et al.* 2010). The neurons included in this study were located in the region between the dorsolateral funiculus (lateral border) and the dorsal root entry zone (medial border) (Fig. 1*A*). The white matter covering this part of lamina I is thin in young rats (Pinto *et al.* 2008*b*), allowing visually controlled tight-seal recordings from the superficial neurons. Large lamina I neurons could be clearly distinguished from deeper located SG neurons whose somata were smaller and appeared as a densely packed cell layer (Szucs *et al.* 2009).

Selection of the ALT-PNs

The percentage of PNs in the entire population of lamina I neurons is low (Spike *et al.* 2003; Todd & Koerber, 2006). However, we have recently found that, among the neurons with large cell bodies (>25 μm) in the lateral SDH, the ALT-PNs represent a majority (Szucs *et al.* 2010). For this reason, we selected as postsynaptic neurons those which had large mediolaterally oriented or round somata with the longest diameter above 25 μm. As putative presynaptic neurons, those with soma diameter above 20 μm were tested. The major types of the somata of large lamina I neurons are shown in Fig. 1*B*. For all postsynaptic neurons described here, the *post hoc* analysis of their axon course (reaching the contralateral ALT) confirmed that they were ALT-PNs.

Recording from postsynaptic neurons

Recordings from the postsynaptic neurons were done in whole-cell mode (Melnick *et al.* 2004*a*,*b*). ACSF contained (in mM): NaCl 115, KCl 3, $CaCl_2$ 2, $MgCl_2$ 1, NaH_2PO_4 1, $NaHCO_3$ 25, and glucose 11 (pH 7.4 when bubbled with 95%–5% mixture of O_2–CO_2). The pipettes were pulled from thick-walled glass (BioMedical Instruments, Germany) and fire-polished (resistance, 4–5 MΩ). The

© 2010 The Authors. Journal compilation © 2010 The Physiological Society

pipette solution contained (in mM): KCl 3, potassium gluconate 150, $MgCl_2$ 1, BAPTA 1, Hepes 10 (pH 7.3 adjusted with KOH, final $[K^+]$ was 160 mM) and 1% biocytin. The amplifier was an EPC10-Double (HEKA, Lambrecht, Germany). The signal was low-pass filtered at 2.9 kHz and sampled at 10 kHz. The traces in Fig. 3*C* were additionally off-line-filtered at 1 kHz. Offset potentials were compensated before seal formation. Liquid junction potentials were calculated (15 mV) and corrected for in all experiments using the compensation circuitry of the amplifier. The blockers CNQX and IEM 1460 were from Sigma and Tocris, respectively.

Stimulation and labelling of presynaptic neurons

Intact presynaptic neurons were selectively stimulated and labelled through the cell-attached pipette containing 500 mM NaCl and 1.5% biocytin. The pairs of monosynaptically connected neurons were identified as described by Santos *et al.* (2007). After the connected neurons have been found, the strength of the current pulse (duration, 1 ms) used for the stimulation of the presynaptic neuron was reduced from 100 nA to the 'threshold + 20 nA' level (Santos *et al.* 2009), to allow a non-damaging stimulation for longer periods of time (up to 1 h 45 min). For most presynaptic neurons in this study, the adjusted stimulation strength was 50–70 nA.

To test whether our stimulation protocol, originally developed for small SG neurons, can be also used for the fast spike initiation in large lamina I neurons, we did control measurements in 15 cells with soma diameter $>20\ \mu$m (not shown). Direct whole-cell recordings of the voltage changes introduced by the cell-attached stimulation (both pipettes were positioned on the same soma) showed that, as in the case of SG neurons (see Fig. 3 from Santos *et al.* 2009), a spike in the axon initial segment of a lamina I neuron was reliably evoked within the 1 ms of the stimulation ($n = 15$). For this reason, the EPSC latencies in connections were calculated from the end of the 1 ms stimulation pulse (to the time moment when the evoked EPSC reached 10% of its peak amplitude).

When recordings from a connection have been completed, the presynaptic neuron was filled by biocytin through the cell-attached pipette (Szucs *et al.* 2009). Biocytin diffusion into the cell was facilitated by applying depolarizing current pulses (duration, 500 ms) of increasing amplitude (1–10 nA, 1 nA increment) at 1 Hz for 10 min.

Criteria for monosynaptic connections

In most cases, the EPSCs evoked by stimulation of a presynaptic neuron consisted of several components corresponding to transmitter release in multiple synapses

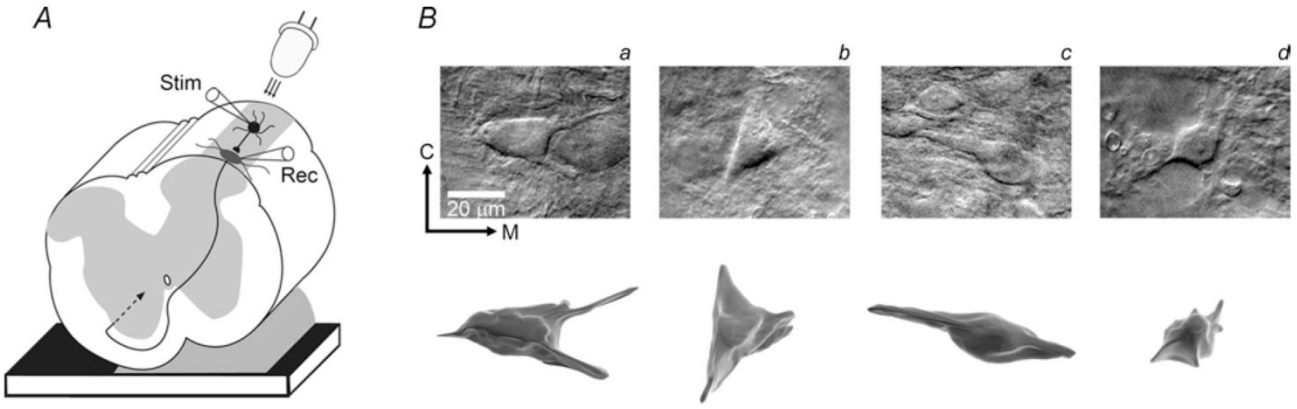


Figure 1. Recording from large lamina I neurons in the isolated spinal cord
A, preparation of the lumbar spinal cord for recordings from pairs of synaptically connected lamina I neurons. An infrared LED was used as a source of oblique illumination for the cell imaging. Both pre- and postsynaptic neurons were located in the region between the dorsolateral funiculus (lateral border) and the dorsal root entry zone (medial border). A *post hoc* analysis of the major axon course was done to prove that the postsynaptic neuron was an ALT-PN. *B*, types of large somata of lamina I neurons seen under our experimental conditions. The 3-D reconstructions (bottom) were done from 5–10 serial images (top) taken in different focal planes (~2 μm step). Contour lines of a soma and initial dendrites were traced in individual images into a 3-D modelling software (Cinema-4D, Maxon). *a*, a polygonal flattened soma (dorsoventral extent, ~10 μm) with three or four major dendrites. This cell body resembled those of flattened neurons (Lima & Coimbra, 1986). *b*, a pyramidal soma with four dendrites leaving from the apices similar to that of a pyramidal neuron (Lima & Coimbra, 1986). *c*, a spindle-shaped soma with dendrites in a bipolar organization resembling those of fusiform cells (Lima & Coimbra, 1986). *d*, a soma appearing as a sphere (diameter, ~20 μm) with numerous, sometimes poorly visible, dendrites; similar to the body of multipolar cells (Lima & Coimbra, 1986). All ALT-PNs ($n = 40$) had somata of the first three types, while the presynaptic neurons had frequently somata of the fourth type. M, medial; C, caudal.

© 2010 The Authors. Journal compilation © 2010 The Physiological Society

of the same axon (see Fig. 3; and Santos *et al.* 2009 for SG neurons). According to our recent estimation, the release probability for a synapse (or a group of synapses with similar spatial location) responsible for the generation of an EPSC component is about 0.5 (Santos *et al.* 2009). Therefore, an EPSC component was identified as monosynaptic if it was observed in at least 7 of 10 consecutive stimulations (1 Hz) and its latency variation was within 1 ms. Neurons in a pair were considered to be connected monosynaptically if at least one EPSC component was identified as monosynaptic.

Histological processing and cell reconstruction

After fixation in 4% paraformaldehyde, the spinal cord was embedded in agar and parasagittal serial sections (thickness, 100 μm) were prepared with a tissue slicer (Leica, VT 1000S). To reveal biocytin, the sections were permeabilized with 50% ethanol and treated according to the avidin-biotinylated horseradish peroxidase method (ExtrAvidin-Peroxidase, diluted 1:1000) followed by a diaminobenzidine chromogen reaction. For 2-D reconstructions, sections were counterstained with 1% toluidine blue, to determine borders of the grey matter and laminae, and mounted in DPX (Fluka). For 3-D reconstructions, sections were treated with 1% OsO_4 and embedded in Durcupan resin. Photomicrographs were taken with a Primo Star (Zeiss) microscope equipped with a Guppy (Allied Vision Technologies, Stadtroda, Germany) digital camera. Contrast and brightness of the images used for the figures were adjusted using Adobe Image Ready software.

The 2-D reconstructions in Figs 4 and 5 were done as follows. A window of the Neurolucida software (MBF Bioscience, Williston, VT, USA, workstation version) was dimmed and superimposed on the live digital image of the section (objective, 40×) by means of the Transparent Windows 2.2 application. All dendrites, somata and axons as well as contours of the grey and white matter were completely traced into a serial section data file in 2-D. During the reconstruction, the microscope stage was aligned manually. The location of the neuronal soma and processes were determined on reconstructions of individual sections where borders of the grey and white matter were clearly identifiable. The 2-D serial sections were overlaid, aligned using Neuroexplorer software (MBF Bioscience) and exported as bitmap images.

The 3-D reconstruction of an ALT-PN (Fig. 7) and a lamina I local-circuit neuron (Fig. 8) for computer modelling was done with the Neurolucida system (MBF Bioscience). Shrinkage was not corrected. The dendrogram in Fig. 7 and the axogram in Fig. 8 were constructed with Neuroexplorer (MBF Bioscience).

Computer simulations

The 3-D reconstructed neurons were imported to NEURON (version 7.1) software (Hines, 1993; Hines & Carnevale, 1997). The dendritic spines forming less than 3% of the dendritic membrane area were ignored. The resolution limit of a light microscope (0.2 μm) was used to set the diameters of all apparently thinner regions of axons and dendrites. The integration step was 50 μs. The spatial grid was set to 0.1 of the characteristic length (λ) for the axon and dendrites. The soma was divided in 10 segments. The specific membrane capacitance (C_m) and specific axial resistance (R_a) were assumed to be 1 μF cm^{-2} and 200 Ω cm, respectively. The specific membrane resistivity (R_m) was uniformly set to 100 kΩ cm^2 to give, in agreement with our measurements, the slowest membrane time constant ($\tau_0 = R_m C_m$) of 100 ms. These settings of passive properties in the model of the ALT-PN gave the input resistance (R_{IN}) of 0.33 GΩ, which was close to the experimentally determined value (0.38 GΩ) for the neuron reconstructed. Simulations were done for the resting/holding potential of −70 mV.

The ALT-PN model was used to analyse passive EPSC propagation in the dendritic tree. The synaptic input was modelled by a two-state kinetic scheme. The synaptic current (I_S) was described by the following equation:

$$I_S = \tau_D/(\tau_D - \tau_R) \times [\exp(-t/\tau_D) - \exp(-t/\tau_R)] \times g_M \times (V - E_{Rev}),$$

where τ_R is the conductance rise time constant (1 ms), τ_D is the conductance decay time constant (10 ms), g_M is the maximum conductance (1.86×10^{-5} μS), V is the membrane potential and E_{Rev} is the reversal potential (0 mV). The synapse locations are specified in Fig. 7.

The model of the lamina I local-circuit neuron was used to analyse the spike propagation time in the axon of the presynaptic neuron. Voltage-gated Na^+ and K^+ channels were inserted at uniform densities in all branches of the axon, whereas soma and dendrites were passive. The channel models and densities were from Melnick *et al.* (2004*b*) with the only modification being that to prevent the spike self-generation in the axon at high densities of Na^+ channels, their steady-state activation variable (m_∞) was set to 0 at potentials negative to −65 mV. Based on our recordings from tonic-firing neurons (Melnick *et al.* 2004*b*), the Na^+ conductance (g_{Na}) was 1800 mS cm^{-2}. Assuming the Na^+ channel conductance in dorsal horn neurons of 11.6 pS (Safronov *et al.* 1997; Safronov, 1999), each μm^2 of the axonal membrane in the model contained 433 channels, 158 of which were available at a resting potential of −70 mV (calculated for voltage steps to +20 mV). The voltage-gated K^+ conductance was 76 mS cm^{-2}. In a uniform axon with a constant diameter of 1 μm, these channel densities allowed generation of a

© 2010 The Authors. Journal compilation © 2010 The Physiological Society

spike with a maximum depolarization rate of 576 V s^{-1} propagating at a conduction velocity of 0.38 m s^{-1}. In the axon with a diameter of 0.2 μm (thinnest axons in our reconstructed neurons), the conduction velocity was 0.16 m s^{-1}. These values were in a good agreement with the highest and lowest conduction velocities measured at 22–24°C for unmyelinated C-fibres in isolated dorsal roots (see Table 2 from Pinto *et al.* 2008*a*).

All data are given as means ± S.E.M.

Results

A total of 199 large lamina I neurons were filled with biocytin in the whole-cell mode. Full recovery of axonal and dendritic trees was achieved for 79 neurons, 44 of which (56%) were identified as ALT-PNs. Detailed anatomical description of a subset of these ALT-PNs is given in Szucs *et al.* (2010). Stable voltage- and current-clamp recordings were obtained from 40 ALT-PNs. For 28 of them, we searched for presynaptic neurons by testing 234 large cells. Monosynaptic connections were found in 11 cases and were all excitatory. We did not observe monosynaptic inhibitory inputs from large neurons; all recorded IPSCs were either polysynaptic or spontaneous. These 40 ALT-PNs, including 11 with paired neurons, form the basis of the present study. According to the morphology of their axon collaterals (Szucs *et al.* 2010), the 11 postsynaptic ALT-PNs were of the dorsal-collateral-type ($n = 1$), ventral-collateral-type ($n = 4$), lateral-collateral-type ($n = 2$), mixed-collateral-type ($n = 2$) and no-collateral-type ($n = 2$). Based on their somatodendritic organization (Lima & Coimbra, 1986), these neurons were classified as fusiform ($n = 3$), flattened ($n = 5$) and pyramidal ($n = 3$).

Passive membrane properties of large ALT-PNs

The resting membrane potential (measured with zeroed amplifier input, Santos *et al.* 2004) was −70.6 ± 1.0 mV ($n = 40$; range, −55 mV to −86 mV). The mean input resistance (R_{IN}) and the slowest membrane time constant (τ_0) measured in the current-clamp mode from a

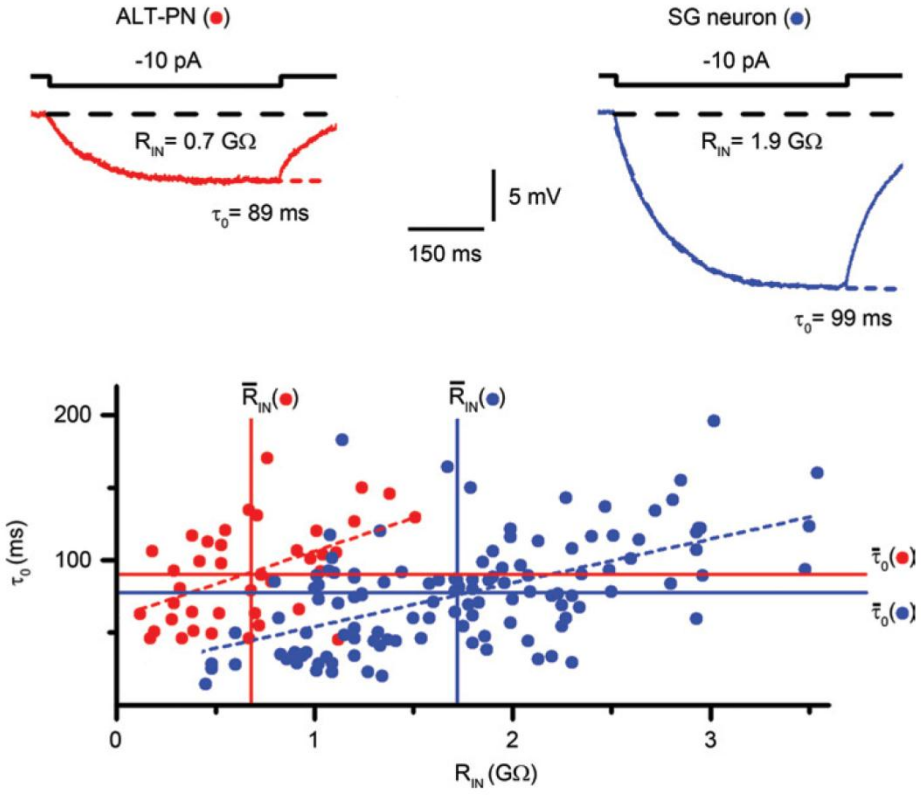


Figure 2. Comparison of passive membrane properties of ALT-PNs and SG neurons
R_{IN} and τ_0 were measured from membrane responses evoked in current-clamp by a 500 ms hyperpolarizing current pulse of −10 pA. The neurons were kept at −70 mV. τ_0 *versus* R_{IN} was plotted for 40 anatomically confirmed ALT-PNs (red circles) and 122 SG neurons (blue circles) from Santos *et al.* (2009). Linear fit of the data points in each group is shown by oblique dashed lines. The mean R_{IN} and τ_0 are indicated by vertical and horizontal continuous lines, respectively. For SG neurons, $R_{IN} = 1.73 \pm 0.06$ GΩ and $\tau_0 = 76.2 \pm 3.4$ ms ($n = 122$). The mean values for ALT-PNs are given in the text.

© 2010 The Authors. Journal compilation © 2010 The Physiological Society

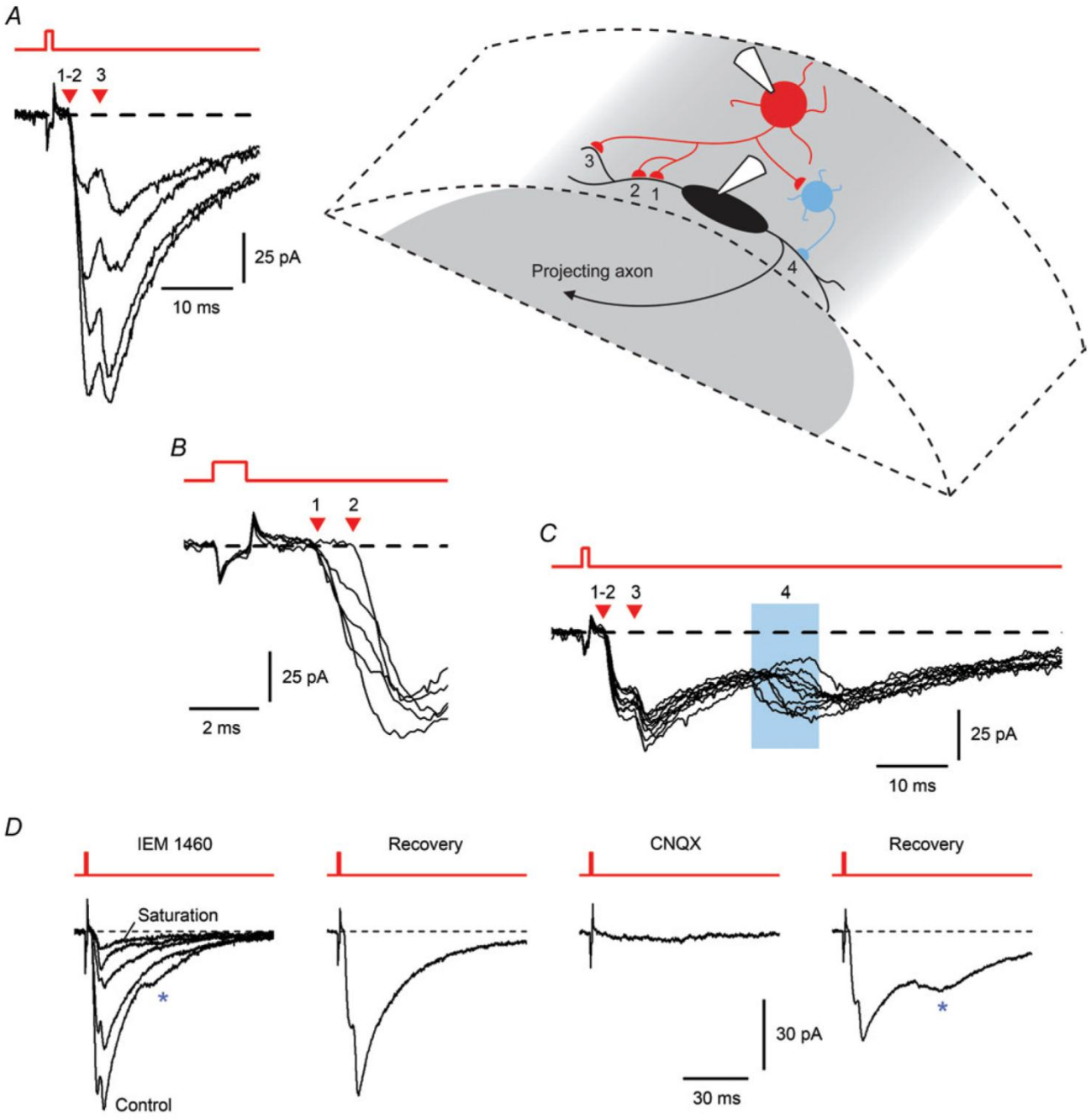


Figure 3. A monosynaptic connection with transmitter release in multiple synapses and activation of CP- and CI-AMPARs

Recordings from a connection with a postsynaptic ALT-PN. The axon of the presynaptic neuron (red) released transmitter in multiple synapses. *A*, the shorter- and longer-latency components of a composite monosynaptic EPSC. Four non-consecutive traces show the EPSC amplitude variation caused by fluctuation of the quantal transmitter release. The longer-latency component corresponded to activation of more remote synapse 3. *B*, fast transitions on the rising phase of the shorter-latency component. Two subcomponents corresponding to activation of synapses 1 and 2 could be activated either individually (no transitions) or together (traces with transitions) (5 non-consecutive traces). *C*, 10 consecutive traces showing a polysynaptic EPSC (synapse 4). Note the lack of failures. A large latency variation (indicated by a blue box) was caused by the variation in the spike initiation time in the intercalated neuron (blue) as described by Santos *et al.* (2009). Laminar location of the intercalated neuron could not be determined. *D*, both CP- and CI-AMPARs are involved in transmission in this connection. Effects of 20 μM IEM 1460 (CP-AMPAR blocker) and 10 μM CNQX (AMPA/kainate receptor blocker) are shown for averaged

© 2010 The Authors. Journal compilation © 2010 The Physiological Society

uniformly preset potential of −70 mV were 0.67 ± 0.06 GΩ and 91.1 ± 5.2 ms, respectively ($n = 40$).

The mean R_{IN} in large ALT-PNs was considerably lower than those measured under our experimental conditions (1 mM BAPTA-buffered pipette solution or perforated-patch recording) in non-identified, mostly medium-sized, lamina I neurons (1.8 GΩ, Pinto *et al.* 2010) and small SG neurons (1.59 to 2.26 GΩ, Santos *et al.* 2007; Santos *et al.* 2009). Lower R_{IN} in ALT-PNs could be explained by a larger neuronal membrane area or a lower specific membrane resistivity (R_m). To distinguish between these two possibilities, we analysed the relationship between R_{IN} and τ_0 in large and small neurons, assuming that, at a uniform specific membrane capacitance (C_m), τ_0 could be used as a measure of R_m ($\tau_0 = R_m C_m$).

In Fig. 2, we compared our measurements for large ALT-PNs (red) and small (soma diameter, ∼10 μm) SG neurons (blue, data from Santos *et al.* 2009). The two groups appeared well-separated in the τ_0 *versus* R_{IN} plot. Within each group, R_{IN} increased with τ_0 (oblique dashed lines) indicating that its reduction was caused, at least in part, by the drop in R_m. However, comparison of the mean values for the two groups has revealed that ALT-PNs had significantly lower R_{IN} ($P < 10^{-5}$, independent Student's *t* test; ratio of mean values was 2.58) but a slightly slower τ_0 (Fig. 2, continuous lines). Therefore, lower mean R_{IN} in ALT-PNs, in comparison with SG neurons, could be explained by a larger area of the neuronal membrane with similar R_m.

Monosynaptic connections with transmitter release in multiple synapses

In 9 of 11 connections with a postsynaptic ALT-PN, stimulation of the presynaptic neuron evoked composite EPSCs corresponding to transmitter release in multiple synapses of the same axon. Detailed analysis of the monosynaptic nature of individual EPSC components was done as described recently (Santos *et al.* 2009). Recordings from an ALT-PN receiving at least three monosynaptic inputs and one polysynaptic input from the same lamina I neuron are shown in Fig. 3.

The shorter- and longer-latency components separated by a time interval of 4 ms could be clearly distinguished (Fig. 3*A*). Stability of the latencies and of the interval between the components was consistent with our criteria for the monosynaptic inputs located at different electrotonic distances from the soma (Santos *et al.* 2009). The rising phase of the longer-latency EPSC (the synapse labelled 3 on the figure) could not be analysed due to the overlap with the preceding component. However, fast transitions on the rising phase of the shorter-latency component (Fig. 3*B*) revealed the presence of two subcomponents corresponding to activation of synapses (labelled 1 and 2) with only a slight difference in their electrotonic distances from the soma (Santos *et al.* 2009).

In addition, the ALT-PN in this connection received a strong polysynaptic input (synapse 4, Fig. 3*C*). Its latency variation of ∼10 ms (indicated by a blue box) was consistent with our estimation for the variation of the spike initiation time in an intercalated neuron (Santos *et al.* 2009). Although activity of the intercalated neuron varied during the experiment, the lack of failures of the polysynaptic EPSC in 10 consecutive stimulations shown in Fig. 3*C* suggested that the presynaptic lamina I neuron could efficiently excite the intercalated neuron. Similar polysynaptic inputs were observed in six other connections. Laminar location of the intercalated neuron could not be determined in our study.

Thus, an ALT-PN can receive multiple synapses from the axon of another lamina I neuron. Distinct groups of synapses can generate EPSC components with different latencies. The presynaptic lamina I neuron can additionally evoke a polysynaptic response by efficiently exciting an intercalated (intact) neuron.

Both CP- and CI-AMPARs are involved in synaptic transmission

Effects of the CP-AMPAR blocker IEM 1460 (20 μM) and the AMPA/kainate receptor blocker CNQX (10 μM) were studied in connections with postsynaptic ALT-PNs (Fig. 3*D*). IEM 1460 reduced the EPSC amplitude by 85.4 ± 4.2% ($n = 4$; range 73 to 90%), while CNQX showed a complete block ($n = 5$).

During the application of the blockers (shown for IEM 1460; Fig. 3*D*, left), the EPSC components were suppressed in a manner consistent with their classification as mono- and polysynaptic. The monosynaptic EPSCs were progressively reduced with the receptor block. In contrast, the polysynaptic component (indicated by an asterisk) disappeared abruptly at the stage of a partial receptor block (judged from the reduction of the

traces (each obtained from 10 consecutive episodes recoded at 1 Hz). For IEM 1460, development of the block is shown. Note that monosynaptic EPSCs (corresponding to synapses 1–2 and 3) are progressively reduced, while the polysynaptic one (synapse 4, indicated by an asterisk) disappears abruptly. Because of the variable latency, the polysynaptic EPSC appears smaller in the averaged trace. The polysynaptic component was recovered only after a long wash-out at the end of the experiment.

© 2010 The Authors. Journal compilation © 2010 The Physiological Society

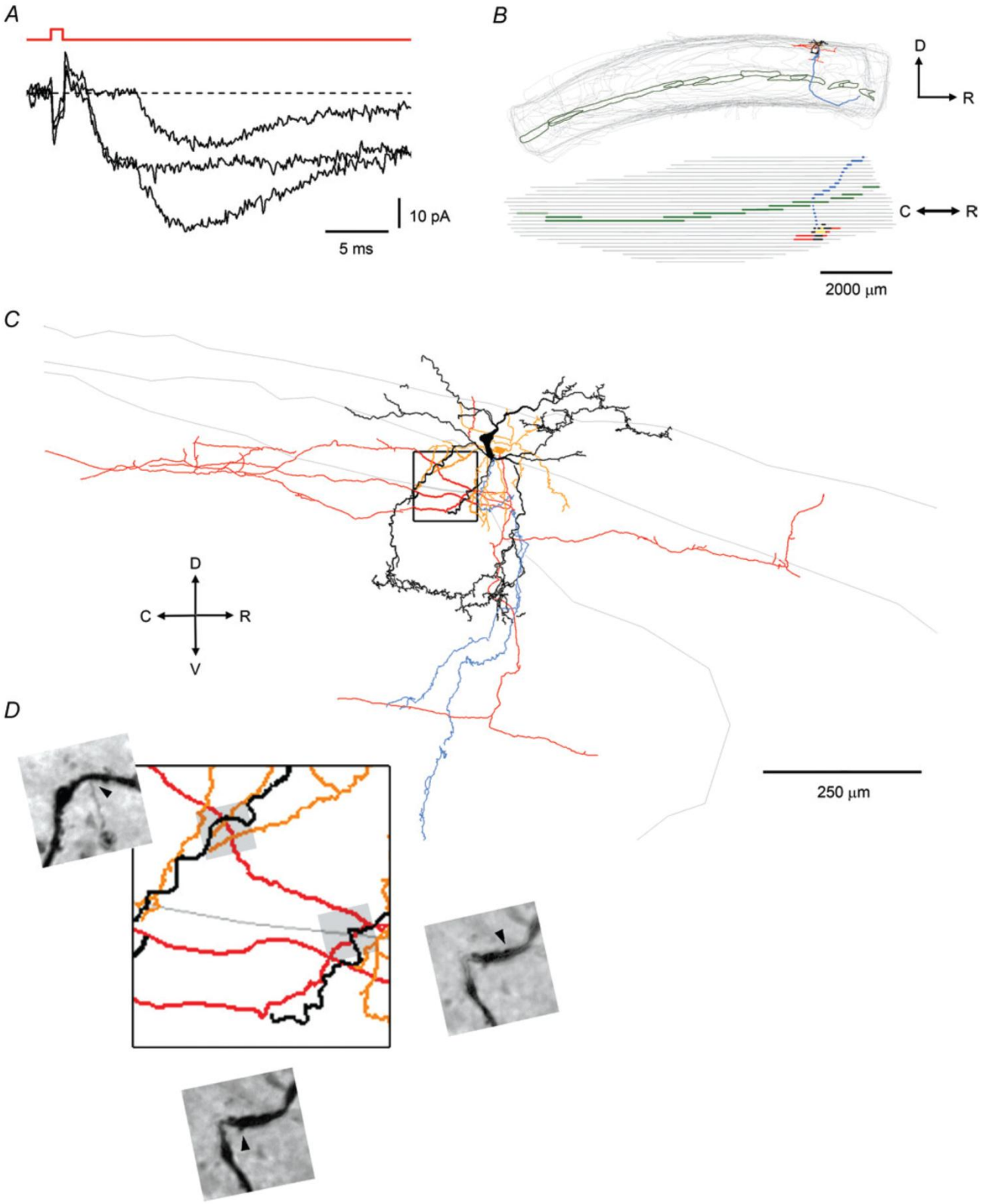


Figure 4. Inputs to an ALT-PN from a lamina I local-circuit neuron
A, monosynaptic EPSCs with at least two components. Non-consecutive traces were chosen to show individual components and the composite EPSC. *B*, 2-D reconstruction from serial sections showing the major axon (blue) of the postsynaptic ALT-PN (soma and dendrites, black) reaching the rostral end of the spinal cord preparation. The presynaptic neuron: orange, soma and dendrites; red, axon. Upper part, a lateral view; lower part, a horizontal

© 2010 The Authors. Journal compilation © 2010 The Physiological Society

monosynaptic EPSCs). Thus, the partial block was already sufficient to reduce depolarization and prevent spike firing in the intercalated neuron ($n = 4$).

Input to an ALT-PN from a local-circuit neuron or another ALT-PN

In 2 of 11 pairs, we also obtained a detailed labelling of the presynaptic neuron. In the pair shown in Fig. 4, the monosynaptic EPSC consisted of at least two components which could be evoked either separately or together (Fig. 4*A*). In the 2-D reconstruction, the major axon of the postsynaptic ALT-PN could be followed until the rostral end of the isolated spinal cord (Fig. 4*B*). The presynaptic cell was a lamina I local-circuit neuron (multipolar type-IIa) with its axon occupying the SDH of one entire segment (Fig. 4*B–C*). Three close appositions between the presynaptic axon and the postsynaptic dendrites (putative synaptic contacts) were revealed (Fig. 4*D*). Two of them were formed by the same presynaptic axon branch (right group), while the third one originated from another branch (left). In another connection (Fig. 5), a simple EPSC corresponding to activation of one synapse was recorded; both cells were ALT-PNs.

Latency and efficacy of inputs

The mean latencies of individual monosynaptic components of composite EPSCs were distributed between 1.5 and 12.4 ms (mean, 4.31 ± 0.55 ms; 21 components analysed). The latencies of the initial monosynaptic components were distributed between 1.5 and 5.0 ms (mean, 2.75 ± 0.31 ms; $n = 11$).

The connection with three monosynaptic contacts (analysed in Fig. 3) showed EPSC components with latencies of 2, 3 and 6 ms (Fig. 6*A*). In the current-clamp mode, release in all three synapses increased the membrane depolarization; however, the composite EPSP did not reach the firing threshold in the postsynaptic ALT-PN.

The input with the longest mean EPSC latency of 12.4 ms was observed in a connection shown in Fig. 6*B*. We did a detailed analysis of the latency variation for this EPSC. The histogram constructed for 47 episodes, revealed a low latency variation typical for a monosynaptic connection. In the current-clamp mode, this input was suprathreshold and EPSPs activated one-to-three spikes in each of six consecutive stimulations.

The EPSP efficacy was tested in nine connections. The postsynaptic ALT-PN was current-clamped at −70 mV. In four pairs, the evoked EPSPs were subthreshold and had maximum amplitudes of 4–11 mV (mean 8.0 ± 1.5 mV; $n = 4$).

In the remaining five pairs, $59.6 \pm 13.4\%$ of the evoked EPSPs elicited spikes (range 23% to 100%; 38 EPSPs analysed). In 2 of these 5 pairs, EPSPs evoked multiple spikes (Fig. 6*B*). Those EPSPs which did not elicit spikes in these five connections showed maximum amplitudes of 6–13 mV.

Thus, release from one lamina I neuron can substantially depolarize and, in many cases, excite an ALT-PN. The monosynaptic responses can have a long latency.

In the following experiments we studied whether such latencies could be explained by the conduction times in pre- and postsynaptic neurons. We assumed that synaptic release is fast (<1 ms) and, therefore, major transmission delay can be caused by the electrotonic EPSC propagation in the dendrites of a large ALT-PN and/or by the active spike propagation in the axon of the presynaptic neuron. To estimate maximum delays, we did computer simulations using the models based on detailed 3-D reconstructions of the dendritic and axonal branches of a representative ALT-PN and a large local-circuit neuron.

EPSC propagation time in the postsynaptic ALT-PN

The reconstructed ALT-PN had four major dendrites (Fig. 7*A* and *B*). The highest order of the dendritic branches was 14 and the maximum dendritic path length was 804 μm (Fig. 7*C*). Eight uniform synapses were inserted in different locations along the somatodendritic domain of the model neuron (1–8) to simulate somatic recordings of the corresponding EPSCs (Fig. 7*D* and *E*). The somatic synapse (labelled 1 on the figure) evoked an EPSC with a short delay of 0.1 ms. The longest delay of 3.9 ms was obtained for the most distal synapse (2) in the large dorsomedial major dendrite (green). In the dendritic branch of the highest order, the most distal synapse (3) showed a delay of 1.9 ms. In the large ventrolateral major dendrite (blue), the maximum delay was 2.7 ms (synapse 4). In shorter dendrites, dorsomedial (purple)

view (green line indicates the central canal). R, rostral; C, caudal; V, ventral; D, dorsal. Grey lines in *B* and *C* indicate the contours of the bottom of the serial sections. For clarity, some contour lines were omitted. *C*, the postsynaptic ALT-PN was a pyramidal neuron of the ventral-collateral-type. The presynaptic cell was a lamina I local-circuit neuron (multipolar type-IIa) with axon arborizations occupying the SDH of one entire segment. The region in the inset is shown amplified in *D*. *D*, three close appositions between the presynaptic axon and the postsynaptic dendrites were revealed (arrowheads). Two of them were formed by the same axon branch (right group).

© 2010 The Authors. Journal compilation © 2010 The Physiological Society

and ventrolateral (orange), the longest EPSC delays were 1.1 ms (synapse 5) and 0.8 ms (synapse 6), respectively.

We also tested whether two spatially close synapses, located, however, in different major dendrites may evoke EPSCs with substantially different propagation times. For synapses 7 and 8 (grey circle), in large dorsomedial (green) and smaller ventrolateral (orange) major dendrites, the EPSC delays were 3.4 and 0.8 ms, respectively (Fig. 7*E*).

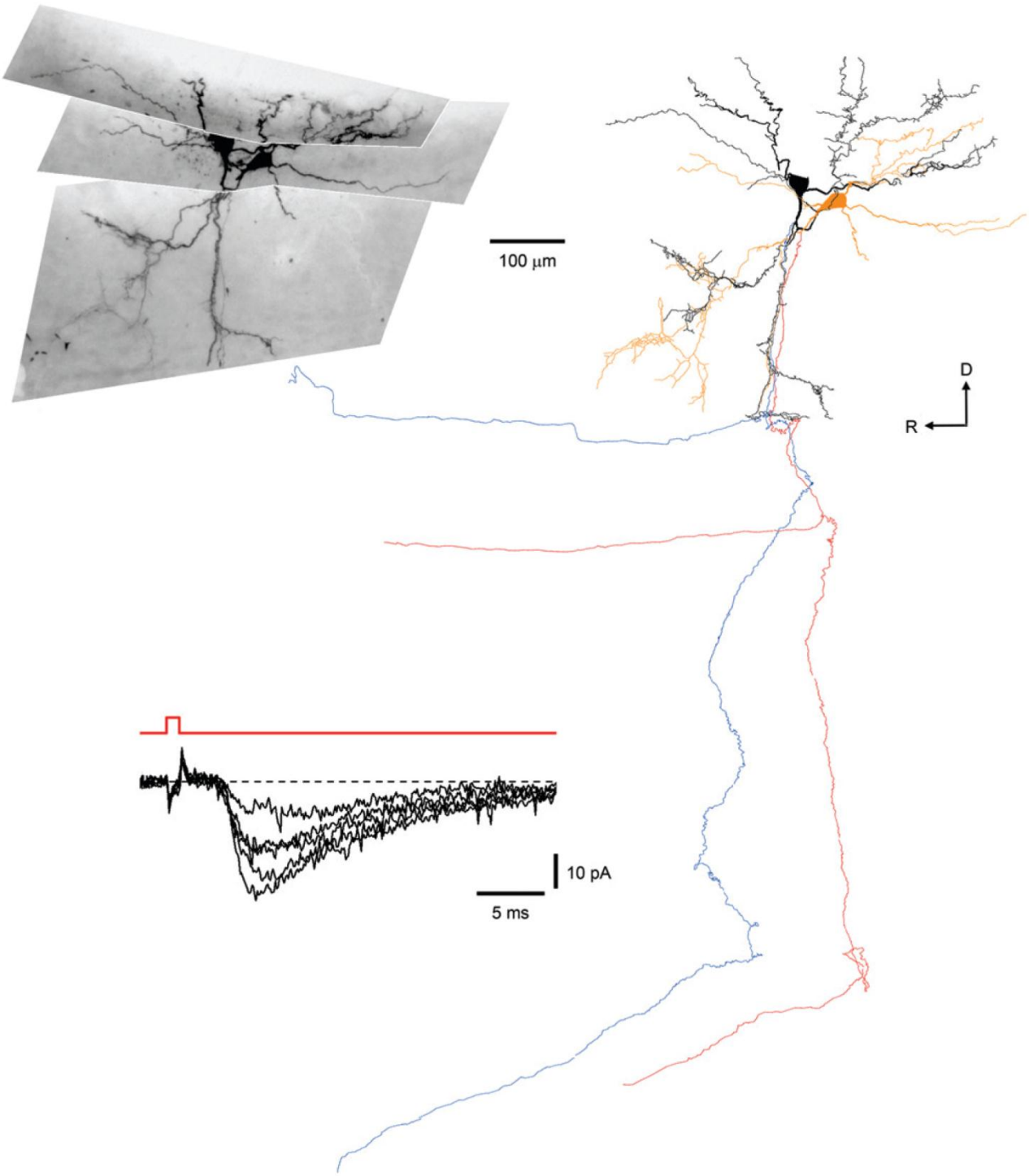


Figure 5. Input to an ALT-PN from another ALT-PN
Microphotographs (from different sections) and the 2-D reconstruction of two ALT-PNs (pyramidal neurons of the lateral-collateral-type). Postsynaptic neuron; soma and dendrites, black; axon, blue. Presynaptic neuron: soma and dendrites, orange; axon, red. The evoked EPSC showed only one component (5 consecutive traces). R, rostral; D, dorsal.

© 2010 The Authors. Journal compilation © 2010 The Physiological Society

Thus, simultaneous release in two spatially close synapses can evoke EPSCs reaching the soma with substantially different delays depending on the electrotonic lengths of the dendritic pathways.

These simulations have shown that the electrotonic propagation of an EPSC in the dendrites of the post-synaptic ALT-PN can take up to 4 ms but, alone, cannot explain the longest latencies observed in our experiments. Therefore, the spike propagation time in the axon of a presynaptic neuron was also estimated.

Conduction time in the axon of a local-circuit neuron

We reconstructed a lamina I local-circuit neuron with its axon covering the SDH area of three segments (Fig. 8*A*), to model possible long conduction times. The axon originated from one of the primary dendrites (Fig. 8*B*) and its length to the first branching point was 228 μm. The axon diameter was 2 μm in the 19 μm-long initial part, but then rapidly decreased to less than 1 μm. The maximum axon path length was 3725 μm (Fig. 8*C*) and the thinnest branches had a diameter of 0.2 μm.

When a 1 ms current pulse was applied to the soma in the model, the spike was initiated in the primary axon, about 20 μm away from its origin (point 0). It took 0.65 ms for the spike to reach the first branching point (1) (Fig. 8*C* and *D*).

We did simulations for several terminal boutons which were within the range of the dendritic field of a typical ALT-PN with the soma located closely to the soma of the reconstructed neuron. Terminal boutons 2 and 3 (Fig. 8*B*) located 64 μm and 118 μm away from the soma (3-D distances) had substantially longer axon paths of 646 μm and 922 μm, respectively (Fig. 8*C*). The spike propagation times to these boutons, located on the same principal branch, were 2.7 and 4.5 ms, respectively (Fig. 8*D*). For the terminal bouton 4 (another axon branch) located 436 μm away from the soma (3-D distance) and connected via the axon path of 952 μm, the spike propagation time was 4.15 ms. For bouton 5, in a dorsomedial position (3-D distance, 585 μm; the axon path length, 2076 μm), the conduction time was 11 ms.

We also did simulations for two terminal boutons located rostrally (6) and caudally (7) beyond the area of a possible contacts with the mediolaterally oriented dendrites of a neighbouring (somata separated by $<$80 μm) ALT-PN. The spike propagation times were 9.2 ms and 10.7 ms, respectively. The longest propagation time (17.4 ms) was obtained for the most remote labelled point (8) of the axon (Fig. 8*C* and *D*).

Thus, a lamina I local-circuit neuron can form synapses with dendrites of neighbouring neurons via long axonal pathways. The conduction in the narrow and highly branched axon may last for about 10 ms. For the

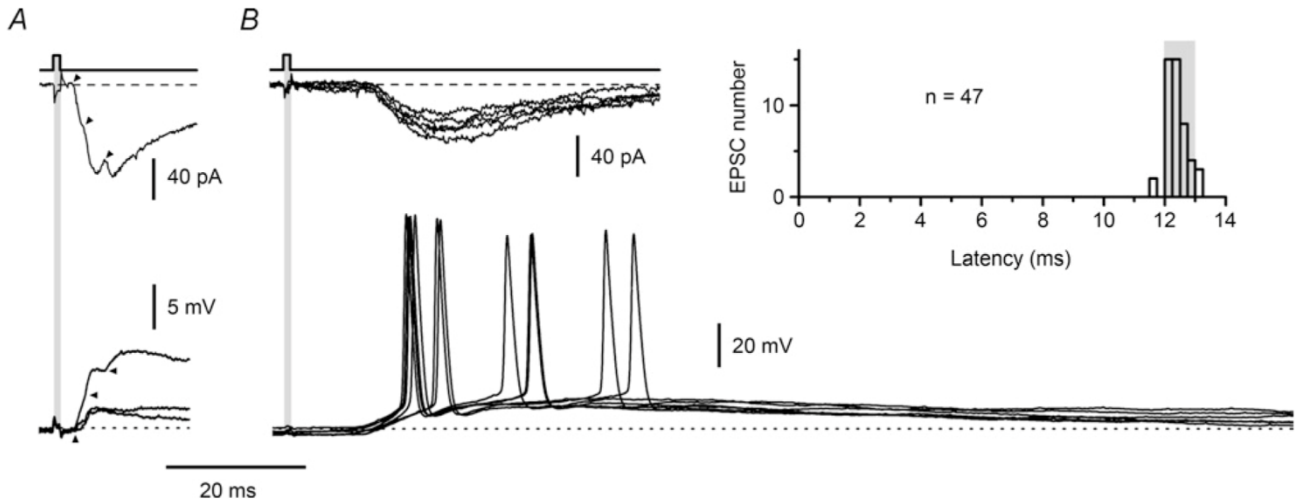


Figure 6. Latency and efficacy of monosynaptic inputs
A, a composite EPSC with three components showing latencies of 2, 3 and 6 ms (indicated by arrowheads). The analysis of the components was done in Fig. 3. In the current-clamp mode, simultaneous activation of all components (uppermost of 3 consecutive traces) increased the membrane depolarization which, however, remained subthreshold. *B*, EPSC evoked in the connection with the longest latency (5 consecutive traces). The histogram shows the distribution of the EPSC latencies measured in 47 episodes. Bin width, 0.25 ms. The mean latency was 12.4 $\pm$ 0.1 ms. For 42 measurements, the latency variation was within 1 ms (a grey bar), and for all 47 measurements within 2 ms. This long-latency input evoked spike firing in each of 6 consecutive stimulations. This connection also showed a shorter-latency monosynaptic component which, however, was not activated in the episodes analysed. In current-clamp, dotted lines indicate a preset potential of $-$70 mV (note different amplifications in *A* and *B*).

© 2010 The Authors. Journal compilation © 2010 The Physiological Society

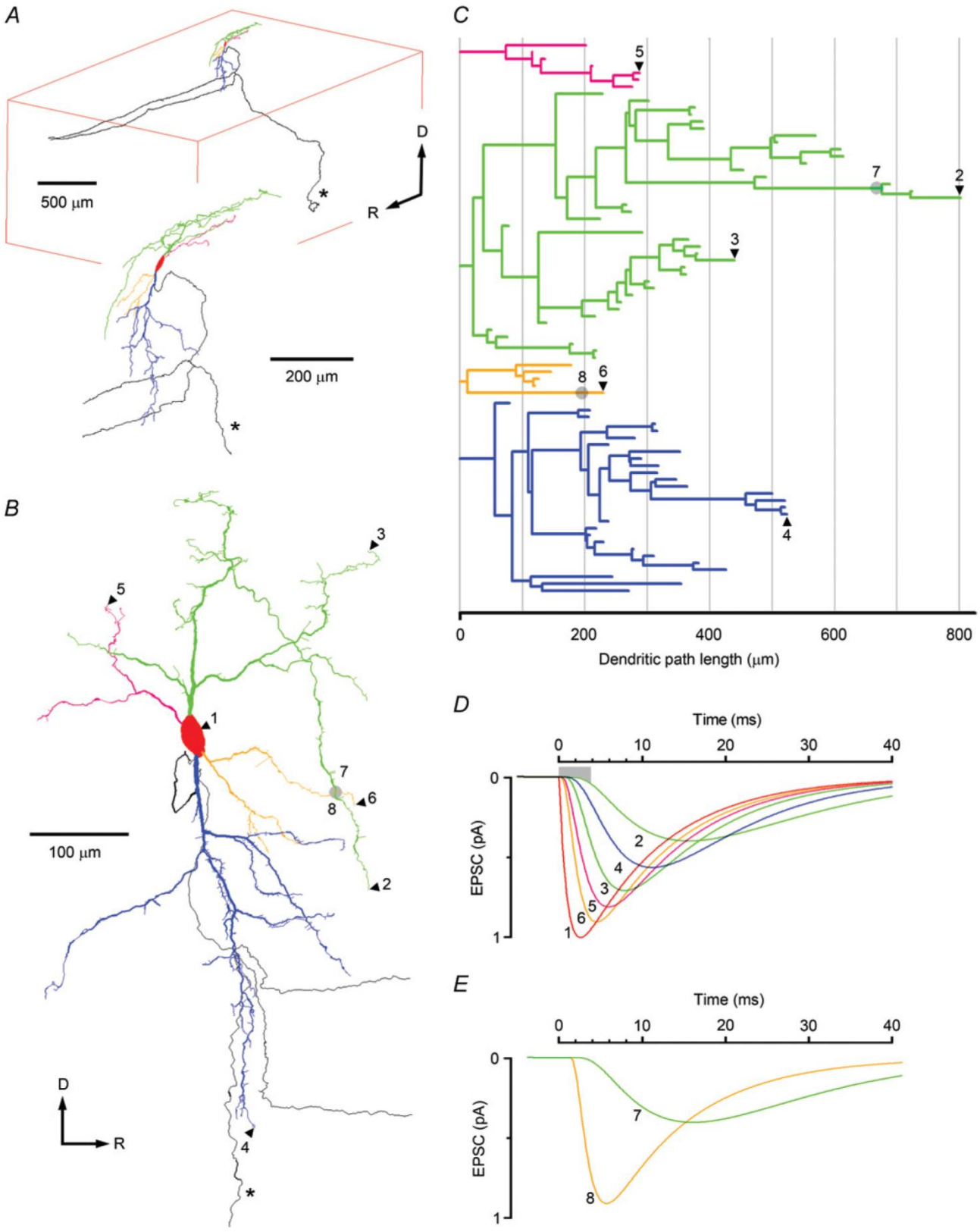


Figure 7. EPSC propagation in the postsynaptic ALT-PN
A, the 3-D reconstruction of the dendrites and axon of an ALT-PN of the lateral-collateral-type. Perspective overview of the neuron depicting the orientation and course of the projecting axon and collaterals. Higher magnification image demonstrates major dendrites restricted to lamina I following the curvature of the dorsal horn surface.

© 2010 The Authors. Journal compilation © 2010 The Physiological Society

connections with more distant neurons, the conduction time may be even longer.

Discussion

We used the isolated spinal cord preparation to record from large lamina I neurons with preserved dendritic trees and axonal arborizations. Our results show that ALT-PNs receive excitatory inputs from other lamina I neurons both directly and indirectly, via intercalated neurons. The axon of a presynaptic neuron forms multiple functional synapses on the dendrites of an ALT-PN and transmitter release activates both CP- and CI-AMPARs. An ALT-PN can receive input from a local-circuit neuron as well as from another ALT-PN. Transmission between lamina I neurons can have a long latency, mostly caused by the spike propagation in the axon of the presynaptic neuron. An input from a lamina I excitatory neuron can be sufficiently strong to evoke spikes in an ALT-PN.

Large lamina I neurons

In our sample from the lateral half of the SDH, 54% of large mediolaterally oriented neurons were identified as ALT-PNs (Szucs *et al.* 2010). The remaining neurons had either a highly branched local axon (like the presynaptic neuron in Fig. 4 and the neuron in Fig. 8) or projected via pathways other than the ALT. In comparison with smaller SG and lamina I neurons (Santos *et al.* 2007, 2009; Pinto *et al.* 2010), the ALT-PNs had lower R_{IN} but a similar slowest membrane time constant, which could be explained by a larger area of the neuronal membrane with a similar density of a K^+ leak conductance. It should be noted that our experiments were focused on large laterally located neurons and, therefore, smaller or medially located ALT-PNs may have different properties.

Organization of synaptic connections in lamina I

Our experiments revealed synaptic connections between large lamina I neurons. The EPSC latencies were distributed in a broad range implying that, in some cases, the signal propagated via long axodendritic pathways.

The postsynaptic delay is caused by the electrotonic EPSC propagation in the dendrites of an ALT-PN. It can be less than 1 ms for synapses in short dendrites or in the proximal parts of long dendrites. However, the propagation may take about 4 ms for distal synapses in long dendrites. This maximum delay was similar to our estimation for SG neurons (Santos *et al.* 2009). In an ALT-PN, different major dendrites may have some overlapping branches. In this case, two spatially close synapses located, however, in different dendritic branches may generate EPSCs with substantially different latencies.

The spike propagation time in the unmyelinated axon of the presynaptic neuron contributes substantially to the EPSC latency. Lamina I local-circuit neurons have extensive and dense axonal arbours and can synapse on ALT-PNs. The axon path can be several times longer than the 3-D distance between the terminal bouton and the soma of the presynaptic neuron. Furthermore, the small diameter of the axon (0.2–1 μm) lowers its conduction velocity, thus increasing the spike propagation time. The architecture of the axon of a local-circuit neuron predicts the spike conduction times of 1–11 ms for a postsynaptic ALT-PN with a closely located soma, and longer times for a more distant neuron. In terms of these findings, shorter EPSC latencies reported by Santos *et al.* (2009) for the SG excitatory interneurons can imply their short axon paths. It is also possible that in that study, using spinal cord slices, the long axodendritic paths were truncated.

In the majority of the cases, an axon of a presynaptic neuron forms multiple synapses on an ALT-PN, which may be a general principle of organization of neuronal connections in the SDH (Santos *et al.* 2009). The inputs from some synapses can be only distinguished on the basis of fast transitions on the EPSC rising phase, whereas others are better separated in time. Each component of a composite EPSC may represent a synapse (or a group of synapses) with its specific dendritic location and presynaptic axon path. Multiple monosynaptic contacts between lamina I neurons may provide a basis for the functional plasticity related to the activation of silent synapses (Santos *et al.* 2009).

In addition to direct contacts, lamina I neurons are also connected to ALT-PNs via intercalated neurons. The polysynaptic inputs show variable latencies consistent with the variation of the spike initiation time in the intercalated neuron (Santos *et al.* 2009). Polysynaptic inputs can be sufficiently strong to increase the excitation of an ALT-PN. Thus, the recruiting of intercalated neurons may

The projecting axon is indicated by an asterisk. Four major dendrites are shown by different colours. *B*, sagittal projection of the reconstructed neuron. Simulations were done for synapses (1–8) inserted on places indicated by arrowheads or a grey circle. *C*, dendrogram (the same colour code and synapse identification numbers as in *B*). *D*, simulations of the somatic voltage-clamp recording of the EPSCs evoked by activation of the corresponding synapses. The delays were measured as a time interval between the transmitter release (0 ms) and the moment when the corresponding EPSC reached 10% of its peak amplitude (shown by a grey bar for the slowest EPSC). *E*, EPSCs arising from two spatially close synapses (7 and 8) located in different major dendrites.

© 2010 The Authors. Journal compilation © 2010 The Physiological Society

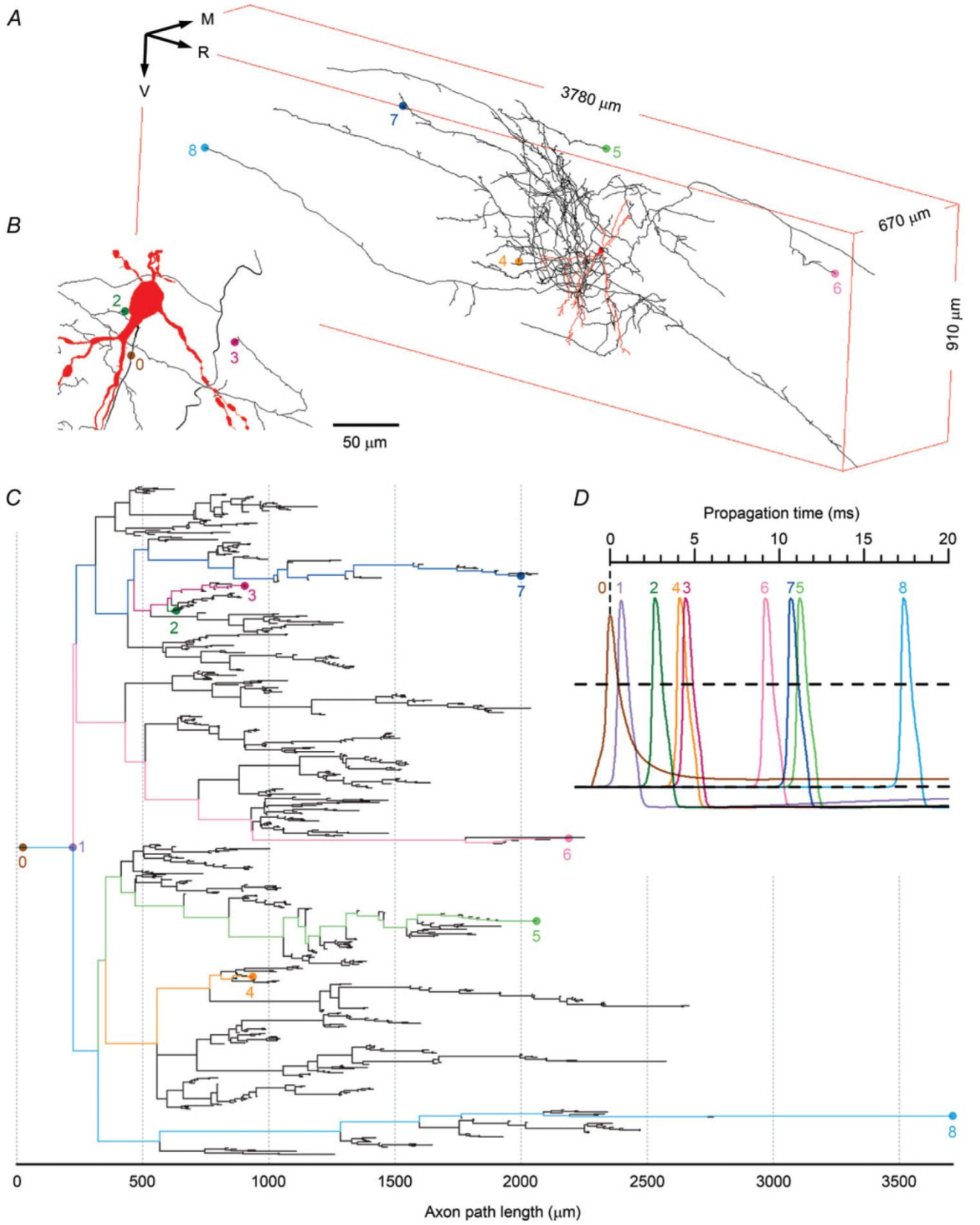


Figure 8. Spike propagation in the axon of a local-circuit neuron
A, the 3-D reconstruction of the axon (black) and dendrites (red) of a large lamina I local-circuit neuron filled with biocytin in whole-cell mode. The highest order of the axon branches was 26. The axon had 647 endings

© 2010 The Authors. Journal compilation © 2010 The Physiological Society

be an additional mechanism increasing efficacy of neuronal connections in the SDH.

We have found that, in many cases, monosynaptic inputs from one neuron can be sufficiently strong to evoke spikes in an ALT-PN. Inputs from different groups of synapses can be integrated to increase the postsynaptic depolarization. Furthermore, monosynaptic connections via different axodendritic paths may broaden the temporal pattern of synaptic input from one neuron. It should be noted that the presence of numerous polysynaptic inputs implied an excitation of an intercalated (intact) neuron. This also supports the idea that release from one SDH neuron can be sufficient to evoke a spike in another neuron (Santos *et al.* 2009).

We show that ALT-PNs communicate with other lamina I neurons via synapses equipped with CP- and CI-AMPARs. Expression of GluR2-lacking CP-AMPARs and GluR2-containing CI-AMPARs in the SDH was shown by immunocytochemistry and EM studies (Nagy *et al.* 2004; Larsson & Broman, 2006; Antal *et al.* 2008; Polgar *et al.* 2008). Physiological activation of CP-AMPARs by transmitter release has recently been reported for synapses formed by the SG excitatory interneurons (Santos *et al.* 2009). CP-AMPARs may provide Ca^{2+} influx and underlie different forms of synaptic plasticity in the SDH (Santos *et al.* 2009) and hippocampus (Oren *et al.* 2009). The CP-AMPAR-dependent plasticity in synapses formed by the interneurons (Santos *et al.* 2009) may be an alternative to the NMDA-receptor-dependent plasticity in the synapses of primary afferents (Ikeda *et al.* 2003). The contribution of CP-AMPARs to transmission in the SDH may further increase under chronic pain conditions (Katano *et al.* 2008; Larsson & Broman, 2008; Vikman *et al.* 2008).

Thus, multiple mono- and polysynaptic inputs from one lamina I neuron can increase its efficacy of exciting an ALT-PN and provide the basis for different forms of functional plasticity.

Lamina I and nociceptive processing

Lamina I is traditionally considered as a relay station conveying thin primary afferent input to supraspinal centres (Molander & Grant, 1995; Lima, 1998; Todd & Koerber, 2006). However, recent studies show that lamina I is an interconnected layer involved in intralaminar, interlaminar and intersegmental spinal processing. Individual lamina I neurons can integrate monosynaptic Aδ- and C-afferent-inputs from several segmental dorsal roots (Pinto *et al.* 2010). Highly branched axons of lamina I local-circuit neurons can interconnect large SDH areas of several segments (Szucs *et al.* 2010; and this study). In addition, the projecting axons of the ALT-PNs give rise to local collaterals connecting lamina I with the dorsal, ventral and lateral spinal cord regions of several neighbouring segments (Szucs *et al.* 2010). As we show here, lamina I neurons are interconnected through groups of functional synapses and intercalated neurons. The intralaminar neuronal connectivity has also been shown by the laser-scanning photostimulation technique (Kato *et al.* 2009). An overall prevalence of local-circuit neurons over the PNs in lamina I (Bice & Beal, 1997; Spike *et al.* 2003; Todd & Koerber, 2006) can further emphasize the functional importance of the intralaminar processing. Therefore, future investigations of the neuronal network organization in lamina I will be necessary for the better understanding of signal processing in this spinal nociceptive projection area.

References

Antal M, Fukazawa Y, Eordogh M, Muszil D, Molnar E, Itakura M, Takahashi M & Shigemoto R (2008). Numbers, densities, and colocalization of AMPA- and NMDA-type glutamate receptors at individual synapses in the superficial spinal dorsal horn of rats. *J Neurosci* **28**, 9692–9701.

Bice TN & Beal JA (1997). Quantitative and neurogenic analysis of the total population and subpopulations of neurons defined by axon projection in the superficial dorsal horn of the rat lumbar spinal cord. *J Comp Neurol* **388**, 550–564.

Cajal RyS (1909). *Histologie du systeme nerveux de l'homme et des vertebres*. A. Maloine, Paris.

Drummond GB (2009). Reporting ethical matters in *The Journal of Physiology*: standards and advice. *J Physiol* **587**, 713–719.

Graham BA, Brichta AM & Callister RJ (2007). Moving from an averaged to specific view of spinal cord pain processing circuits. *J Neurophysiol* **98**, 1057–1063.

Grudt TJ & Perl ER (2002). Correlations between neuronal morphology and electrophysiological features in the rodent superficial dorsal horn. *J Physiol* **540**, 189–207.

and 4588 varicosities. Note that some of the longest branches were truncated. Axonal points for which the spike propagation simulation was done are labelled by coloured circles. *B*, higher magnification image demonstrating the axon (black) in the vicinity of the soma (red). The axon originated from a primary dendrite (red). In simulation, the spike was initiated in the primary axon at point 0 (stimulation was applied to the soma). *C*, axogram with indication of simulation points and their axon paths (indicated by the corresponding colours). The common parts of the axon paths are shown by the colour of the longer path. *D*, simulation of the spike propagation to points 1–8. The propagation time was counted from the moment of the spike initiation in the primary axon (point 0). Dashed lines correspond to potentials of 0 mV and −70 mV.

© 2010 The Authors. Journal compilation © 2010 The Physiological Society

Hines M (1993). NEURON – A program for stimulation of nerve equation. In *Neural Systems: Analysis and Modeling*, ed. Eeckman F, pp. 127–136. Kluwer Academic Publishers, Boston.

Hines ML & Carnevale NT (1997). The NEURON simulation environment. *Neural Comput* **9**, 1179–1209.

Ikeda H, Heinke B, Ruscheweyh R & Sandkuhler J (2003). Synaptic plasticity in spinal lamina I projection neurons that mediate hyperalgesia. *Science* **299**, 1237–1240.

Katano T, Furue H, Okuda-Ashitaka E, Tagaya M, Watanabe M, Yoshimura M & Ito S (2008). N-ethylmaleimide-sensitive fusion protein (NSF) is involved in central sensitization in the spinal cord through GluR2 subunit composition switch after inflammation. *Eur J Neurosci* **27**, 3161–3170.

Kato G, Kawasaki Y, Koga K, Uta D, Kosugi M, Yasaka T, Yoshimura M, Ji RR & Strassman AM (2009). Organization of intralaminar and translaminar neuronal connectivity in the superficial spinal dorsal horn. *J Neurosci* **29**, 5088–5099.

Larsson M & Broman J (2006). Pathway-specific bidirectional regulation of Ca^{2+}/calmodulin-dependent protein kinase II at spinal nociceptive synapses after acute noxious stimulation. *J Neurosci* **26**, 4198–4205.

Larsson M & Broman J (2008). Translocation of GluR1-containing AMPA receptors to a spinal nociceptive synapse during acute noxious stimulation. *J Neurosci* **28**, 7084–7090.

Lima D (1998). Anatomical basis for the dynamic processing of nociceptive input. *Eur J Pain* **2**, 195–202.

Lima D & Almeida A (2002). The medullary dorsal reticular nucleus as a pronociceptive centre of the pain control system. *Prog Neurobiol* **66**, 81–108.

Lima D & Coimbra A (1986). A Golgi study of the neuronal population of the marginal zone (lamina I) of the rat spinal cord. *J Comp Neurol* **244**, 53–71.

Lu Y & Perl ER (2005). Modular organization of excitatory circuits between neurons of the spinal superficial dorsal horn (laminae I and II). *J Neurosci* **25**, 3900–3907.

Melnick IV, Santos SF & Safronov BV (2004*a*). Mechanism of spike frequency adaptation in substantia gelatinosa neurones of rat. *J Physiol* **559**, 383–395.

Melnick IV, Santos SF, Szokol K, Szucs P & Safronov BV (2004*b*). Ionic basis of tonic firing in spinal substantia gelatinosa neurons of rat. *J Neurophysiol* **91**, 646–655.

Molander C & Grant G (1995). Spinal cord cytoarchitecture. In *The Rat Nervous System*, 2nd edn, ed. Paxinos G, pp. 39–44. Academic Press, San Diego.

Nagy GG, Al-Ayyan M, Andrew D, Fukaya M, Watanabe M & Todd AJ (2004). Widespread expression of the AMPA receptor GluR2 subunit at glutamatergic synapses in the rat spinal cord and phosphorylation of GluR1 in response to noxious stimulation revealed with an antigen-unmasking method. *J Neurosci* **24**, 5766–5777.

Oren I, Nissen W, Kullmann DM, Somogyi P & Lamsa KP (2009). Role of ionotropic glutamate receptors in long-term potentiation in rat hippocampal CA1 oriens-lacunosum moleculare interneurons. *J Neurosci* **29**, 939–950.

Pinto V, Derkach VA & Safronov BV (2008*a*). Role of TTX-sensitive and TTX-resistant sodium channels in Aδ- and C-fiber conduction and synaptic transmission. *J Neurophysiol* **99**, 617–628.

Pinto V, Szucs P, Derkach VA & Safronov BV (2008*b*). Monosynaptic convergence of C- and Aδ-afferent fibres from different segmental dorsal roots on to single substantia gelatinosa neurones in the rat spinal cord. *J Physiol* **586**, 4165–4177.

Pinto V, Szucs P, Lima D & Safronov BV (2010). Multisegmental Aδ- and C-fiber input to neurons in lamina I and the lateral spinal nucleus. *J Neurosci* **30**, 2384–2395.

Polgar E, Watanabe M, Hartmann B, Grant SG & Todd AJ (2008). Expression of AMPA receptor subunits at synapses in laminae I–III of the rodent spinal dorsal horn. *Mol Pain* **4**, 5.

Safronov BV (1999). Spatial distribution of Na^+ and K^+ channels in spinal dorsal horn neurones: role of the soma, axon and dendrites in spike generation. *Prog Neurobiol* **59**, 217–241.

Safronov BV, Pinto V & Derkach VA (2007). High-resolution single-cell imaging for functional studies in the whole brain and spinal cord and thick tissue blocks using light-emitting diode illumination. *J Neurosci Methods* **164**, 292–298.

Safronov BV, Wolff M & Vogel W (1997). Functional distribution of three types of Na^+ channel on soma and processes of dorsal horn neurones of rat spinal cord. *J Physiol* **503**, 371–385.

Santos SF, Luz LL, Szucs P, Lima D, Derkach VA & Safronov BV (2009). Transmission efficacy and plasticity in glutamatergic synapses formed by excitatory interneurons of the substantia gelatinosa in the rat spinal cord. *PLoS One* **4**, e8047.

Santos SF, Melnick IV & Safronov BV (2004). Selective postsynaptic inhibition of tonic-firing neurons in substantia gelatinosa by mu-opioid agonist. *Anesthesiology* **101**, 1177–1183.

Santos SF, Rebelo S, Derkach VA & Safronov BV (2007). Excitatory interneurons dominate sensory processing in the spinal substantia gelatinosa of rat. *J Physiol* **581**, 241–254.

Spike RC, Puskar Z, Andrew D & Todd AJ (2003). A quantitative and morphological study of projection neurons in lamina I of the rat lumbar spinal cord. *Eur J Neurosci* **18**, 2433–2448.

Szucs P, Luz LL, Lima D & Safronov BV (2010). Local axon collaterals of lamina I projection neurons in the spinal cord of young rats. *J Comp Neurol* **518**, 2645–2665.

Szucs P, Pinto V & Safronov BV (2009). Advanced technique of infrared LED imaging of unstained cells and intracellular structures in isolated spinal cord, brainstem, ganglia and cerebellum. *J Neurosci Methods* **177**, 369–380.

Todd AJ & Koerber R (2006). Neuroanatomical substrates of spinal nociception. In *Wall and Melzack's Textbook of Pain*, 5th edn, ed. McMahon SB & Koltzenburg M, pp. 73–90. Churchill Livingstone, Edinburgh, UK.

Todd AJ, McGill MM & Shehab SA (2000). Neurokinin 1 receptor expression by neurons in laminae I, III and IV of the rat spinal dorsal horn that project to the brainstem. *Eur J Neurosci* **12**, 689–700.

Vikman KS, Rycroft BK & Christie MJ (2008). Switch to Ca^{2+}-permeable AMPA and reduced NR2B NMDA receptor-mediated neurotransmission at dorsal horn nociceptive synapses during inflammatory pain in the rat. *J Physiol* **586**, 515–527.

Waldeyer W (1889). *Das Gorilla-Rückenmark*. Königliche Akademie der Wissenschaften, Berlin.

© 2010 The Authors. Journal compilation © 2010 The Physiological Society

Willis WD & Coggeshall RE (1991). *Sensory Mechanisms of the Spinal Cord*. John Wiley & Sons, New York.

Author contributions

The experiments were performed in IBMC (University of Porto). All authors have contributed to (1) conception and design of the experiments, (2) collection, analysis and interpretation of data, and (3) drafting the article or revising it critically for important intellectual content. All authors approved the final version of the manuscript.

Acknowledgements

The work was supported by the grant from the Portuguese Foundation for Science and Technology funded by COMPETE and FEDER. We thank Miklós Antal for providing the Neurolucida system.

© 2010 The Authors. Journal compilation © 2010 The Physiological Society

Publication III

Morphological analysis of lamina I local-circuit neurons of the lumbar spinal dorsal horn of rats (In preparation)

Szucs P, Luz LL, Pinho R, Aguiar P, Antal Zs, Tiong SY, Todd A, Safronov BV.

The third task of my work was to characterize non-projecting neurons in lamina I. Although these neurons give the majority of the lamina I neuronal population and most likely fall into the already established somatodendritic groups, almost nothing is known about their axons and synaptic contacts. While characterizing the axon trajectories and connectivity of lamina I projection neurons (Szucs et al., 2010; Luz et al., 2010), we have encountered an intriguing population of lamina I neurons, named local-circuit neurons (LCNs), defined by an extensive local axon and characteristic discharge patterns in response to the depolarizing current injections. We have recorded and filled 97 neurons that were identified as LCNs based on the lack of a projection axon in the contralateral white matter and the presence of a dense local axon with numerous varicosities. In 76 cases we revealed sufficient amount of axon to perform quantitative analysis on the axon and these 76 cells form the base of this study. The electrophysiology and morphology methods used in this study were identical to those utilized in the previous two. The result of this work is presently being prepared for publication. Below, a short summary of the major findings is given.

Morphological features of LCNs

Neurons in this group mostly had relatively large somata, comparable to those of the ALT-projection neurons in the previous two studies (longest cross-sectional soma diameter: 20-30 micrometers). With a few exceptions that could not be classified based on the criteria of Lima and Coimbra (1986), they were of the flattened and multipolar (usually large multipolar) types (Figure 1A-B). Dendrites in both cases were extensive; however in case of large multipolar neurons apparent ventral dendrites, reaching down into lamina II-III, were always present (Figure 1C). Dendritic spines were encountered less frequently and in smaller numbers than in case of ALT-projection neurons.

The initial myelinated part of the axon frequently had a contorted path (with dorsoventral and/or mediolateral loops) while giving rise to several unmyelinated small-diameter branches running either rostrally or caudally and branching further in acute angles. The axons had a complicated branching pattern, often with branches above the 20th branching order (see Figure 8 in Luz *et al.*, 2010). Distal and terminal branches had densely packed large (1-2 micrometers)

varicosities. The complete axon showed an extensive rostrocaudal (up to 3-4 segments) and mediolateral (covering almost the whole extent of the dorsal horn) distribution. The axons also protruded ventrally into deeper layers of the dorsal horn, reaching lamina III-IV (Figure 1D). Although this dense local axon appears to be similar, the axonal branching pattern, varicosity densities along the axonal tree and terminal field locations seem to show substantial heterogeneity within the population.

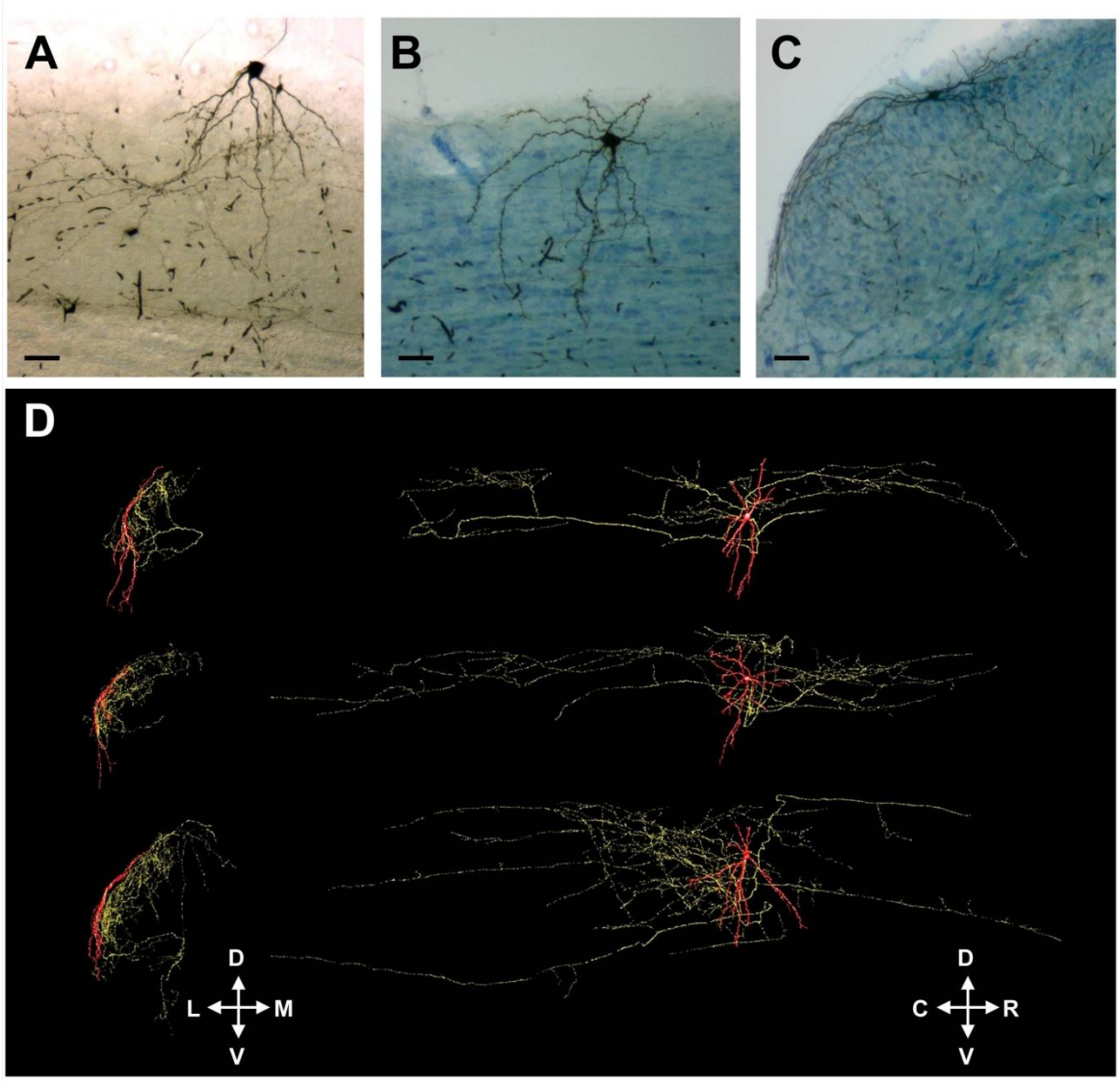


Figure 1 – Different appearance of LCNs. **A-B**: Low-magnification images of two LCNs with distinct types of large somata (A - flattened type; B - multipolar type; scale bar: 50 µm). **C**: Example of large multipolar neuron with clear ventral dendrites, reaching down into lamina II-III (scale bar: 50 µm). **D**: 3-D reconstruction of the dendrites and densely branching axon of 3 LCNs. Note that these axons have an extensive mediolateral distribution and also protruded ventrally into deeper layers of the dorsal horn, which can reach lamina III-IV (soma and dendrites – red; axon - yellow).

Neurochemical characteristics of LCNs

In an international collaboration with Andrew Todd (Glasgow, UK) we have performed double and triple immunocytochemistry on individually labelled LCNs to reveal the neurotransmitter content of their axon terminals. From the 21 neurons that were used for immunocytochemical analysis of the neurotransmitter content of their axon varicosities, 16 were immunoreactive for vesicular GABA transporter (VGAT) and negative for vesicular glutamate transporter 2 (VGLUT2). The immunostaining was not conclusive in 4 neurons, most likely due to fixation problems or the deterioration of the tissue during the experiments, while 1 neuron was negative for both VGAT and VGLUT2.

In a collaboration with Zita Puskar (Budapest, Hungary) we also showed that the somata and dendrites of LCNs occasionally expressed the NK1r (Figure 2A). We also performed pharmacology experiments to clarify this result and found that one-third of the tested LCNs (13 out of 39) responded to the application of Substance P (1µM) with a characteristic inward current (Figure 2B). When recorded in current-clamp mode the same current caused depolarization that was often suprathreshold and resulted in sustained action potential firing (not shown).

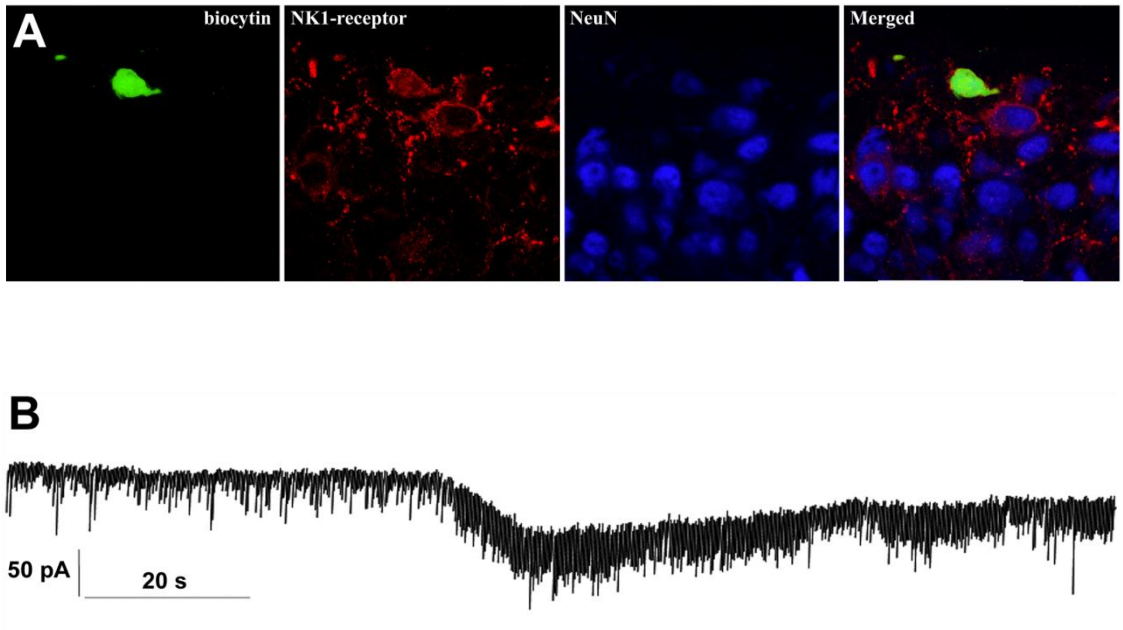


Figure 2 – Presence of NK1r in lamina I LCNs. **A**: These images shows a confocal optical slice through part of lamina I in a section immunostained to reveal the expression of NK1r (shown in red), the neuronal marker NeuN (shown in blue). **B**: Voltage-clamp recording of a LCN during substance P application (1microM).

Electrophysiology of LCNs

All recorded LCNs shared a common feature of responding with tonic discharge to depolarizing current injections. They presented a variable amplitude afterhyperpolarization and occasionally showed an additional after depolarization. When compared their average resting membrane potential and input resistance to the ALT-projection neurons from our previous two papers, they were lower and higher, respectively. Interestingly some of the LCNs showed rhythmic activity (i.e. spontaneous rhythmic action potential discharge) at resting membrane potentials. This feature to our knowledge is unique in the spinal dorsal horn.

Conclusions

Recently, Pinto et al. (2010) reported that some lamina I neurons receive (and most likely integrate) monosynaptic primary afferent input from up to six segmental dorsal roots. Although morphological recovery in that study was not conclusive, the occasional partially recovered neurons showed similar features to the LCNs in this study.

Taken together, these data allow to suggest that we described a well-defined, most likely inhibitory interneuron population in lamina I. In our previous work on the local synaptic connections of lamina I ALT-projection neurons we could not find any inhibitory connections onto ALT-projection neurons when selecting presynaptic neurons in lamina I. Thus it is likely that this inhibitory LCN population do not target ALT-projection neurons in lamina I. Judging from the axon distribution of the LCNs, their potential targets may reside in lamina I (neurons other than ALT-projection neurons) and also in lamina II-IV. Dendritic distribution patterns and their NK1r expression suggest that LCNs receive similar (if not identical) input as ALT-projection neurons and they distribute this information along several segments and laminae. Thus our observations indicate that these neurons act as intersegmental as well as interlaminar integrators, providing anatomical substrate for rostrocaudal "processing units" in the dorsal horn.

FINAL REMARKS

Lamina I is a major pain processing area in the spinal cord. Although morphology and physiology of supraspinally-projecting neurons and interneurons have been intensively studied, the complex pattern of neuronal connections in this region is still poorly understood.

This deficit of knowledge was, at least in part, due to the lack of approaches enabling recording from visually-identified neurons in their natural environment. However, the recent development of the infrared-light emitting diode (IR-LED) oblique illumination technique allowed to perform electrophysiological recordings from visually-identified lamina I neurons in the intact spinal cord (Szucs *et al.*, 2009). With this approach we were able to reveal the complex structure of labelled lamina I neurons and follow both axons and dendrites for several hundreds of micrometers along the rostrocaudal, mediolateral and dorsoventral axes. The major findings that emerged from this study are listed below.

1. **Local axon collaterals of lamina I projection neurons**

The role of a neuron in a network is determined by two key factors, input and output, which, from an anatomical point of view, depend on the organization of its dendritic and axonal trees, respectively. The dendritic structure of lamina I neurons has been extensively studied (Ramon y Cajal, 1909; Light *et al.*, 1979; Lima & Coimbra, 1986). Although the key function of lamina I projection neurons in nociceptive processing has long been described, the organization of the axon collaterals of these neurons is still largely elusive. Authors generally agree that local axon collaterals may have a significant contribution to intraspinal connections, however, collaterals of lamina I projection neurons have not been described systematically.

In the first publication, we performed 2-D reconstructions of complete lamina I biocytin-labelled neurons projecting in the contralateral ALT. We observed that almost ¾ of the ALT-projection neurons gave rise to various types of axon collaterals on the ipsilateral side. Based on the trajectory and location of collaterals (dorsal, lateral and ventral), we could propose distinct ipsilateral target areas for the

different projection neuron types giving rise to one type of collaterals (or combination of them; mixed-collateral type).

The distribution of dorsal collaterals suggests that their postsynaptic target include neighbouring areas within lamina I (dorsal-collateral type I) or laminae II–IV (dorsal-collateral type II neurons). The rostrocaudal extent of these collaterals suggests that their postsynaptic targets are located within the same segment. These results strongly support the idea that some lamina I neurons may have both segmental and supraspinal connections. Projection neurons could recruit neighbouring lamina I neurons, some of which may also be projection neurons targeting the same (or other) supraspinal areas.

Lateral collaterals occupied the dorsal part of the lateral funiculus targeting rostral segments and, occasionally, extending caudally. Several studies demonstrated that multisegmental integration can occur within lamina I, and most authors attributed this role to specific sets of propriospinal neurons. However, our results imply that some of these propriospinal axons are ipsilateral collaterals of ALT-projection neurons located in the lateral half of lamina I. Furthermore, the trajectory of the lateral collaterals of ALT-projection neurons revealed in our study strongly supports the idea that these collaterals may provide input for the LSN. Taken together, our data suggest that, besides their principal function, lamina I projection neurons with lateral collaterals can be involved in inter- and/or multisegmental integration and can provide input for LSN neurons.

Ventral collaterals typically had a limited rostrocaudal spread but also larger and variable mediolateral and dorsoventral extents. This distribution suggests that neurons giving rise to ventral collaterals establish connections with neurons in deeper laminae (V–VII). A recent study by Braz & Basbaum (2009) demonstrated that neurons in deep laminae (III–V) receive polysynaptic inputs from unmyelinated primary afferents. The authors presumed that this input is via interneurons of laminae I–II. Apart from some lamina II islet and stalked neurons projecting to deeper laminae (Eckert *et al.*, 2003), the ventral collaterals of ventral-collateral type (VCT) and mixed-collateral type (MCT) lamina I neurons described here may also establish such connections. In this way, the ventral collaterals can link parallel pain pathways originating from laminae I and V (Braz *et al.*, 2005). Thus, our findings further support the hypothesis of sensory information “flow” from

superficial to deeper laminae of the dorsal horn (Wall, 1960; Braz & Basbaum, 2009).

Identifying the postsynaptic targets of ipsilateral collaterals may reveal local network functions of lamina I projection neurons. Collaterals of other principal neurons in the spinal cord are known to contribute to such networks (Renshaw, 1946; Morgan *et al.*, 1991). To the best of our knowledge, involvement of ALT-projection neurons in local spinal processing has not been described so far. From this point of view, MCT cells with their diverse types of collaterals form probably the most intriguing group of lamina I neurons. They seem to play a very complex role involving participation in local circuits, establishing propriospinal connections, and at the same time serving as major supraspinal output elements of the dorsal horn network. MCT neurons with extensive dendritic trees and diverse axon collaterals are capable of interconnecting broad spinal cord regions.

In conclusion, lamina I ALT-projection neurons give rise to distinct types of ipsilateral axon collaterals. We propose that these collaterals are important determinants of the complex function of projection neurons and can serve as basis for their classification. Eventually, detailed description of collateral connections of lamina I projection neurons will be crucial for a better understanding of their roles in spinal sensory processing.

2. Organization of synaptic connections in lamina I

As mentioned above, the role of a neuron in a network is determined by two key factors, input and output. Although we know sufficiently about the supraspinal targets of ALT-projection neurons, their input from neighbouring lamina I neurons was poorly understood. Therefore, in the second part of the work (second publication) we studied synaptic connections between lamina I neurons.

In this publication we demonstrate that an ALT-projection neuron can receive input from a LCN as well as from another ALT-projection neuron and in the majority of the cases, the axon of these presynaptic neurons forms multiple synapses along the somatodendritic domain of the ALT-projection neuron. These results support our earlier suggestion that this may be a general principle of organization of neuronal connections in the spinal dorsal horn (Santos *et al.*, 2009). Each component of a

composite excitatory postsynaptic current (EPSC) may represent one of these synapses (or a group of synapses) with its specific dendritic location and presynaptic axon path. In addition to direct contacts, lamina I neurons are also connected to ALT-projection neurons via intercalated neurons. The polysynaptic inputs show variable latencies consistent with the variation of the spike initiation time in the intercalated neuron (Santos *et al.*, 2009). We have also found that, in many cases, monosynaptic inputs from one neuron can be sufficiently strong to evoke spikes in an ALT-projection neuron. Inputs from different groups of synapses can be integrated to increase the postsynaptic depolarization.

Since in our experiments the EPSC latencies were distributed in a broad range, we decided to study whether such latencies could be explained by the conduction times in pre- and postsynaptic neurons. To estimate these delays, we did computer simulations using the models based on detailed 3-D reconstructions of the dendritic and axonal branches of a postsynaptic projection neuron and a presynaptic lamina I LCN. The postsynaptic delay is caused by the electrotonic EPSC propagation in the dendrites of an ALT-projection neuron and it can be between 1-4 ms. The maximum delay was similar to Santos *et al.* (2009) estimation for lamina II neurons. The spike propagation time in the unmyelinated axon of the presynaptic neuron also contributes substantially to the EPSC latency. As lamina I LCNs can synapse on ALT-projection neurons and they have extensive axons, we decided to do simulation of spike propagation delay in a 3-D reconstruction of one of these neurons. The axonal architecture of a LCN predicts spike conduction times of 1-11 ms. In the light of these findings, shorter EPSC latencies reported by Santos *et al.* (2009) for the lamina II excitatory interneurons can either imply inherent shorter axo-dendritic paths or that by using spinal cord slices, the long axo-dendritic paths were truncated.

To elucidate the type of postsynaptic neurotransmitter receptors on ALT-projection neurons we studied the effects of specific blockers. The experiments allowed us to conclude that ALT-projection neurons communicate with other lamina I neurons via synapses equipped with Ca^{2+} permeable (CP)- and Ca^{2+} impermeable (CI)-AMPARs. CP-AMPARs may provide Ca^{2+} influx and underlie different forms of synaptic plasticity in the SDH (Santos *et al.*, 2009) and hippocampus (Oren *et al.*, 2009). The CP-AMPAR-dependent plasticity in synapses formed by the interneurons (Santos *et al.*, 2009) may be an alternative to the NMDA-receptor-dependent plasticity in the synapses of primary afferents (Ikeda *et al.*, 2003). The contribution of CP-AMPARs

to transmission in the superficial dorsal horn may further increase under chronic pain conditions (Larsson & Broman, 2008; Vikman *et al.*, 2008; Kato *et al.*, 2009).

From this study we concluded that besides their main function of projecting to supraspinal areas, ALT-projection neurons are also involved in intralaminar connections with other lamina I neurons. Lamina I ALT-projection neurons can receive excitatory inputs from other lamina I neurons, like LCNs or others ALT-projection neurons (directly and indirectly). The axon of a presynaptic neuron forms multiple functional synapses on the dendrites of an ALT-projection neuron and the transmitter release activates both CP- and CI-AMPARs. The transmission between lamina I neurons can have a long latency, mostly caused by the spike propagation in the axon of the presynaptic neuron. An input from a lamina I excitatory neuron can be sufficiently strong to evoke spikes in an ALT-projection neuron.

3. Morphological description of LCNs

We have revealed an intriguing neuronal population in lamina I, defined by an extensive local axon collateral network and characteristic discharge patterns in response to depolarizing current pulse injection. For the medullary dorsal horn of rats, Li et al. (2000) described large local axonal arbors in the vicinity of the somata of putative projection neurons. The overall appearance of some of those cells was very similar to that of our LCNs. Typically, the initial myelinated part of the axon gave rise to several unmyelinated small-diameter branches, showing an extensive rostrocaudal, mediolateral and dorsoventral distribution. Although the axonal distribution pattern of these LCNs appear to be homogenous, their initial branching order, varicosity densities along axonal tree and terminal field locations seem to show substantial heterogeneity within the population.

Furthermore, the dendritic distribution patterns and their NK1r expression suggest that LCNs receive similar input as ALT-projection neurons and they distribute this information along several segments and laminae. Our preliminary immunocytochemical results indicate that a subset of these neurons are inhibitory. Taking into consideration the results in our previous work (second publication), where we could not find any inhibitory input to ALT-projection neurons from other lamina I neurons, one could assume that this subpopulation of inhibitory neurons does not target large ALT-projection neurons.

In conclusion, our results suggested that LCNs form intersegmental as well as interlaminar connections and may regulate several neuronal ensembles, providing anatomical substrate for rostrocaudal “processing units” in the dorsal horn.

The data forming the basis of this dissertation allow us to conclude that the structural organization of lamina I neurons is far more complicated than previously thought. The detailed study of their axonal morphologies may be the key to the understanding of their complex function. We have shown that lamina I neurons can form intralaminar, interlaminar as well as intersegmental connections. These findings provide new important perspectives for understanding the functional and structural organization of neuronal circuits in this principal spinal nociceptive projecting area.

4. Remaining questions and future directions

"Somewhere, something incredible is waiting to be known".
Dr. Carl Sagan (1934-1996)

The results of this study have important implications on our current understanding of the functional significance of lamina I neurons within the dorsal horn network. Some questions, however, remain open and new ones also emerge:

- Our sample was biased because small and medium-sized neurons were not studied and neurons in the medial part of lamina I close to the dorsal root entry zone were not accessible. Are these neurons different from the anatomical point of view?
- Frequently, in more than 2/3 of the cases, the main axon of ALT-projection neurons branched from a stem dendrite, instead of originating directly from the cell body. What is the functional significance of this dendritic origin? How different is the intermittent dendritic region in relation to the expression pattern of transmitter receptors and voltage-gated ion channels?
- What are the major local spinal inputs and outputs of LCNs?
- What is the neurochemical nature of LCNs and what kind of neurotransmitters do they release for their synaptic transmission?
- What are the functional consequences of the complex topology of the axons of the LCNs for conduction delay and transmitter release at thousands of axonal synapses?

REFERENCES

Al-Khater KM, Kerr R & Todd AJ. (2008). A quantitative study of spinothalamic neurons in laminae I, III, and IV in lumbar and cervical segments of the rat spinal cord. *J Comp Neurol* 511, 1-18.

Al-Khater KM & Todd AJ. (2009). Collateral projections of neurons in laminae I, III, and IV of rat spinal cord to thalamus, periaqueductal gray matter, and lateral parabrachial area. *J Comp Neurol* 515, 629-646.

Al Ghamdi KS, Polgar E & Todd AJ. (2009). Soma size distinguishes projection neurons from neurokinin 1 receptor-expressing interneurons in lamina I of the rat lumbar spinal dorsal horn. *Neuroscience* 164, 1794-1804.

Almeida TF, Roizenblatt S & Tufik S. (2004). Afferent pain pathways: a neuroanatomical review. *Brain Res* 1000, 40-56.

Alvarez FJ, Villalba RM, Carr PA, Grandes P & Somohano PM. (2000). Differential distribution of metabotropic glutamate receptors 1a, 1b, and 5 in the rat spinal cord. *J Comp Neurol* 422, 464-487.

Antal M, Petko M, Polgar E, Heizmann CW & Storm-Mathisen J. (1996). Direct evidence of an extensive GABAergic innervation of the spinal dorsal horn by fibres descending from the rostral ventromedial medulla. *Neuroscience* 73, 509-518.

Antal M, Polgar E, Chalmers J, Minson JB, Llewellyn-Smith I, Heizmann CW & Somogyi P. (1991). Different populations of parvalbumin- and calbindin-D28k-immunoreactive neurons contain GABA and accumulate 3H-D-aspartate in the dorsal horn of the rat spinal cord. *J Comp Neurol* 314, 114-124.

Averill S, McMahon SB, Clary DO, Reichardt LF & Priestley JV. (1995). Immunocytochemical localization of trkA receptors in chemically identified subgroups of adult rat sensory neurons. *Eur J Neurosci* 7, 1484-1494.

Basbaum AI, Bautista DM, Scherrer G & Julius D. (2009). Cellular and molecular mechanisms of pain. *Cell* 139, 267-284.

Basbaum AI & Jessel TM. (2000). The Perception of Pain. In *Principles of Neural Science*, 4th edn, ed. Kandel ER, Schwartz JH & Jessell TM, pp. 472-491. McGraw-Hill, New York.

Beal JA, Penny JE & Bicknell HR. (1981). Structural diversity of marginal (lamina I) neurons in the adult monkey (Macaca mulatta) lumbosacral spinal cord: a golgi study. *J Comp Neurol* 202, 237-254.

Bennett GJ, Abdelmoumene M, Hayashi H, Hoffert MJ & Dubner R. (1981). Spinal cord layer I neurons with axon collaterals that generate local arbors. *Brain Res* 209, 421-426.

Bernard JF & Besson JM. (1990). The spino(trigemino)pontoamygdaloid pathway: electrophysiological evidence for an involvement in pain processes. *J Neurophysiol* 63, 473-490.

Berthele A, Boxall SJ, Urban A, Anneser JM, Zieglgansberger W, Urban L & Tolle TR. (1999). Distribution and developmental changes in metabotropic glutamate receptor messenger RNA expression in the rat lumbar spinal cord. *Brain Res Dev Brain Res* 112, 39-53.

Bice TN & Beal JA. (1997a). Quantitative and neurogenic analysis of neurons with supraspinal projections in the superficial dorsal horn of the rat lumbar spinal cord. *J Comp Neurol* 388, 565-574.

Bice TN & Beal JA. (1997b). Quantitative and neurogenic analysis of the total population and subpopulations of neurons defined by axon projection in the superficial dorsal horn of the rat lumbar spinal cord. *J Comp Neurol* 388, 550-564.

Biella G, Riva L & Sotgiu ML. (1997). Interaction between neurons in different laminae of the dorsal horn of the spinal cord. A correlation study in normal and neuropathic rats. *Eur J Neurosci* 9, 1017-1025.

Bing Z, Villanueva L & Le Bars D. (1990). Ascending pathways in the spinal cord involved in the activation of subnucleus reticularis dorsalis neurons in the medulla of the rat. *J Neurophysiol* 63, 424-438.

Bowker RM, Westlund KN & Coulter JD. (1981). Origins of serotonergic projections to the spinal cord in rat: an immunocytochemical-retrograde transport study. *Brain Res* 226, 187-199.

Braz JM & Basbaum AI. (2009). Triggering genetically-expressed transneuronal tracers by peripheral axotomy reveals convergent and segregated sensory neuron-spinal cord connectivity. *Neuroscience* 163, 1220-1232.

Braz JM, Nassar MA, Wood JN & Basbaum AI. (2005). Parallel "pain" pathways arise from subpopulations of primary afferent nociceptor. *Neuron* 47, 787-793.

Broman J. (1994). Neurotransmitters in subcortical somatosensory pathways. *Anat Embryol (Berl)* 189, 181-214.

Burstein R, Cliffer KD & Giesler GJ, Jr. (1987). Direct somatosensory projections from the spinal cord to the hypothalamus and telencephalon. *J Neurosci* 7, 4159-4164.

Burstein R, Cliffer KD & Giesler GJ, Jr. (1990a). Cells of origin of the spinohypothalamic tract in the rat. *J Comp Neurol* 291, 329-344.

Burstein R, Dado RJ & Giesler GJ, Jr. (1990b). The cells of origin of the spinothalamic tract of the rat: a quantitative reexamination. *Brain Res* **511,** 329-337.

Calvino B & Grilo RM. (2006). Central pain control. *Joint Bone Spine* 73, 10-16.

Chery N & De Koninck Y. (1999). Junctional versus extrajunctional glycine and GABA(A) receptor-mediated IPSCs in identified lamina I neurons of the adult rat spinal cord. *J Neurosci* 19, 7342-7355.

Cheunsuang O & Morris R. (2000). Spinal lamina I neurons that express neurokinin 1 receptors: morphological analysis. *Neuroscience* 97, 335-345.

Christensen BN & Perl ER. (1970). Spinal neurons specifically excited by noxious or thermal stimuli: marginal zone of the dorsal horn. *J Neurophysiol* 33, 293-307.

Cliffer KD, Burstein R & Giesler GJ, Jr. (1991). Distributions of spinothalamic, spinohypothalamic, and spinotelencephalic fibers revealed by anterograde transport of PHA-L in rats. *J Neurosci* 11, 852-868.

Coggeshall RE & Carlton SM. (1997). Receptor localization in the mammalian dorsal horn and primary afferent neurons. *Brain Res Brain Res Rev* 24, 28-66.

Cruz F, Lima D & Coimbra A. (1987). Several morphological types of terminal arborizations of primary afferents in laminae I–II of the rat spinal cord, as shown after HRP labeling and Golgi impregnation. *J Comp Neurol* 261, 221-236.

D'Mello R & Dickenson AH. (2008). Spinal cord mechanisms of pain. *Br J Anaesth* 101, 8-16.

Dostrovsky JO & Craig AD. (1996). Cooling-specific spinothalamic neurons in the monkey. *J Neurophysiol* 76, 3656-3665.

Eckert WA, 3rd, McNaughton KK & Light AR. (2003). Morphology and axonal arborization of rat spinal inner lamina II neurons hyperpolarized by mu-opioid-selective agonists. *J Comp Neurol* 458, 240-256.

Fields HL, Basbaum AI & Heinricher MM. (2006). Central nervous system mechanisms of pain molulation. In *Wall and Melzack´s Textbook of Pain*, Fifth edn, ed. McMahon SB & Koltzenburg M, pp. 125 - 142. Elsevier Churchill Livingstone, Philadelphia.

Gardner EP, Martin JM & Jessel TM. (2000). The Bodily Senses. In *Principles of Neural Science*, 4th edn, ed. Kandel ER, Schwartz JH & Jessell TM, pp. 430–449. McGraw-Hill, New York.

Gebhart GF. (2004). Descending modulation of pain. *Neurosci Biobehav Rev* 27, 729-737.

Gobel S. (1978). Golgi studies of the neurons in layer I of the dorsal horn of the medulla (trigeminal nucleus caudalis). *J Comp Neurol* 180, 375-393.

Graham BA, Brichta AM & Callister RJ. (2004). In vivo responses of mouse superficial dorsal horn neurones to both current injection and peripheral cutaneous stimulation. *J Physiol* 561, 749-763.

Graham BA, Brichta AM & Callister RJ. (2007). Moving from an averaged to specific view of spinal cord pain processing circuits. *J Neurophysiol* 98, 1057-1063.

Grudt TJ & Perl ER. (2002). Correlations between neuronal morphology and electrophysiological features in the rodent superficial dorsal horn. *J Physiol* 540, 189-207.

Han ZS, Zhang ET & Craig AD. (1998). Nociceptive and thermoreceptive lamina I neurons are anatomically distinct. *Nat Neurosci* 1, 218-225.

Harmann PA, Carlton SM & Willis WD. (1988). Collaterals of spinothalamic tract cells to the periaqueductal gray: a fluorescent double-labeling study in the rat. *Brain Res* 441, 87-97.

Hochman S, Garraway SM & Pockett S. (1997). Membrane properties of deep dorsal horn neurons from neonatal rat spinal cord in vitro. *Brain Res* 767, 214-219.

Hunt SP & Mantyh PW. (2001). The molecular dynamics of pain control. *Nat Rev Neurosci* 2, 83-91.

Hylden JL, Anton F & Nahin RL. (1989). Spinal lamina I projection neurons in the rat: collateral innervation of parabrachial area and thalamus. *Neuroscience* 28, 27-37.

Hylden JL, Hayashi H & Bennett GJ. (1986a). Lamina I spinomesencephalic neurons in the cat ascend via the dorsolateral funiculi. *Somatosens Res* 4, 31-41.

Hylden JL, Hayashi H, Dubner R & Bennett GJ. (1986b). Physiology and morphology of the lamina I spinomesencephalic projection. *J Comp Neurol* 247, 505-515.

Ikeda H, Heinke B, Ruscheweyh R & Sandkuhler J. (2003). Synaptic plasticity in spinal lamina I projection neurons that mediate hyperalgesia. *Science* 299, 1237-1240.

Jia H, Rustioni A & Valtschanoff JG. (1999). Metabotropic glutamate receptors in superficial laminae of the rat dorsal horn. *J Comp Neurol* 410, 627-642.

Jones SL. (1991). Descending noradrenergic influences on pain. *Prog Brain Res* 88, 381-394.

Katano T, Furue H, Okuda-Ashitaka E, Tagaya M, Watanabe M, Yoshimura M & Ito S. (2008). N-ethylmaleimide-sensitive fusion protein (NSF) is involved in central sensitization in the spinal cord through GluR2 subunit composition switch after inflammation. *Eur J Neurosci* 27, 3161-3170.

Kato G, Kawasaki Y, Koga K, Uta D, Kosugi M, Yasaka T, Yoshimura M, Ji RR & Strassman AM. (2009). Organization of intralaminar and translaminar neuronal connectivity in the superficial spinal dorsal horn. *J Neurosci* 29, 5088-5099.

Keller AF, Coull JA, Chery N, Poisbeau P & De Koninck Y. (2001). Region-specific developmental specialization of GABA-glycine cosynapses in laminas I-II of the rat spinal dorsal horn. *J Neurosci* 21, 7871-7880.

Kevetter GA & Willis WD. (1982). Spinothalamic cells in the rat lumbar cord with collaterals to the medullary reticular formation. *Brain Res* 238, 181-185.

Kevetter GA & Willis WD. (1983). Collaterals of spinothalamic cells in the rat. *J Comp Neurol* 215, 453-464.

Khasabov SG, Rogers SD, Ghilardi JR, Peters CM, Mantyh PW & Simone DA. (2002). Spinal neurons that possess the substance P receptor are required for the development of central sensitization. *J Neurosci* 22, 9086-9098.

King AE, Ackley MA & Slack JR. (1997). Profile of neuronal excitation following selective activation of the neurokinin-1 receptor in rat deep dorsal horn in vitro. *Brain Res* 767, 55-63.

Kuru M. (1949). *The sensory paths in the spinal cord and brainstem of man.* Sogensya, Tokyo.

LaMotte C. (1977). Distribution of the tract of Lissauer and the dorsal root fibers in the primate spinal cord. *J Comp Neurol* 172, 529-561.

Larsson M & Broman J. (2008). Translocation of GluR1-containing AMPA receptors to a spinal nociceptive synapse during acute noxious stimulation. *J Neurosci* 28, 7084-7090.

Lawson SN, Crepps BA & Perl ER. (1997). Relationship of substance P to afferent characteristics of dorsal root ganglion neurones in guinea-pig. *J Physiol* 505 (Pt 1), 177-191.

Li YQ, Li H, Yang K, Kaneko T & Mizuno N. (2000). Morphologic features and electrical membrane properties of projection neurons in the marginal layer of the medullary dorsal horn of the rat. *J Comp Neurol* 424, 24-36.

Light AR & Perl ER. (1979). Reexamination of the dorsal root projection to the spinal dorsal horn including observations on the differential termination of coarse and fine fibers. *J Comp Neurol* 186, 117-131.

Light AR, Trevino DL & Perl ER. (1979). Morphological features of functionally defined neurons in the marginal zone and substantia gelatinosa of the spinal dorsal horn. *J Comp Neurol* 186, 151-171.

Lima D. (1990). A spinomedullary projection terminating in the dorsal reticular nucleus of the rat. *Neuroscience* 34, 577-589.

Lima D. (1998). Anatomical basis for the dynamic processing of nociceptive input. *Eur J Pain* 2, 195-202.

Lima D & Almeida A. (2002). The medullary dorsal reticular nucleus as a pronociceptive centre of the pain control system. *Prog Neurobiol* 66, 81-108.

Lima D & Coimbra A. (1983). The neuronal population of the marginal zone (lamina I) of the rat spinal cord. A study based on reconstructions of serially sectioned cells. *Anat Embryol (Berl)* 167, 273-288.

Lima D & Coimbra A. (1986). A Golgi study of the neuronal population of the marginal zone (lamina I) of the rat spinal cord. *J Comp Neurol* 244, 53-71.

Lima D & Coimbra A. (1988). The spinothalamic system of the rat: structural types of retrogradely labelled neurons in the marginal zone (lamina I). *Neuroscience* 27**,** 215-230.

Lima D & Coimbra A. (1989). Morphological types of spinomesencephalic neurons in the marginal zone (lamina I) of the rat spinal cord, as shown after retrograde labelling with cholera toxin subunit B. *J Comp Neurol* 279, 327-339.

Lima D & Coimbra A. (1990). Structural types of marginal (lamina I) neurons projecting to the dorsal reticular nucleus of the medulla oblongata. *Neuroscience* 34, 591-606.

Littlewood NK, Todd AJ, Spike RC, Watt C & Shehab SA. (1995). The types of neuron in spinal dorsal horn which possess neurokinin-1 receptors. *Neuroscience* 66, 597-608.

Liu RP. (1986). Spinal neuronal collaterals to the intralaminar thalamic nuclei and periaqueductal gray. *Brain Res* 365, 145-150.

Lopez-Garcia JA & King AE. (1994). Membrane properties of physiologically classified rat dorsal horn neurons in vitro: correlation with cutaneous sensory afferent input. *Eur J Neurosci* 6, 998-1007.

Lu Y & Perl ER. (2005). Modular organization of excitatory circuits between neurons of the spinal superficial dorsal horn (laminae I and II). *J Neurosci* 25, 3900-3907.

Luz LL, Szucs P, Pinho R & Safronov BV. (2010). Monosynaptic excitatory inputs to spinal lamina I anterolateral-tract-projecting neurons from neighbouring lamina I neurons. *J Physiol* 588, 4489-4505.

Mantyh PW, Allen CJ, Ghilardi JR, Rogers SD, Mantyh CR, Liu H, Basbaum AI, Vigna SR & Maggio JE. (1995). Rapid endocytosis of a G protein-coupled receptor: substance P evoked internalization of its receptor in the rat striatum in vivo. *Proc Natl Acad Sci U S A* 92, 2622-2626.

Mantyh PW, Rogers SD, Honore P, Allen BJ, Ghilardi JR, Li J, Daughters RS, Lappi DA, Wiley RG & Simone DA. (1997). Inhibition of hyperalgesia by ablation of lamina I spinal neurons expressing the substance P receptor. *Science* 278, 275-279.

Marshall GE, Shehab SA, Spike RC & Todd AJ. (1996). Neurokinin-1 receptors on lumbar spinothalamic neurons in the rat. *Neuroscience* 72, 255-263.

McMahon SB & Wall PD. (1983). A system of rat spinal cord lamina 1 cells projecting through the contralateral dorsolateral funiculus. *J Comp Neurol* 214, 217-223.

McMahon SB & Wall PD. (1985). Electrophysiological mapping of brainstem projections of spinal cord lamina I cells in the rat. *Brain Res* 333, 19-26.

Melzack R & Wall PD. (1965). Pain mechanisms: a new theory. *Science* 150, 971-979.

Menetrey D, Chaouch A, Binder D & Besson JM. (1982). The origin of the spinomesencephalic tract in the rat: an anatomical study using the retrograde transport of horseradish peroxidase. *J Comp Neurol* 206, 193-207.

Millan MJ. (1999). The induction of pain: an integrative review. *Prog Neurobiol* 57, 1-164.

Millan MJ. (2002). Descending control of pain. *Prog Neurobiol* 66, 355-474.

Molony V, Steedman WM, Cervero F & Iggo A. (1981). Intracellular marking of identified neurones in the superficial dorsal horn of the cat spinal cord. *Q J Exp Physiol* 66, 211-223.

Morgan CW, de Groat WC, Felkins LA & Zhang SJ. (1991). Axon collaterals indicate broad intraspinal role for sacral preganglionic neurons. *Proc Natl Acad Sci U S A* 88, 6888-6892.

Nakaya Y, Kaneko T, Shigemoto R, Nakanishi S & Mizuno N. (1994). Immunohistochemical localization of substance P receptor in the central nervous system of the adult rat. *J Comp Neurol* 347, 249-274.

Oren I, Nissen W, Kullmann DM, Somogyi P & Lamsa KP. (2009). Role of ionotropic glutamate receptors in long-term potentiation in rat hippocampal CA1 oriens-lacunosum moleculare interneurons. *J Neurosci* 29, 939-950.

Pertovaara A. (2006). Noradrenergic pain modulation. *Prog Neurobiol* 80, 53-83.

Pin JP & Bockaert J. (1995). Get receptive to metabotropic glutamate receptors. *Curr Opin Neurobiol* 5, 342-349.

Pin JP & Duvoisin R. (1995). The Metabotropic Glutamate Receptors - Structure and Functions. *Neuropharmacology* 34, 1-26.

Pinault D. (1996). A novel single-cell staining procedure performed in vivo under electrophysiological control: morpho-functional features of juxtacellularly labeled thalamic cells and other central neurons with biocytin or Neurobiotin. *J Neurosci Methods* 65, 113-136.

Pinto V, Szucs P, Lima D & Safronov BV. (2010). Multisegmental A{delta}- and C-fiber input to neurons in lamina I and the lateral spinal nucleus. *J Neurosci* 30, 2384-2395.

Polgar E, Al Ghamdi KS & Todd AJ. (2010a). Two populations of neurokinin 1 receptor-expressing projection neurons in lamina I of the rat spinal cord that differ in AMPA receptor subunit composition and density of excitatory synaptic input. *Neuroscience* 167, 1192-1204.

Polgar E, Hughes DI, Riddell JS, Maxwell DJ, Puskar Z & Todd AJ. (2003). Selective loss of spinal GABAergic or glycinergic neurons is not necessary for development of thermal hyperalgesia in the chronic constriction injury model of neuropathic pain. *Pain* 104, 229-239.

Polgar E, Watanabe M, Hartmann B, Grant SG & Todd AJ. (2008). Expression of AMPA receptor subunits at synapses in laminae I-III of the rodent spinal dorsal horn. *Mol Pain* 4, 5.

Polgar E, Wright LL & Todd AJ. (2010b). A quantitative study of brainstem projections from lamina I neurons in the cervical and lumbar enlargement of the rat. *Brain Res* 1308, 58-67.

Prescott SA & De Koninck Y. (2002). Four cell types with distinctive membrane properties and morphologies in lamina I of the spinal dorsal horn of the adult rat. *J Physiol* 539, 817-836.

Ramon y Cajal S. (1909). *Histologie du systeme nerveux de l'homme et des vertebres*. A. Maloine, Paris.

Renshaw B. (1946). Central effects of centripetal impulses in axons of spinal ventral roots. *J Neurophysiol* 9, 191-204.

Rethelyi M, Light AR & Perl ER. (1989). Synaptic ultrastructure of functionally and morphologically characterized neurons of the superficial spinal dorsal horn of cat. *J Neurosci* 9, 1846-1863.

Rexed B. (1952). The cytoarchitectonic organization of the spinal cord in the cat. *J Comp Neurol* 96, 414-495.

Ruscheweyh R, Ikeda H, Heinke B & Sandkuhler J. (2004). Distinctive membrane and discharge properties of rat spinal lamina I projection neurones in vitro. *J Physiol* 555, 527-543.

Ruscheweyh R & Sandkuhler J. (2002). Lamina-specific membrane and discharge properties of rat spinal dorsal horn neurones in vitro. *J Physiol* 541, 231-244.

Safronov BV, Pinto V & Derkach VA. (2007). High-resolution single-cell imaging for functional studies in the whole brain and spinal cord and thick tissue blocks using light-emitting diode illumination. *J Neurosci Methods* 164, 292-298.

Santos SF, Luz LL, Szucs P, Lima D, Derkach VA & Safronov BV. (2009). Transmission efficacy and plasticity in glutamatergic synapses formed by excitatory interneurons of the substantia gelatinosa in the rat spinal cord. *PLoS One* 4, e8047.

Santos SF, Rebelo S, Derkach VA & Safronov BV. (2007). Excitatory interneurons dominate sensory processing in the spinal substantia gelatinosa of rat. *J Physiol* 581, 241-254.

Shigemoto R, Nakanishi S & Mizuno N. (1992). Distribution of the mRNA for a metabotropic glutamate receptor (mGluR1) in the central nervous system: an in situ hybridization study in adult and developing rat. *J Comp Neurol* 322, 121-135.

Snider WD & McMahon SB. (1998). Tackling pain at the source: new ideas about nociceptors. *Neuron* 20, 629-632.

Spike RC, Kerr RC, Maxwell DJ & Todd AJ. (1998). GluR1 and GluR2/3 subunits of the AMPA-type glutamate receptor are associated with particular types of neurone in laminae I-III of the spinal dorsal horn of the rat. *Eur J Neurosci* 10, 324-333.

Spike RC, Puskar Z, Andrew D & Todd AJ. (2003). A quantitative and morphological study of projection neurons in lamina I of the rat lumbar spinal cord. *Eur J Neurosci* 18, 2433-2448.

Steedman WM, Molony V & Iggo A. (1985). Nociceptive neurones in the superficial dorsal horn of cat lumbar spinal cord and their primary afferent inputs. *Exp Brain Res* 58, 171-182.

Suzuki R, Morcuende S, Webber M, Hunt SP & Dickenson AH. (2002). Superficial NK1-expressing neurons control spinal excitability through activation of descending pathways. *Nat Neurosci* 5, 1319-1326.

Swett JE, McMahon SB & Wall PD. (1985). Long ascending projections to the midbrain from cells of lamina I and nucleus of the dorsolateral funiculus of the rat spinal cord. *J Comp Neurol* 238, 401-416.

Szentagothai J. (1964). Neuronal and synaptic arrangement in the substantia gelatinosa rolandi. *J Comp Neurol* 122, 219 –239.

Szucs P, Pinto V & Safronov BV. (2009). Advanced technique of infrared LED imaging of unstained cells and intracellular structures in isolated spinal cord, brainstem, ganglia and cerebellum. *J Neurosci Methods* 177, 369-380.

Tavares I & Lima D. (2002). The caudal ventrolateral medulla as an important inhibitory modulator of pain transmission in the spinal cord. *J Pain* 3, 337-346.

Tavares I & Lima D. (2007). From neuroanatomy to gene therapy: searching for new ways to manipulate the supraspinal endogenous pain modulatory system. *J Anat* 211, 261-268.

Thomson AM, West DC & Headley PM. (1989). Membrane Characteristics and Synaptic Responsiveness of Superficial Dorsal Horn Neurons in a Slice Preparation of Adult Rat Spinal Cord. *Eur J Neurosci* 1, 479-488.

Todd AJ. (2010). Neuronal circuitry for pain processing in the dorsal horn. *Nat Rev Neurosci* 11, 823-836.

Todd AJ, Hughes DI, Polgar E, Nagy GG, Mackie M, Ottersen OP & Maxwell DJ. (2003). The expression of vesicular glutamate transporters VGLUT1 and

VGLUT2 in neurochemically defined axonal populations in the rat spinal cord with emphasis on the dorsal horn. *Eur J Neurosci* 17, 13-27.

Todd AJ & Koerber R. (2006). Neuroanatomical substrates of spinal nociception. In *Wall and Melzack's Textbook of Pain*, 5 edn, ed. McMahon SB & Koltzenburg M, pp. 73-90. Churchill Livingstone, Edinburgh, UK.

Todd AJ, McGill MM & Shehab SA. (2000). Neurokinin 1 receptor expression by neurons in laminae I, III and IV of the rat spinal dorsal horn that project to the brainstem. *Eur J Neurosci* 12, 689-700.

Todd AJ, Puskar Z, Spike RC, Hughes C, Watt C & Forrest L. (2002). Projection neurons in lamina I of rat spinal cord with the neurokinin 1 receptor are selectively innervated by substance p-containing afferents and respond to noxious stimulation. *J Neurosci* 22, 4103-4113.

Todd AJ & Ribeiro-da-Silva A. (2005). Molecular Architecture of the Dorsal horn. In *The Neurobiology of Pain (Molecular and Cellular Neurobiology)*, ed. Hunt SP & Koltzenburg M, pp. 65-94. Oxford University Press, London.

Todd AJ & Spike RC. (1993). The localization of classical transmitters and neuropeptides within neurons in laminae I-III of the mammalian spinal dorsal horn. *Prog Neurobiol* 41, 609-645.

Todd AJ, Spike RC, Chong D & Neilson M. (1995). The relationship between glycine and gephyrin in synapses of the rat spinal cord. *Eur J Neurosci* 7, 1-11.

Todd AJ, Spike RC & Polgar E. (1998). A quantitative study of neurons which express neurokinin-1 or somatostatin sst2a receptor in rat spinal dorsal horn. *Neuroscience* 85, 459-473.

Todd AJ, Spike RC, Russell G & Johnston HM. (1992). Immunohistochemical evidence that Met-enkephalin and GABA coexist in some neurones in rat dorsal horn. *Brain Res* 584, 149-156.

Todd AJ, Spike RC, Young S & Puskar Z. (2005). Fos induction in lamina I projection neurons in response to noxious thermal stimuli. *Neuroscience* 131, 209-217.

Todd AJ & Sullivan AC. (1990). Light microscope study of the coexistence of GABA-like and glycine-like immunoreactivities in the spinal cord of the rat. *J Comp Neurol* 296, 496-505.

Todd AJ, Watt C, Spike RC & Sieghart W. (1996). Colocalization of GABA, glycine, and their receptors at synapses in the rat spinal cord. *J Neurosci* 16, 974-982.

Tracey DJ. (2004). Ascending and Descending Pathways in the Spinal cord. In *The Rat Nervous System*, Thirth edn, ed. Paxinos G, pp. 149-164. Elsevier Academic Press, San Diego.

Valtschanoff JG, Weinberg RJ, Rustioni A & Schmidt HH. (1992). Nitric oxide synthase and GABA colocalize in lamina II of rat spinal cord. *Neurosci Lett* 148, 6-10.

Vidnyanszky Z, Hamori J, Negyessy L, Ruegg D, Knopfel T, Kuhn R & Gorcs TJ. (1994). Cellular and subcellular localization of the mGluR5a metabotropic glutamate receptor in rat spinal cord. *Neuroreport* 6, 209-213.

Vikman KS, Rycroft BK & Christie MJ. (2008). Switch to Ca2+-permeable AMPA and reduced NR2B NMDA receptor-mediated neurotransmission at dorsal horn nociceptive synapses during inflammatory pain in the rat. *J Physiol* 586, 515-527.

Wall PD. (1960). Cord cells responding to touch, damage, and temperature of skin. *J Neurophysiol* 23, 197-210.

Willis WD & Coggeshall RE. (1991). *Sensory Mechanisms of the Spinal Cord*. John Wiley & sons, New York.

Willis WD & Coggeshall RE. (2004). *Sensory Mechanisms of the Spinal Cord*, vol. 1. Kluwer Academic / Plenum Publishers, New York.

Willis WD, Kenshalo DR, Jr. & Leonard RB. (1979). The cells of origin of the primate spinothalamic tract. *J Comp Neurol* 188, 543-573.

Willis WD & Westlund KN. (1997). Neuroanatomy of the pain system and of the pathways that modulate pain. *J Clin Neurophysiol* 14, 2-31.

Willis WD, Westlund KN & Carlton SM. (2004). Pain System. In *The Rat Nervous System*, Third edn, ed. Paxinos G, pp. 853 - 890. Elsevier Academic Press, San Diego.

Woolf CJ & Fitzgerald M. (1983). The properties of neurones recorded in the superficial dorsal horn of the rat spinal cord. *J Comp Neurol* 221, 313-328.

Yoshimura M & Jessell T. (1990). Amino acid-mediated EPSPs at primary afferent synapses with substantia gelatinosa neurones in the rat spinal cord. *J Physiol* 430, 315-335.

Yoshimura M & Nishi S. (1992). Excitatory amino acid receptors involved in primary afferent-evoked polysynaptic EPSPs of substantia gelatinosa neurons in the adult rat spinal cord slice. *Neurosci Lett* 143, 131-134.

Zoli M, Jansson A, Sykova E, Agnati LF & Fuxe K. (1999). Volume transmission in the CNS and its relevance for neuropsychopharmacology. *Trends Pharmacol Sci* 20, 142-150.

Zou X, Lin Q & Willis WD. (2000). Enhanced phosphorylation of NMDA receptor 1 subunits in spinal cord dorsal horn and spinothalamic tract neurons after intradermal injection of capsaicin in rats. *J Neurosci* 20, 6989-6997.

ABSTRACT

Spinal lamina I is a key area for relaying and integrating information from nociceptive primary afferents with various other sources of input, including descending control from supraspinal areas and local spinal input. The dendritic organization of lamina I neurons have been extensively studied, however, little is known about their complex axonal architecture and synaptic connections.

Combining the oblique infrared-LED illumination technique, paired electrophysiological recordings, 3-D reconstructions of biocytin-labelled neurons and computer simulations we studied: 1) the organization of the axon collaterals of projection neurons, 2) the axonal structure of lamina I local-circuit neurons and 3) local neuronal networks formed by these neurons.

In our studies, we demonstrate that the major axon of projection neurons from the lateral aspect of lamina I give rise to various types of ipsilateral collaterals (dorsal, ventral and lateral). These data suggest that projection neurons can additionally function as local-circuit and propriospinal neurons participating in intra- and intersegmental spinal processing. The projection neurons can receive input (direct or indirect) from both local-circuit cells and other projection neurons in lamina I. Local-circuit neurons in lamina I are characterized by an extensive local axon network. We show that a subpopulation of these local-circuit neurons with large somata is inhibitory. Their dendritic patterns and NK1r expression suggest that the local-circuit neurons receive similar input as projection neurons and distribute this information over several spinal segments and laminae.

In summary, our data suggest that both local-circuit and projection neurons in lamina I are involved in intralaminar, interlaminar and also intersegmental spinal processing. Still, the overall prevalence of local-circuit cells over projection neurons in lamina I emphasizes the functional importance of intralaminar processing. Therefore, future investigations of the neuronal network organization in lamina I will be necessary for the better understanding of signal processing in this spinal nociceptive projection area.

RESUMO

A lâmina I da medula espinhal é uma área fundamental na transmissão e integração de informações provenientes de aferentes primários nociceptivos com outras fontes de *input*, incluindo o controlo descendente de áreas supra-espinhais e o *input* espinhal local. A organização dendrítica dos neurónios da lâmina I tem sido extensivamente estudada, no entanto pouco se sabe sobre sua complexa arquitectura axonal e conexões sinápticas.

Através da combinação da técnica de iluminação oblíqua de LED infravermelho, registos electrofisiológicos em pares de neurónios, reconstruções em 3-D de neurónios preenchidos com biocitina e simulações computacionais, estudamos: 1) a organização dos colaterais locais do axónio de neurónios de projecção, 2) a estrutura axonal dos neurónios de "circuito-local" da lâmina I e 3) as redes neuronais locais formadas por estes neurónios.

Nos nossos estudos, demonstramos que o axónio principal de neurónios de projecção na região lateral da lâmina I dá origem a vários tipos de colaterais ipsilaterais (dorsal, ventral e lateral). Estes dados sugerem que os neurónios de projecção podem também funcionar como neurónios de "circuito local" e proprioespinhais, participando no processamento espinhal intra- e intersegmental. Estes neurónios de projecção podem receber *input* (directo ou indirecto) tanto de células de "circuito-local" como de outros neurónios de projecção da lâmina I. Os neurónios de "circuito-local" da lâmina I são caracterizados por uma extensa rede local de axónio. Os nossos resultados indicam que uma subpopulação destes neurónios de "circuito-local", com um grande corpo celular, é inibitória. Os seus padrões dendríticos e a expressão de NK1r sugerem que os neurónios de "circuito-local" recebem *inputs* similares aos recebidos pelos neurónios de projecção e distribuem esta informação sobre vários segmentos e lâminas da medula espinhal.

Em resumo, estes dados sugerem que ambos, os neurónios de "circuito-local" e de projecção da lâmina I, estão envolvidos no processamento espinhal intralaminar, interlaminar, e também intersegmental. Para além disso, a prevalência global de células de "circuito-local" sob neurónios de projecção na lâmina I realça a importância funcional do processamento intralaminar. Deste modo, investigações futuras sobre a organização da rede neuronal na lâmina I serão necessárias para

uma melhor compreensão do processamento de sinal nesta área de projecção nociceptiva da medula espinhal.

Cover illustration: Representative example of a lamina I local-circuit neuron (soma and dendrites – red; axon – black).